ANTENNA LABORATORY

Technical Report No. 67

APPLICATION OF CROSS-CORRELATION TECHNIQUES TO LINEAR ANTENNA ARRAYS

by

ROBERT H. MacPHIE

Contract No. AF33(657)-10474
High Element Number 62405484
760 D-Project 6278, Task 6278-01

March 1963

Sponsored by
AERONAUTICAL SYSTEMS DIVISION
WRIGHT-PATTERSON AIR FORCE BASE, OHIO
Project Engineer — James Rippin — ASRNCF-3

ELECTRICAL ENGINEERING DEPARTMENT
ENGINEERING EXPERIMENT STATION
UNIVERSITY OF ILLINOIS
URBANA, ILLINOIS

Antenna Laboratory

Technical Report No. 67

APPLICATION OF CROSS-CORRELATION TECHNIQUES TO LINEAR ANTENNA ARRAYS

by

Robert H. MacPhie

Contract No. AF33(657)-10474
Hitch Element Number 62405484
760 D-Project 6278, Task 6278-01

March 1963

Sponsored by

AERONAUTICAL SYSTEMS DIVISION

WRIGHT-PATTERSON AIR FORCE BASE, OHIO

Project Engineer - James Rippin - ASRNCF-3

Electrical Engineering Research Laboratory
Engineering Experiment Station
University of Illinois
Urbana, Illinois

ABSTRACT

This thesis is concerned with the application of cross-correlation techniques to linear antenna arrays. The basic cross-correlation system, which is considered, consists of two linear receiving arrays excited by a distribution of remote radio sources. The terminal voltage of each array is passed through a narrow-band RF filter and the two resulting signals are cross-correlated. It is demonstrated that this system can measure the mutual coherence function of the source distribution. To do this the patterns of the two antennas must be scanned independently. A Fourier analysis shows that the cross-correlation system's output is a filtered version of the mutual coherence function. From this output a three-dimensional principal solution can be deduced; it is a generalization of the one-dimensional principal solution given by Bracewell and Roberts in connection with radio astronomy.

In addition to cross-correlating the voltages obtained from two distinct arrays one can perform a cross-correlation of signals obtained from one of the arrays. By dividing the signal from each element into two parts (with predetermined weighting), and by combining additively each set of signals, one obtains two output voltages from what are effectively two coincident arrays. These signals are then cross-correlated in the usual fashion. A similar cross-correlation can be performed on the voltages obtained from the other array of the system. Finally, a fourth cross-correlation function results when the signals of the two arrays are combined in reverse order and it is the complex conjugate of the original cross-correlation function. These four distinct outputs are the elements of the 2 x 2 correlation matrix of the system. A Fourier analysis of the correlation matrix leads to a more general principal solution for the system as a whole which yields considerably more information about the source

ACKNOWLEDGMENT

It has been my privilege to prepare this thesis and technical report under the direction of Professor George A. Deschamps. It is with a deep sense of gratitude that I take this opportunity to thank him for his sound advice and helpful criticism during the course of this work. I also want to thank Professor Y. T. Lo for his continued interest and many suggestions. During my stay at the Antenna Laboratory I was able to discuss my work with a great many individuals and I appreciate very much their comments and criticism.

I also would like to express my appreciation to Miss Nanita Patterson, who typed my numerous rough drafts, and to Mrs. Arlene Albert and her staff in the publications office. Finally I want to thank the sponsor of my work, Aeronautical Systems Division, Wright-Patterson Air Force Base, Ohio, for their continued support.

CONTENTS

CONTENTS (continued)

ILLUSTRATIONS

1. INTRODUCTION

The concept of correlation has been used to advantage for many years in various branches of mathematical science. It is basically a statistical concept and such well-known statisticians as Karl Pearson[1] and A. A. Chuprov[2] have employed it extensively in their work. For example, Pearson defined the correlation coefficient of two sets of numbers x_{-n}, x_{-n+1}, ..., x_{n-1}, x_n, and y_{-n}, y_{-n+1}, ..., y_{n-1}, y_n, to be

$$r = \frac{\sum_{i=-n}^{n} x_i\, y_i}{\sqrt{\sum_{i=-n}^{n} (x_i)^2}\ \sqrt{\sum_{i=-n}^{n} (y_i)^2}}$$

which is the cosine of the angle in 2n+1-space between the two vectors X and Y.

If the elements of X and Y are samples of a time sequence, it is of interest to obtain a correlation coefficient between the two sequences when one of them is shifted in time, time being represented by the index of the correlated data. Hence we can write

$$r_k = \lim_{n \to \infty} \frac{1}{2n+1} \sum_{\ell=-n}^{n} x_\ell\, y_{\ell-k} .$$

If the values x_k and y_k are complex, we modify the above expression as follows

$$r_k = \lim_{n \to \infty} \frac{1}{2n+1} \sum_{\ell=-n}^{n} x_\ell\, y^*_{\ell-k}$$

where the superscript * indicates the complex conjugate of the quantity. The above expression, as a function of the index k, is the cross-correlation between the two time series X and Y. It is a simple step to the generalization of these discrete time series to continuous ones and the resulting cross-correlation function for the continuous case is

$$R(\tau) = \lim_{T \to \infty} \frac{1}{2T} \int_{-T}^{T} x(t)\, y^{*}(t-\tau)\, dt$$

where τ is the time delay of one function relative to the other. Norbert Wiener[3,4] has made a thorough study of stationary time series and has shown that the methods of Fourier analysis can be carried over into the domain of such functions in spite of their statistical nature.

In the case of antennas the time series represent signals which originate from remote radio sources distributed in various directions. Consequently the cross-correlation function of a pair of signals should now be written as

$$T(\tau,u,v) = \lim_{T \to \infty} \frac{1}{2T} \int_{-T}^{T} V(t,u)\, V^{*}(t-\tau,v)\, dt\ .$$

There are now two additional variables, u and v, which represent the directions from which the signals originate.

There is a considerable literature on the subject of such spatio-temporal cross-correlation functions or mutual coherence functions[5] as they are usually called, most of it having originated in optical studies. The mutual coherence function of two light disturbances is analogous to the cross-correlation function of two voltages. Complete correlation and

zero correlation correspond to coherence and incoherence respectively. More generally one speaks of partial coherence. Historically, the theory of partial coherence, according to Wolf[5], dates back to Verdet[6]. More recent contributors have been Von Laue[7], Van Cittert[8], Zernike[9], Wolf[10,11,12], Blanc-Lapierre and Dumontet[13], Beran[14], and Parrent[15,16]. Although developed primarily to describe optical phenomena, the theory of partial coherence can also be used to describe the correlation properties of radio fields.

It is the role of the receiving antenna to act as a device which responds to the fields from the remote radio sources. In many practical cases the antenna consists of a number of smaller elementary antennas, which are located on a straight line in space. Only such composite antennas, called linear arrays, will be considered in this thesis. They were chosen not only because they are widely used but because they lend themselves readily to mathematical analysis. In this connection the concept of the linear antenna array as a filter of spatial frequencies[17] has become quite widespread in recent years. The definitive paper on the subject, by Bracewell and Roberts[18], appeared in 1954 in connection with radio astronomy. A remote source distribution (e.g., the extraterrestrial radio sources), can be analyzed as a function of direction by Fourier techniques to yield a spectrum of spatial frequency components. One can show that a finite antenna acts as a low-pass spatial frequency filter. In the time domain there is usually a narrow-band RF filter associated with the antenna. Thus the antenna can be thought of as a spatio-temporal filter of the incoming radio signals.

The basic cross-correlation antenna system consists of two antennas whose terminal voltages are cross-correlated. There are several techniques

to do this electrically[19,20]. The first practical example of such a system appears to have been the Mill's Cross[21] which consists of two long arrays intersecting at right angles. When the array voltages are cross-correlated with $\tau = 0$, the power pattern of the system is the product of the two field strength patterns of the arrays. This product pattern is practically zero except in the region where the fan-shaped beams of the two arrays intersect at right angles. This produces a pencil beam which is the same as that of the field strength pattern of a rectangular planar antenna whose dimensions are given by the lengths of the two arrays. Another well known example of this type of system is the Compound Interferometer[22] in which a uniformly weighted linear aperture of length L is placed adjacent to a simple two-element interferometer of the same length. The cross-correlation output (again with $\tau = 0$) yields a product pattern which is the same as the field strength pattern of a uniformly weighted linear aperture of length 4L. Both of these systems are used in radio astronomy.

Taking inspiration from the success in this field, many workers have extended the use of cross-correlation techniques to radio direction finding, radar, and general communication antenna systems. Some of these contributors are: Arsac[23], Barber[24,25], Berman and Clay[26], Drane and Parrent[27,28], Hanbury Brown and Twiss[29,30], Linder[31], MacPhie[32,33,34], Pedinoff and Ksienski[35], Price[36], Welsby and Tucker[37], White, Ball and Deckett[38], and Young[39]. Since some of the above investigators deal with single and multiple products of antenna voltages the resulting outputs no longer are related to inputs by the law of superposition. Consequently, the generic terms "nonlinear antenna systems" or "data processing antenna systems" have become associated with these various schemes.

In this thesis a general theory of mapping the mutual coherence function, $T(\tau,u,v)$, of a distribution of remote radio sources is presented for the first time. Previous workers considered only the case of incoherent sources[18] and zero time shift ($\tau=0$). It will be shown that $T(\tau,u,v)$ can be measured with a correlation antenna system whose two linear arrays are scanned independently. Four distinct outputs from the system are obtained. These four correlation functions are the elements of the correlation matrix of the system. A three-dimensional Fourier analysis shows that each of the system outputs is a filtered version of the mutual coherence function of the source distribution. The analysis is for a partially coherent distribution, but the limiting cases of complete coherence and incoherence are considered and are shown to give rise to special types of system outputs. Consequently, if one or the other of these types of outputs is observed in practice, one can infer that the source distribution is completely coherent or incoherent as the case may be. The problem of taking a finite time-average in measuring the correlation of signals is also considered.

It is shown that when one compares cross-correlation with conventional antenna systems the comparison should be made between the cross-correlated output of the former and the square-law detected output of the latter system. Indeed it is shown that the square-law detected output is a degenerate case of the correlation output. An example of the improvement obtainable by using the cross-correlation system is given for the case of the optimum Dolph-Chebyshev array design[40].

The generalization of a two-antenna correlation system to one containing N antennas is analyzed. It is shown that such a system yields information about the higher order moments of the temporal probability distribution

of the sources. The methods of Fourier analysis used in the single correlation case can be generalized to more dimensions in the multiple correlation case.

Finally, a new type of radar system employing cross-correlation is described and analyzed in detail. Just as a cross-correlation receiving system employs two antennas, the radar system uses two antennas for both transmitting and receiving, four antennas in all. It is shown that such a system has distinct advantages over conventional systems employing a single antenna. An improved Dolph-Chebyshev design becomes possible and interference noise can be suppressed. The system could also be used to determine possible correlation between the returns from various targets.

2. LINEAR ARRAY THEORY

A linear array consists of a number of elementary antennas which are colinear, i.e., are located on a straight line in space. If, as is customary, the array elements are identical, then the array's radiation pattern is factorable; it is the product of the element pattern and the pattern of the array when its elements are replaced by isotropic antennas. Consequently in linear array theory we need consider only arrays of isotropic antennas knowing that for any specific type of element, e.g., a half-wave dipole, we can obtain the actual array pattern by multiplying the element pattern by the pattern of the isotropic array. We should also note that the polarization response of the array is the same as that of its elements. Thus by removing the element factor we are reducing linear antenna array theory from a vector to a scalar formulation.

If the elements of an array of finite length are increased in number without limit and the element spacing approaches zero, we obtain a "continuous array", as opposed to the discrete array mentioned above. In what follows we will refer to both continuous and discrete arrays, whose elements are located on a straight line, simply as <u>linear antennas</u>.

Now as is shown in Figure 1, two linear antennas (with isotropic elements) are located on the x axis of a convenient coordinate system. One is of length L_A and the other, located a distance ℓ to the right of the first, is of length L_B. It is well known that except for a constant factor, the far field patterns of the antennas[4] operating at frequency ω_o are given by

$$A(u) = \frac{1}{\sqrt{2\pi}} \int_{-L_A/2}^{L_A/2} a(x) e^{jux} dx \qquad (1)$$

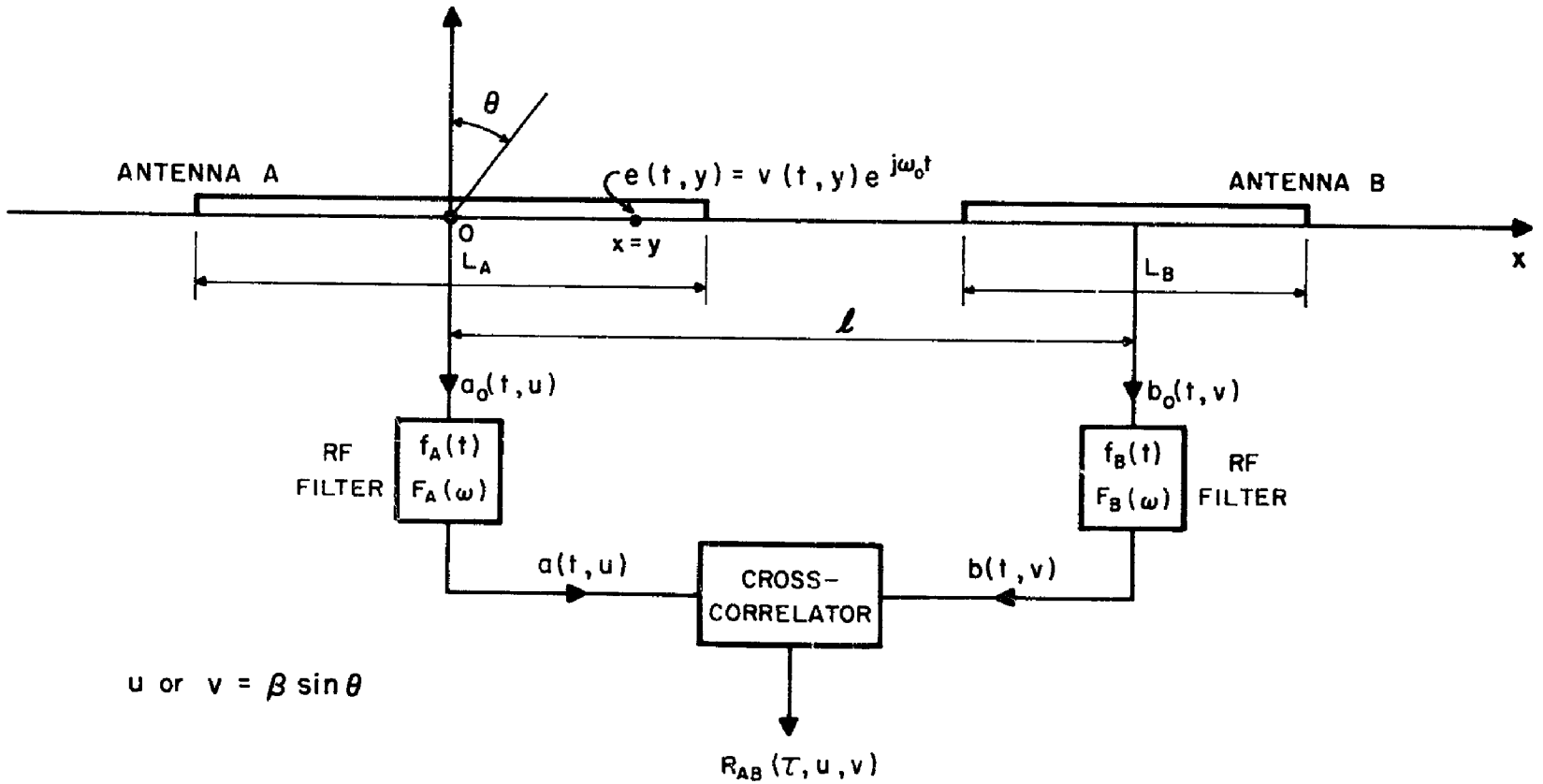

Figure 1. The Two-Antenna Cross-Correlation System.

and

$$B(u) = \frac{1}{\sqrt{2\pi}} \int_{-L_B/2 + \ell}^{L_B/2 + \ell} b(x) e^{jux}\, dx \qquad (2)$$

where $u = \beta \sin \theta$,

β = phase constant,

θ = angle measured from the normal to the antenna aperture,

x = aperture coordinate,

$a(x)$ = antenna A's aperture weighting function,

$b(x)$ = antenna B's aperture weighting function.

Note that the time-harmonic far fields are represented by complex quantities according to the usual convention. We will use this convention throughout the thesis for both fields and voltages. However, in cases where two voltages are being multiplied one must consider the product to be the product of two real quantities. The real part of the product of the corresponding complex voltages is not the same as the product of the real voltages. Consequently, in any case such as this, the notation "Re...." will be inserted to describe the operation precisely.

Since $a(x)$ and $b(x)$ are identically zero for $|x| > L_A/2$ and $|x-\ell| > L_B/2$ respectively, it can be seen from Equations (1) and (2) that $A(u)$ is the Fourier transform of $a(x)$, while $B(u)$ is the Fourier transform of $b(x)$. Consequently we can use the shifting theorem to show that if for example, $a(x)$ is changed to $a(x)\, e^{-ju_s x}$, the pattern becomes

$$A(u-u_s) = \frac{1}{\sqrt{2\pi}} \int_{-\infty}^{\infty} [a(x) e^{-ju_s x}]\, e^{jux}\, dx\,. \qquad (3)$$

The pattern can be shifted or scanned by introducing a progressive phase shift of $u_s = \beta \sin \theta_s$ radians per meter across the aperture. This is called electrical scanning and will be the only type considered in this thesis.* It also follows that the inverse Fourier transforms of A(u) and B(v) are the weighting functions

$$a(x) = \frac{1}{\sqrt{2\pi}} \int_{-\infty}^{\infty} A(u)\, e^{-jux}\, du \tag{4}$$

and

$$b(y) = \frac{1}{\sqrt{2\pi}} \int_{-\infty}^{\infty} B(v)\, e^{-jvy}\, dv, \tag{5}$$

It will be observed that these antennas are essentially "one-dimensional" since they are described by one-dimensional aperture and pattern functions. In physical (three-dimensional) space the angle θ = constant describes a cone whose apex is at the origin and whose axis is the x axis. When the antenna is receiving, all incident signals whose propagation vectors are parallel to any generator of this cone are indistinguishable by the antenna. Their phasor sum, as "seen" by the antenna, is taken as the field of "a source"

*It should be noted that in practice, electrical scanning is complicated by a number of factors. For example, suppose the antenna is matched to the load when its pattern is beamed in the broadside direction ($u_s = 0$); then in order to scan the pattern to the $u_s = v$ direction, a progressive phase shift, which of course changes the aperture's weighting function, must be introduced. This will, in general, result in a mismatch between the antenna and the load. The mutual impedance effects of the antenna elements also complicate the analysis of electrical scanning. Thus in Equation (3) we have hopefully assumed that these impedance problems have been solved and we can perform an ideal scan of the pattern in the u domain. However, when considered as a function of angle θ the pattern becomes distorted when scanned.

in the θ = constant direction. In addition, by thinking of β as the propagation vector $\vec{\beta}$, which indicates the direction as well as the frequency of the signals, we see that $u = \beta \sin \theta$ is actually the three-dimensional scalar product of $\vec{\beta}$ with a unit vector $\hat{x}$ parallel to the antenna axis.*

$$u = \vec{\beta} \cdot \hat{x} = \beta \cos (\pi/2-\theta)$$

or

$$u = \beta \sin \theta . \tag{6}$$

The two-dimensional counterparts of linear antennas are planar antennas whose elements are located, for example, in the $z = 0$ plane of a cartesian coordinate system. The one-dimensional Fourier analysis of linear antennas can be extended to these two-dimensional antennas with the transform coordinates being given by x, y, and $u = \beta \sin \theta \cos \varphi$, $v = \beta \sin \theta \sin \varphi$. In this case the propagation vector can be represented as a point on a sphere whose coordinates are (β,θ,φ) and by analogy with the one-dimensional case we have

$$\begin{aligned} u &= \vec{\beta} \cdot \hat{x} = \beta \sin \theta \cos \varphi , \\ v &= \vec{\beta} \cdot \hat{y} = \beta \sin \theta \sin \varphi . \end{aligned} \tag{7}$$

*In Appendix A is a more detailed account of the relation between the three-dimensional physical space and its projected counterparts in both one and two dimensions.

Admittedly, such antennas are of much greater practical value than linear antennas. However the method of analysis is essentially the same for both and for simplicity of notation we will restrict ourselves to the one-dimensional case. Generalization to the planar antenna of the results obtained is quite straightforward.

3. DESCRIPTION OF THE SOURCE DISTRIBUTION

In almost all cases of practical interest the exact nature of the source distribution is unknown; if it were known exactly a priori, it would never be necessary to build an antenna to measure it. However, we can make some reasonable assumptions about the distribution which are deduced from some of its known physical properties. Furthermore, the statistical description, which proved so useful in communication theory[3,4], will be used here. The basic concepts of this type of approach are embodied in the theory of partial coherence as developed by Born and Wolf[5] and Parrent[15,16].

3.1 Assumptions

It will be assumed that the source distribution possesses the following physical and statistical properties:

1) The sources are remote from the receiving antenna and fixed in space during the observation.

2) The direction of "a source" is given by the single parameter $u = \beta \sin \theta$.

3) In the time domain the sources are stationary; they emit random signals whose statistical properties are invariant under a shift of the time origin[42].

4) The sources are ergodic; the time averages of various quantities are equivalent to their mathematical expectations or statistical averages[42].

5) The signals emitted by the sources are described by zero-mean complex random variables with statistically independent real and imaginary parts.

6) The signals from sources in different directions are not necessarily statistically independent.

7) The statistics of the signals are gaussian[43].

8) The signals are quasi-monochromatic. The bandwidth $2 \Delta \omega$ is much less than the carrier frequency ω_o.

The above properties constitute an acceptable description of many sources encountered by the antenna engineer. For example, remote communication transmitters, radar targets, radio stars, and even earth satellites, produce signals whose general description is given above.

Since the sources are remote, the field due to each is incident on the antenna system in the form of a plane wave. The RF field at time t, at the origin of the antenna system (see figure 1), which is due to the source in the u direction, can be written as

$$e(t,u) = V(t,u)\, e^{j\omega_o t} \tag{8}$$

where the complex scalar function, e (t,u), can be thought of as one of the components of the electric field vector due to the remote source, i.e., the component to which the antenna elements respond. V (t,u) is the complex modulation envelope of the carrier signal at frequency ω_o and is the zero-mean random variable with independent real and imaginary parts mentioned above. This signal contains the desired information about the source. Accordingly, let us suppress the carrier factor in Equation (8) and focus our attention on the coherence properties of V (t,u).

3.2 Coherence Theory

Following Born and Wolf[5], we define the complex degree of coherence between the fields from the source in the u direction and the source in the v direction[+] as

$$\gamma(\tau,u,v) = \frac{\langle V(t,u)\, V^*(t-\tau,v)\rangle}{\left[\sqrt{\langle |V(t,u)|^2\rangle}\ \sqrt{\langle |V(t,v)|^2\rangle}\right]} \tag{9}$$

where $\langle f(t) \rangle$ denotes the time-average of f(t), i.e.,

$$\langle f(t) \rangle = \lim_{T\to\infty} \frac{1}{2T} \int_{-T}^{T} f(t)dt\,. \tag{10}$$

One signal is delayed by τ seconds relative to the other before their Hermitian product is formed and time-averaged.[*] The normalized form of this average is $\gamma(\tau,u,v)$ and it can be easily shown that

$$0 \le \left|\gamma(\tau,u,v)\right| \le 1\,. \tag{11}$$

[+] Both u and v are independent running variables in the $\beta \sin\theta$ domain, i.e., we could write $u = \beta \sin\theta_u$ and $v = \beta \sin\theta_v$. They should not be confused with the orthogonal coordinates u and v in the two-dimensional antenna case.

[*] More specifically, Born and Wolf use the total complex phasor $V(t,u)e^{j\omega_o t}$, rather than just the envelope V(t,u). Their complex degree of coherence differs from Equation (9) by an RF phase factor $e^{j\omega_o \tau}$.

If $|\gamma(\tau,u,v)| = 0$, for $u \neq v$, the two sources are completely incoherent while if $|\gamma(\tau,u,v)| = 1$ they are completely coherent. Note that $\gamma(\tau,u,v)$ is a function only of the difference τ, of the time arguments of the two field phasors $V(t,u)$ and $V^*(t-\tau,v)$. This is a consequence of the stationary nature of the sources. Let us define

$$T(\tau,u,v) = \langle V(t,u)\, V^*(t-\tau,v) \rangle \tag{12}$$

to be the mutual coherence function of the source distribution*. For $\tau = 0$ and $u = v$, this function is real and is proportional to the average power radiated by the source in the u direction toward the antenna, i.e., it is a measure of the temperature brightness of the source.

In practice it is the temperature brightness of the two-dimensional distribution of remote sources which we wish to measure. Appendix A is devoted to a description of a planar array which can measure such a distribution. The effect of the element pattern and of changing variables from the (u,v) domain to the (θ,ϕ) domain is considered. Nevertheless, such an analysis is simply a generalization of the one-dimensional case which for simplicity of notation we are considering in the main body of this thesis.

Since we have assumed that all of the sources are remote, they must

---

*Born and Wolf define the mutual coherence function as $\Gamma(\tau,u,v) = T(\tau,u,v)\, e^{j\omega_o\tau}$.

lie in the so-called visible range of the antennas. Consequently we can write

$$V(t,u) \equiv 0, \quad \text{for } |u| > \beta,$$

$$\gamma(\tau,u,v) \equiv 0, \quad \text{for } |u| > \beta \text{ or } |v| > \beta, \tag{13}$$

and

$$T(\tau,u,v) \equiv 0, \quad \text{for } |u| > \beta \text{ or } |v| > \beta.$$

In the terminology of distribution theory[44,45,46] we say that $\gamma(\tau,u,v)$ and $T(\tau,u,v)$ have a finite support in the uv domain while $V(t,u)$'s support is finite in the u domain.

3.3 Fourier Analysis

3.3.1 Time Domain

Since $V(t,u)$ is a sample function of a stationary random process its inverse Fourier transform in the time domain does not exist, i.e., $V(t,u)$ is not absolute-square integrable;

$$\lim_{T \to \infty} \int_{-T}^{T} |V(t,u)|^2 dt = \infty. \tag{14}$$

However, the complex mutual coherence function, $T(\tau,u,v)$, which may be written as

$$T(\tau,u,v) = \lim_{T\to\infty} \frac{1}{2T} \int_{-T}^{T} V(t,u)\, V^{*}(t-\tau,v)\,dt \qquad (15)$$

does exist. This means that there is a finite average cross-power between the signals from the u and v directions, as observed at the antenna system's origin.

Thus we define the cross-power spectral density or power spectrum to be the inverse Fourier transform of $T(\tau,u,v)$,

$$\bar{t}(\omega,u,v) = \frac{1}{\sqrt{2\pi}} \int_{-\infty}^{\infty} T(\tau,u,v) e^{-j\omega\tau} d\tau. \qquad (16)$$

It also follows that

$$T(\tau,u,v) = \frac{1}{\sqrt{2\pi}} \int_{-\infty}^{\infty} \bar{t}(\omega,u,v) e^{j\omega\tau} d\omega. \qquad (17)$$

3.3.2 Space Domain

Because $V(t,u)$, as a function of u, has a finite support ($V(t,u) \equiv 0$ for $|u| > \beta$) and is square integrable, it is possible to define its inverse Fourier transform in the space or spatial frequency domain. Thus we let its spatial frequency spectrum at time t be

$$v(t,x) = \frac{1}{\sqrt{2\pi}} \int_{-\infty}^{\infty} V(t,u) e^{jux} du$$

$$= \frac{1}{\sqrt{2\pi}} \int_{-\beta}^{\beta} V(t,u) e^{jux} du \quad . \tag{18}$$

The designation "spatial frequency spectrum" is used as a term which is analogous to "temporal frequency spectrum" in the time domain. Physically, $v(t,y)$ is the complex envelope of the field which exists at a point on the x axis which is y units from the origin (see Figure 1). This field is the integral of all the plane waves from the remote sources modified by the phase factor e^{juy}. On the other hand we can recover the complex field due to the source in the u direction as follows

$$V(t,u) = \frac{1}{\sqrt{2\pi}} \int_{-\infty}^{\infty} v(t,x) e^{-jux} dx \quad . \tag{19}$$

Let us define

$$\bar{\bar{t}}(\tau,x,y) = \left\langle v(t,x)\, v^{*}(t-\tau,y) \right\rangle \tag{20}$$

to be the mutual coherence function between the field envelopes at the points x and y. If we substitute Equation (19) into the above expression, there results

$$\bar{\bar{t}}\ (\tau, x, y) = \left\langle \frac{1}{2\pi} \int_{-\beta}^{\beta} V\ (t,u) e^{jux} du \int_{-\beta}^{\beta} V^{*}(t-\tau, v) e^{-jvy} dv \right\rangle \qquad (21)$$

$$= \frac{1}{2\pi} \int_{-\beta}^{\beta} \int_{-\beta}^{\beta} \left\langle V(t,u)\ V^{*}(t-\tau, v) \right\rangle e^{j(ux-vy)} dudv \qquad (22)$$

or

$$\bar{\bar{t}}\ (\tau, x, y) = \frac{1}{2\pi} \int_{-\beta}^{\beta} \int_{\beta}^{\beta} T(\tau, u, v) e^{j(ux-vy)} dudv\ . \qquad (23)$$

Thus for a given time delay τ, the spatial frequency spectrum of $T(\tau, u, v)$ is given by the mutual coherence function $\bar{\bar{t}}(\tau, x, y)$ as defined by Equation (23).

3.3.3 Combined Time and Space Domain

Using Equations (16) and (23) we can immediately define the combined temporal and spatial spectrum of $T(\tau, u, v)$ as

$$t(\omega, x, y) = \frac{1}{(2\pi)^{3/2}} \int_{-\infty}^{\infty} \int_{-\beta}^{\beta} \int_{-\beta}^{\beta} T(\tau, u, v) e^{-j(\omega\tau + ux + vy)} d\tau du dv \qquad (24)$$

and of course the inverse is

$$T(\tau,u,v) = \frac{1}{(2\pi)^{3/2}} \int_{-\infty}^{\infty} \int_{-\beta}^{\beta} \int_{-\beta}^{\beta} t(\omega,x,y) e^{j(\omega\tau \mp ux+vy)} d\omega dx dy . \qquad (25)$$

Note that the argument of the exponential function in each transform is $\pm(\omega\tau + ux - vy)$. The negative sign associated with vy occurs because the mutual coherence functions are expected values of a Hermitian product, i.e., the product of one complex function and the complex conjugate of another. This taking of the conjugate gives rise to the negative sign as can be seen in Equations (20) to (23).

3.4 Special Limiting Cases

3.4.1 The Coherent Limit

The limit of complete coherence between sources in the u and v directions has been defined by Parrent[15] to mean that

$$\left| \gamma\ (\tau,u,v) \right| \equiv 1 \qquad (26)$$

for all values of τ. However, Parrent has shown that only a strictly monochromatic source distribution will satisfy Equation (26). The mutual coherence function of such a distribution can be written as

$$T\ (\tau,u,v) = V\ (u)\ V^{*}(v) \qquad (27)$$

where V (u) is a fixed amplitude and phase factor associated with the source in the u direction.

In practice one can at best deal with quasi-monochromatic signals for which the power spectrum $\bar{t}\ (\omega,u,v)$ is practically zero except for $|\omega| < \Delta\omega$ where $\Delta\omega \lll \omega_0$. In such a situation one defines a coherent quasi-monochromatic source distribution[15] to be one for which

$$T\ (\tau,u,v) = V\ (u)\ V^*(v),\ \text{for}\ |\tau| \ll \frac{2\pi}{\Delta\omega}\ . \tag{28}$$

The mutual coherence function is independent of τ (for $\tau \ll \frac{2\pi}{\Delta\omega}$), and separable into the cartesian product of two functions V(u) and $V^*(v)$ which are complex conjugates. Since $T\ (\tau,u,v)$ is separable for small τ it follows that the spatial frequency spectrum is also separable.

$$\bar{\bar{t}}\ (\tau,x,y) = v\ (x)\ v^*(y),\ \text{for}\ |\tau| \ll \frac{2\pi}{\Delta\omega}\ . \tag{29}$$

Thus for small values of τ, the coherent quasi-monochromatic distribution behaves as one which is strictly monocromatic.

3.4.2 The Incoherent Limit

Complete incoherence between the sources in the u and v directions is characterized by

$$T\ (\tau,u,v) = T\ (\tau,u,u)\ \delta(u-v) \tag{30}$$

where $\delta(u)$ is the Dirac delta.

The mutual coherence function is non-zero only when u=v, in which case we obtain the self-coherence or autocorrelation function of the source in the u direction. The spatial frequency spectrum of the incoherent distribution is

$$\bar{\bar{t}}\ (\tau, x, y) = \frac{1}{2\pi} \int_{-\beta}^{\beta} \int_{\beta}^{\beta} T\ (\tau, u, u)\ \delta(u-v) e^{j(ux-vy)}\, dudv \qquad (31)$$

or

$$\bar{\bar{t}}\ (\tau, x-y) = \frac{1}{2\pi} \int_{-\beta}^{\beta} T\ (\tau, u, u) e^{ju(x-y)}\, du\ . \qquad (32)$$

The spatial frequency spectrum for incoherent sources is a function only of the difference, x-y, of the spatial frequency coordinates. If we let x-y = z we can define a one-dimensional spatial frequency spectrum as

$$\bar{\bar{t}}\ (\tau, z) = \frac{1}{\sqrt{2\pi}} \int_{-\beta}^{\beta} T\ (\tau, u) e^{juz}\, du \qquad (33)$$

where

$$T\ (\tau, u) = \frac{T\ (\tau, u, u,)}{\sqrt{2\pi}} \qquad (34)$$

in the incoherent case. In addition, one can use Equation (12) to show

that T (o,u,u) and hence T (o,u) are real and non-negative functions of u. Physically, this means that the average energy flow from the remote sources is non-negative.

4. THE GENERAL THEORY OF CROSS-CORRELATION

Before turning our attention to the specific case of the two-antenna cross-correlation system, we will consider the cross-correlation of two arbitrary narrow-band RF signals. We will show that a complex cross-correlation function is associated with these two real signals. Then we will consider in some detail a practical RF cross-correlator; this device can be used to measure the real and imaginary parts of the complex cross-correlation function.

When the two signals are indentical the cross-correlation becomes an autocorrelation. If the two signals are combined in reverse order, another cross-correlation results which is the complex conjugate of the original. The two cross-correlations and the two autocorrelations can be arranged as the elements of a 2 x 2 matrix, the correlation matrix, which completely characterizes the correlation properties of the two signals.* This matrix is analogous to the well known coherency matrix[4,5] used in the study of the polarization of light.

Finally, we will return to the cross-correlator to consider the practical problem of taking finite time-averages instead of the infinite time averages which are formally specified in the definitions of the correlation functions.

---

*See Davenport and Root[43], page 60.

4.1 The Complex Cross-Correlation Function

Let us consider two RF voltages whose cross-correlation function is to be determined. We can represent them by

$$a(t) = \mathrm{Re}\ A(t)e^{j\omega_o t} \tag{35}$$

$$b(t) = \mathrm{Re}\ B(t)e^{j\omega_o t} \tag{36}$$

where A(t) and B(t) are slowly varying complex modulation envelopes. The cross-correlation of the two real voltages is, by definition,

$$\bar{R}'_{AB}(\tau) = \lim_{T\to\infty} \frac{1}{2T}\int_{-T}^{T} a(t)\, b(t-\tau)\, dt\,. \tag{37}$$

In complex notation this becomes

$$\bar{R}'_{AB}(\tau) = \frac{1}{2}\,\mathrm{Re}\,\left\langle A(t)\, B(t-\tau)e^{j\omega_o(2t-\tau)}\right\rangle + \frac{1}{2}\,\mathrm{Re}\,\left\langle A(t)\, B^{*}(t-\tau)e^{j\omega_o\tau}\right\rangle . \tag{38}$$

The first term on the right side of the above equation is the double

$$R_{AB}(\tau) = \overline{R}_{AB}(\tau) e^{-j\omega_o \tau} \tag{43}$$

or

$$R_{AB}(\tau) = \langle A(t)\, B^*(t-\tau) \rangle \quad . \tag{44}$$

This, of course, is a shift of the cross-correlation spectrum from ω_o to 0 and removes the RF "carrier" factor, $e^{j\omega_o \tau}$, from the correlation function.

We see that a complex cross-correlation function is associated with any pair of real, narrow-band, RF voltages. In the following section we will show that the real and imaginary parts of this complex function can be measured by a system employing synchronous detection.

4.2 The Cross-Correlator

We will now describe a device which will cross-correlate the two real RF voltages a(t) and b(t). In practice the Compound Interferometer[22] employs this type of cross-correlator. Now, as is shown in Figure 2, one of the signals, b(t), is delayed by the variable amount τ before it is fed into a frequency shifter. The frequency shifter increases the carrier frequency of the signal from ω_o to $\omega_o + \omega_1$ with $\omega_o >>> \omega_1$. The output of this device can be written as

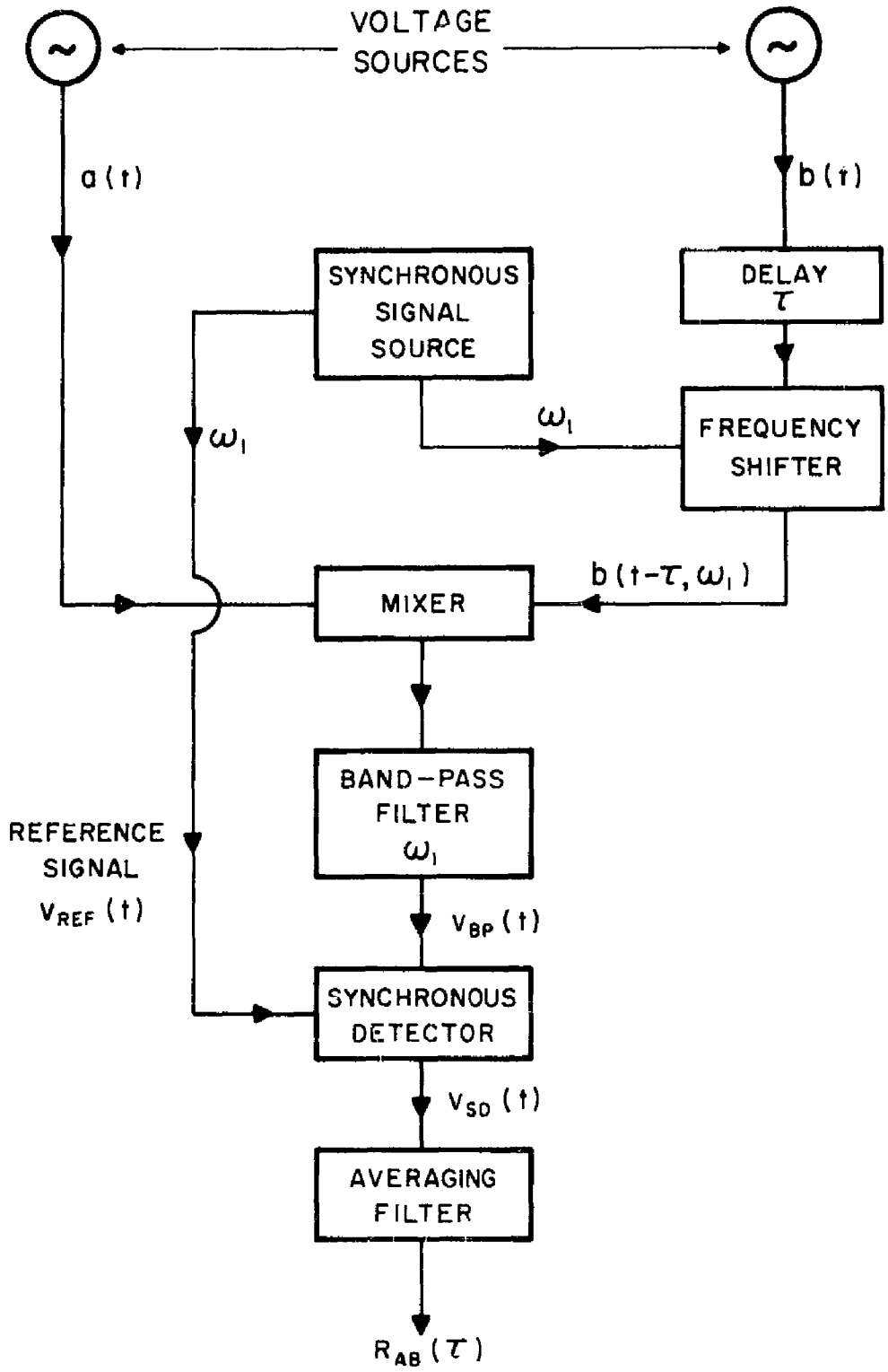

Figure 2. The Cross-Correlator.

$$b(t-\tau,\omega_1) = \mathrm{Re}\ B\ (t-\tau)e^{j[\omega_o\tau - (\omega_o+\omega_1)t]} . \qquad (45)$$

This signal along with a(t), enters a mixer which forms the square of their sum,

$$[\ a(t) + b(t-\tau,\omega_1)\ ]^2 =$$

$$\frac{1}{2}\ \mathrm{Re}\left\{\left[A^2(t) + B^2(t-\tau)e^{-j[2\omega_o\tau - 2\omega_1 t]} + A(t)\ B(t-\tau)e^{-j[\omega_o\tau - \omega_1 t]}\right] e^{j2\omega_o t}\right\}$$

$$+ \frac{1}{2}\ \mathrm{Re}\left\{|A(t)|^2 + |B(t-\tau)|^2 + A(t)\ B^*(t-\tau)e^{j[\omega_o\tau - \omega_1 t]}\right\} . \qquad (46)$$

The first term on the right side of the above equation is the double frequency component of the mixer output. If a band-pass filter with center frequency at $\omega = \omega_1$ is used to reject this signal as well as the signal whose spectrum is centered at $\omega = 0$, we obtain as the filter output

$$V_{BP}(t) = \frac{1}{2}\ \mathrm{Re}\left\{A(t)\ B^*(t-\tau)e^{j[\omega_o\tau - \omega_1 t]}\right\} . \qquad (47)$$

This is possible only if $\omega_1 > \Delta\omega$ where $\Delta\omega$ is the bandwidth of the modulation signals A(t) and B(t).

This filtered signal is fed into a synchronous detector along with a reference signal given by

$$V_{REF}(t) = \mathrm{Re}\ e^{j\omega_1 t} . \tag{48}$$

The detector output is the low-frequency component of the product of these two voltages. It can be written as

$$V_{SD}(t) = \frac{1}{2}\,\mathrm{Re}\,A(t)\,B^*(t-\tau)e^{j\omega_o\tau} . \tag{49}$$

Finally, this signal is fed into an averaging filter. If, for simplicity, we assume that the averager has the following ideal, (but physically unrealizable), impulse response

$$v_o(t) = \frac{1}{2T} \quad , \quad \text{for} \quad 0 < t < 2T, \tag{50}$$

$$= 0 \quad , \quad \text{otherwise,}$$

the averager output , and indeed the system output, after $2T$ seconds of averaging, is

$$\bar{R}'_{AB}(T,\tau) = \frac{1}{2}\,\mathrm{Re}\left\{\left[\frac{1}{2T}\int_o^{2T} A(T-t_1)\,B^*(T-t_1-\tau)dt_1 e^{j\omega_o\tau}\right]\right\} . \tag{51}$$

Letting $t = T-t_1$, this becomes

$$\bar{R}'_{AB}(T,\tau) = \frac{1}{2}\,\mathrm{Re}\left\{\frac{1}{2T}\int_{-T}^{T} A(t)\,B^*(t-\tau)dt\,e^{j\omega_o\tau}\right\}. \tag{52}$$

In the limit as $T\to\infty$ the system output becomes

$$\lim_{T\to\infty}\bar{R}'_{AB}(T,\tau) = \frac{1}{2}\,\mathrm{Re}\left\{\lim_{T\to\infty}\frac{1}{2T}\int_{-T}^{T} A(t)\,B^*(t-\tau)dt\,e^{j\omega_o\tau}\right\}$$

$$= \frac{1}{2}\,\mathrm{Re}\left\{\langle A(t)\,B^*(t-\tau)\rangle\,e^{j\omega_o\tau}\right\}. \tag{53}$$

Comparing this result with Equations (39) and (41) see that

$$\lim_{T\to\infty}\bar{R}'_{AB}(T,\tau) = \bar{R}'_{AB}(\tau) = \frac{1}{2}\,\mathrm{Re}\,\bar{R}_{AB}(\tau) \tag{54}$$

where $\bar{R}_{AB}(\tau)$ is the RF complex cross-correlation function. Consequently by time-averaging the output of the synchronous detector we obtain half of the real part of the RF complex cross-correlation function which is defined by Equation (42).

To obtain the imaginary part we simply perform the same cross-correlation of the two signals a(t) and b(t) except that this time they are taken in phase-quadrature. More specifically we cross-correlate

$$a(t) = \text{Re } A(t) e^{j\omega_o t} \tag{55}$$

and

$$b'(t) = \text{Re } B(t) e^{j(\omega_o t + \pi/2)}$$

$$= \text{Re } j \; B(t) e^{j\omega_o t}, \tag{56}$$

Letting

$$B'(t) = j \, B(t) \tag{57}$$

the correlator output, as $T \to \infty$, is

$$\bar{R}'_{AB'}(\tau) = \frac{1}{2} \text{Re} \left\{ \langle A(t) \, B'^{*}(t-\tau) \rangle \; e^{j\omega_o \tau} \right\} \tag{58}$$

which becomes

$$\bar{R}''_{AB}(\tau) = \frac{1}{2} \text{Im} \left\{ \langle A(t) \, B^{*}(t-\tau) \rangle \; e^{j\omega_o \tau} \right\}. \tag{59}$$

Consequently we can form the complex sum

$$\bar{R}_{AB}(\tau) = 2\left[\bar{R}'_{AB}(\tau) + j\bar{R}''_{AB}(\tau)\right] \tag{60}$$

$$= \langle A(t)\, B^*(t-\tau)\rangle e^{j\omega_o \tau} \tag{61}$$

to obtain the complex cross-correlation function of the two complex RF signals $A(t)e^{j\omega_o t}$ and $B(t)e^{j\omega_o t}$. As before, we can multiply both sides of Equation (61) by $e^{-j\omega_o t}$ and obtain

$$R_{AB}(\tau) = \langle A(t)\, B^*(t-\tau)\rangle \tag{62}$$

which is the complex cross-correlation function of A(t) and B(t).

4.3 The Autocorrelation Functions

The complex autocorrelation function of say A(t) is defined to be

$$R_{AA}(\tau) = \lim_{T\to\infty} \frac{1}{2\tau} \int_{-T}^{T} A(t)\, A^*(t-\tau)\, dt$$

$$= \langle A(t)\, A^*(t-\tau)\rangle \quad . \tag{63}$$

It can be measured in the same manner as the cross-correlation function,

$R_{AB}(\tau)$. To do this, we divide a(t) into two equal parts and "cross-correlate" the two signals as if they were distinct. The complex correlator output, except for the factor 1/4, will be $R_{AA}(\tau)$, as given by Equation (63) above. The complex autocorrelation function of the second signal B(t) is

$$R_{BB}(\tau) = \langle B(t)\, B^{*}(t-\tau) \rangle \tag{64}$$

and it too can be measured by the correlator which is described in the preceeding section.

4.4 The Correlation Matrix

Let us consider the two signals A(t) and B(t) as the elements of the following two-dimensional complex vector

$$\vec{\zeta}\,(t) = \begin{bmatrix} A(t) \\ \\ B(t) \end{bmatrix} . \tag{65}$$

The correlation matrix associated with the two signals is defined as

$$R(\tau) = \langle \vec{\zeta}\,(t)\, \vec{\zeta}^{\dagger}(t-\tau) \rangle \tag{66}$$

where the dagger, $\dagger$, indicates the transpose conjugate of the vector. Using Equation (65) it can easily be shown that

$$R(\tau) = \begin{bmatrix} \langle A(t) \quad A^*(t-\tau) \rangle & \langle A(t) \quad B^*(t-\tau) \rangle \\ \langle B(t) \quad A^*(t-\tau) \rangle & \langle B(t) \quad B^*(t-\tau) \rangle \end{bmatrix} \tag{67}$$

and in view of Equations (62), (63), and (64), this becomes

$$R(\tau) = \begin{bmatrix} R_{AA}(\tau) & R_{AB}(\tau) \\ R_{BA}(\tau) & R_{BB}(\tau) \end{bmatrix} . \tag{68}$$

The second cross-correlation function, $R_{BA}(\tau)$, is related to $R_{AB}(\tau)$ by Hermitian symmetry

$$R_{AB}(\tau) = R^*_{BA}(-\tau) . \tag{69}$$

The correlation matrix has as its four elements the four correlation functions that can be obtained from the two signals A(t) and B(t). It completely characterizes the correlation properties of these signals.

4.5 The Effect of Finite Averaging Time

In practice, of course, one cannot go to the limit of the infinite averaging time which is formally required by the correlation integral (see Equation (37)). It is of some interest therefore to investigate the effects of a finite averaging time $2T$, on the system output. The latter generally will differ from that which results in the limiting case of an infinite time average. We will obtain expressions for the expected value and variance of the complex cross-correlation system output as functions of T. In an earlier analysis[31], Linder has dealt with the effect of finite averaging time on the statistics of the real output of an RF correlation detector. Since what we present here is intended as only an outline of the problem we refer the interested reader to Linder's paper for a more detailed analysis.

Assuming that the signal voltages a(t) and b(t) are ergodic random processes, we can write the expected value of the complex system output after 2T seconds of averaging as

$$E\left\{R_{AB}(T,\tau)\right\} = E\left\{\frac{1}{2T}\int_{-T}^{T} A(t)\ B^{*}(t-\tau)dt\right\} \tag{70}$$

$$= \frac{1}{2T}\int_{-T}^{T} E\left\{A(t)\ B^{*}(t-\tau)\right\} dt \tag{71}$$

$$= E\left\{A(t)\ B^{*}(t-\tau)\right\} \tag{72}$$

where $E\{f(t)\}$ is the expected value (mathematical expectation) of f(t). But by the ergodic hypothesis we have, with probability 1,

$$E\left\{A(t)\ B^{*}(t-\tau)\right\} = \langle A(t)\ B^{*}(t-\tau)\rangle \quad . \tag{73}$$

Consequently, in view of Equation (62), we can write

$$E\left\{R_{AB}(T,\tau)\right\} = R_{AB}(\tau) \tag{74}$$

which is the desired output obtained after an infinite time average. Thus the output error has an expected value of zero, which is independant of the length of the averaging time.

We will now determine the system output variance, a real positive number which can be written as

$$\sigma^{2}_{AB}(T,\tau) = E\left\{|R_{AB}(T,\tau)|^{2}\right\} - |E\left\{R_{AB}(T,\tau)\right\}|^{2} \quad . \tag{75}$$

It can be thought of as the fluctuating a-c. power of the output which exists along with the desired d-c. power, $|R_{AB}(\tau)|^{2}$. We can write the first term on the right side of Equation (75) as

$$E\left\{\left|R_{AB}(T,\tau)\right|^2\right\} = E\left\{\frac{1}{4T^2}\int_{-T}^{T}\int_{-T}^{T} A(t_1)\, B^*(t_1-\tau)\, A^*(t_2) B(t_2-\tau) dt_1 dt_2\right\} \quad (76)$$

$$= \frac{1}{4T^2}\int_{-T}^{T}\int_{-T}^{T} E\left\{A(t_1)B^*(t_1-\tau)A^*(t_2)B(t_2-\tau)\right\}\, dt_1 dt_2 \,. \quad (77)$$

Until now the probability distribution of the random signals has not been specified. It could be quite arbitrary. However if the signals have a gaussian joint probability distribution it can be shown[47] that

$$E\left\{A(t_1)\, B^*(t_1-\tau)\, A^*(t_2)\, B(t_2-\tau)\right\} =$$

$$E\left\{A(t_1)\, B^*(t_1-\tau)\right\}\; E\left\{A^*(t_2)\, B(t_2-\tau)\right\}$$

$$+ E\left\{A(t_1)\, A^*(t_2)\right\}\; E\left\{B^*(t_1-\tau)\, B(t_2-\tau)\right\} \quad (78)$$

and by using the ergodic property of the signals we have

$$E\left\{A(t_1)\, B^*(t_1-\tau) A^*(t_2)\, B(t_2-\tau)\right\} =$$

$$R_{AB}(\tau)\, R^*_{AB}(\tau) + R_{AA}(t_1-t_2)\, R^*_{BB}(t_1-t_2) \quad . \tag{79}$$

Substituting this result back into Equation (77) gives

$$E\left\{\left|R_{AB}(T,\tau)\right|^2\right\} = \frac{1}{4T^2}\int_{-T}^{T}\int_{-T}^{T} R_{AA}(t_1-t_2)\, R^*_{BB}(t_1-t_2)\,dt_1 dt_2$$

$$+ \left|R_{AB}(\tau)\right|^2 \quad . \tag{80}$$

In view of Equations (74) and (75), the variance can be written as

$$\sigma^2_{AB}(T,\tau) = \frac{1}{4T^2}\int_{-T}^{T}\int_{-T}^{T} R_{AA}(t_1-t_2)\, R^*_{BB}(t_1-t_2)\, dt_1 dt_2 \, . \tag{81}$$

Letting $t_1-t_2 = t$ it can be shown that we can reduce the above double integral to

$$\sigma^2_{AB}(T,\tau) = \mathrm{Re}\left\{\frac{1}{T}\int_0^{2T}\left(1-\frac{t}{2T}\right) R_{AA}(t)\, R^*_{BB}(t)\,dt\right\} \quad . \quad (82)$$

Note that this is independent of the time delay τ.

The above expression is clearly dependent on the nature of auto-correlation functions $R_{AA}(\tau)$ and $R_{BB}(\tau)$. If, for analytical purposes, we assume that the signals' power spectra are both uniform in the band $|\omega| < \Delta\omega$ and are zero outside, then

$$R_{AA}(\tau) = R_{BB}(\tau) = R_o \frac{\sin \Delta\omega\tau}{\Delta\omega\tau} \quad . \quad (83)$$

The output variance is

$$\sigma^2_{AB}(T,\tau) = \frac{R_o^2}{T}\int_o^{2T}\left(1-\frac{t}{2T}\right)\left(\frac{\sin \Delta\omega t}{\Delta\omega t}\right)^2 dt \quad (84)$$

which after some manipulation can be shown to be

$$\sigma^2_{AB}(T,\tau) = R_o^2 \frac{Si(4\Delta\omega T)}{2\Delta\omega T} +$$

$$\frac{R_o^2}{2(\Delta\omega T)^2}\left[Ci(4\Delta\omega T) - 1 - \gamma - \ln(2T) + 2\Delta\omega \frac{\cos 4\Delta\omega T}{4\Delta\omega T}\right] . \quad (85)$$

where Si (x) and Ci (x) are the sine and cosine integrals* respectively, and $\gamma = .5772...$ is Euler's constant. This is a rather complicated result, but for large T we have

$$\sigma^2_{AB}(T,\tau)\Big|_{T \gg \frac{2\pi}{\Delta\omega}} \simeq R_o^2 \frac{Si(4\Delta\omega\, T)}{2\,\Delta\omega\, T} = \pi \frac{R_o^2}{4\Delta\omega\, T} . \qquad (86)$$

The output variance is inversely proportional to T for T large. Although this has been shown for the particular case of uniform power spectra it can be demonstrated that even for arbitrary power spectra $\sigma^2_{AB}(T,\tau)$ is inversely proportional to T when $T \gg \frac{2\pi}{\Delta\omega}$.

On the other hand for T small, $(T \ll \frac{2\pi}{\Delta\omega})$, the correlation functions in Equation (82) are essentially constant over the entire range of integration and we can write

$$\sigma^2(T,\tau)\Big|_{T \ll \frac{2\pi}{\Delta\omega}} \simeq R_{AA}(o)\, R^*_{BB}(o) \qquad (87)$$

which for uniform power spectra in the interval $|\omega| \leq \Delta\omega$ gives

*See for example, Schelkunoff, "Applied Mathematics for Engineers and Scientists," Chapter 18, Van Nostrand, 1948.

$$\sigma^2(T,\tau)\Big|_{T \ll \frac{2\pi}{\Delta\omega}} \simeq R_o^2 \tag{88}$$

Since it can be shown* that

$$\left| R_{AB}(\tau) \right| \leq \left(R_{AA}(o)\, R^*_{BB}(o) \right)^{\frac{1}{2}} \tag{89}$$

it follows that the standard deviation of the system output for small T is equal to or greater than its expected absolute value. For meaningful results one must therefore take reasonably long averaging times. Although we have considered only the statistics of the output of the cross-correlator it is obvious that the results apply to the autocorrelation outputs also. Thus

$$E\left\{ R_{AA}(T,\tau) \right\} = R_{AA}(\tau) \tag{90}$$

and

$$\sigma^2_{AA}(T,\tau) = \frac{1}{T}\int_o^{2T} (1 - \frac{t}{2T}) \left| R_{AA}(t) \right|^2 dt \tag{91}$$

Similar expressions obtain for the autocorrelation of b(t).

*See Davenport and Root[43], p. 61.

5. THE TWO-ANTENNA CROSS-CORRELATION SYSTEM

We will not consider the cross-correlation of the voltages obtained from the two linear antennas when they are excited by an arbitrary distribution of remote radio sources. It will be recalled that the source distribution can be described by its mutual coherence function $T(\tau,u,v)$. We will show that the two-antenna correlation system can measure this function. The patterns of the two antennas are scanned independently, one in the u direction and the other in the v direction, and when the voltages from the antennas are cross-correlated we obtain a complex cross-correlation output function which can be written as

$$R_{AB}(\tau,u,v) = T(\tau,u,v) \quad * \quad C_{AB}(\tau,u,v) \tag{92}$$

where * is the symbol for convolution (in three dimensions), and $C_{AB}(\tau,u,v)$ is the complex system function which will be defined in Section 5.2.

A Fourier analysis of this output will be made and from the analysis we will be able to define a principal solution $T_{AB}(\tau,u,v)$ for the cross-correlation antenna system. This principal solution is a generalization of the one-dimensional principal solution $T_o(u)$ which was first proposed by Bracewell and Roberts[18] in connection with radio astronomy.

5.1 Description of the Antenna Voltages

A diagram of the two-antenna cross-correlation system is shown in Figure 1. Before entering the cross-correlator, each of the terminal

voltages $a_o(t,u)$ and $b_o(t,u)$ of the two linear antennas is passed through narrow-band RF filter*. The two filtered signals can be represented by

$$A(t,u) = \int_0^{\infty} \int_{-\beta}^{\beta} V(t-t_1, u_1)\, A(u_1-u)du_1\, f_A(t_1)\, dt_1 \tag{93}$$

$$B(t,v) = \int_0^{\infty} \int_{-\beta}^{\beta} V(t-t_2, v_1)\, B(v_1-v)dv_1\, f_B(t_2)dt_2 \tag{94}$$

where $f_A(t)$ and $f_B(t)$ are the envelopes of the impulse responses of the two filters and the RF carrier factor $e^{j\omega_o t}$ has been suppressed. Note that the patterns of antennas A and B are scanned independently in the u and v directions respectively. The source density function V(t,u), weighted by these pattern functions, is integrated over the visible range to yield the terminal voltages which then are convoluted with the filter response functions. If we define the mirror image, or reverse, of a function to be

$$\overset{\vee}{g}(x) = g(-x) \tag{95}$$

we can write the above equations as

*We have tacitly assumed that the frequency response of each antenna itself is essentially constant over the bandwidth of its RF filter.

$$A(t,u) = V(t,u) * f_A(t) \overset{\vee}{A}(u) \tag{96}$$

$$B(t,v) = V(t,v) * f_B(t) \overset{\vee}{B}(v) . \tag{97}$$

The convolution sign applies to both variables, t and u in Equation (96), and t and v in Equation (97).

These two equations show that each antenna with its associated RF filter acts as a combination spatio-temporal frequency filter of the two-dimensional space-time signal V(t,u). As is indicated in Figure 1 it is the two output voltages from these filters that will be cross-correlated.

5.2 Cross-Correlation of the Antenna Voltages

Comparing Equations (35), (36) and (96), (97) we see that the complex cross-correlation output function of the antenna system can be written down by replacing A(t) and B(t) by A(t,u) and B(t,v) respectively, in the various correlation equations. Thus the complex system output, after 2T seconds of averaging, is

$$R_{AB}(T,\tau,u,v) = \frac{1}{2T}\int_{-T}^{T} A(t,u)\, B^*(t-\tau,v)\, dt \tag{98}$$

and the expected value is

$$R_{AB}(\tau,u,v) = \langle A(t,u)\, B^*(t-\tau,v) \rangle . \tag{99}$$

Substituting the expressions for $A(t,u)$ and $B(t,v)$ given by Equations (96) and (97) into the above, we obtain

$$R_{AB}(\tau,u,v) = \left\langle \left(V(t,u) * f_A(t) \overset{\vee}{A}(u)\right) \left(V^*(t-\tau,v) * f_B^*(t-\tau)\overset{\vee *}{B}(v)\right) \right\rangle \tag{100}$$

$$= \int_0^\infty \int_0^\infty \int_{-\beta}^{\beta} \int_{-\beta}^{\beta} \left\langle V(t-t_1,u_1)V^*(t-\tau-t_2,v_1)\right\rangle f_A(t_1) f_B^*(t_2)\,dt_1\,dt_2 \overset{\vee}{A}(u-u_1)\overset{\vee *}{B}(v-v_1)\,du_1\,dv_1 . \tag{101}$$

In view of Equation (12), we can write

$$\left\langle V(t-t_1,u_1)\ V^*(t-\tau-t_2,v_1)\right\rangle = T(\tau-t_1+t_2,u_1,v_1) \tag{102}$$

and Equation (101) becomes

$$R_{AB}(\tau,u,v) = T(\tau,u,v) * f_{AB}(\tau)\ \overset{\vee}{A}(u)\ \overset{\vee *}{B}(v) \tag{103}$$

where

$$f_{AB}(\tau) = f_A(\tau) \; * \; \overset{\vee}{f}_B^{\,*}(\tau) \; . \tag{104}$$

Thus we can write

$$R_{AB}(\tau,u,v) = T(\tau,u,v) \; * \; C_{AB}(\tau,u,v) \tag{105}$$

where we have defined the complex cross-correlation system function to be

$$C_{AB}(\tau,u,v) = f_{AB}(\tau) \; \overset{\vee}{A}(u) \; \overset{\vee}{B}^{*}(v) \; . \tag{106}$$

Equation (105) is the fundamental equation of the cross-correlation process. It shows how the system function $C_{AB}(\tau,u,v)$ operates on the source function $T(\tau,u,v)$, (by convolution in three dimensions), to give the output complex cross-correlation function $R_{AB}(\tau,u,v)$.

5.3 Fourier Analysis of the System Output

In a manner similar to that which led to the definition of the combined spatio-temporal spectrum of $T(\tau,u,v)$ as given by Equation (24) of Chapter 3, we define the spatio-temporal spectrum of the complex cross-correlation system output $R_{AB}(\tau,u,v)$ to be

$$r_{AB}(\omega,x,y) = \frac{1}{(2\pi)^{3/2}} \int_{-\infty}^{\infty}\int_{-\infty}^{\infty}\int_{-\infty}^{\infty} R_{AB}(\tau,u,v)e^{-j(\omega\tau-ux+vy)}\,d\tau du dv . \quad (107)$$

Substituting the expression for $R_{AB}(\tau,u,v)$ of Equation (105) into the above gives

$$r_{AB}(\omega,x,y) = \frac{1}{(2\pi)^{3/2}} \int_{-\infty}^{\infty}\int_{-\infty}^{\infty}\int_{-\infty}^{\infty} T(\tau,u,v) * C_{AB}(\tau,u,v)e^{-j(\omega\tau-ux+vy)}\,d\tau du dv. \quad (108)$$

We can invoke the convolution theorem to write

$$r_{AB}(\omega,x,y) = (2\pi)^{3/2}\, t(\omega,x,y)\, c_{AB}(\omega,x,y) \quad (109)$$

where $c_{AB}(\omega,x,y)$ is the inverse Fourier transform of the system function $C_{AB}(\tau,u,v)$. Using the expression for $C_{AB}(\tau,u,v)$ given by Equation (106) we obtain

$$c_{AB}(\omega,x,y) = \frac{1}{(2\pi)^{3/2}} \int_{-\infty}^{\infty}\int_{-\infty}^{\infty}\int_{-\infty}^{\infty} f_A(\tau) * f_B^*(\tau)\, V_A(u)\, V_B^*(v)$$

$$e^{-j(\omega\tau-ux+vy)}\,d\tau du dv . \quad (110)$$

By again using the convolution theorem we can write

$$c_{AB}(\omega,x,y) = \sqrt{2\pi}\quad F_A(\omega)\ F_B^*(\omega)\ a\ (x)\ b^*(y) \tag{111}$$

where $F_A(\omega)$ and $F_B(\omega)$, the inverse Fourier transforms of $f_A(\tau)$ and $f_B(\tau)$ respectively, are the frequency response characteristics of the two RF filters, and where a(x) and b(y) are the aperture weighting functions of the antennas. Thus

$$\begin{aligned} r_{AB}(\omega,x,y) &= 4\pi^2 t(\omega,x,y)\ F_A(\omega)\ F_B^*(\omega)\ a\ (x)\ b^*(y) \\ &= (2\pi)^{\frac{3}{2}}\ t(\omega,x,y)\ c_{AB}(\omega,x,y)\ . \end{aligned} \tag{112}$$

Equation (112) is the fundamental equation in the frequency domain. It shows that the spectrum of the output is proportional to the spectrum of the mutual coherence function weighted by the system's frequency response function which is factorable.

5.4 The Principal Solution

Our main purpose is of course to measure $T(\tau,u,v)$, or equivalently, its spectrum $t(\omega,x,y)$. However, if the bandwidth of the RF filters are both say $2\Delta\omega$, it follows that $F_A(\omega)\ F_B^*(\omega) \simeq 0$ for $|\omega| > \Delta\omega$. The system passes only those temporal frequencies of the source distribution which lie in the narrow RF band $|\omega-\omega_o| < \Delta\omega$. To investigate the pass-bands of spatial frequencies of the system we note from Figure 1

that $a(x) \equiv 0$ for $|x| > L_A/2$ and $b(x) \equiv 0$ for $|x-\ell| > L_B/2$ where L_A and L_B are the lengths of the two apertures. Consequently, it is clear that the Cartesian product $a(x)\, b^*(y) \equiv 0$ except when $|x| \leq L_A/2$ and $|y-\ell| \leq L_B/2$. In Figure 3 this region in the xy plane is shown cross-hatched and labeled $\bar{Q}_{AB}$. Note that the spacing ℓ between apertures causes the region to move away from the origin. Finally we can define a three-dimensional region Q_{AB} which delimits the spatio-temporal "aperture" of the system. This region is shown in the diagram of Figure 4. Strictly speaking, since the functions $F_A(\omega)$ and $F_B^*(\omega)$ are analytic in a half plane [4], they are not identically zero outside of Q_{AB}. However in practice there is negligible error in assuming that they are zero.

Now from Equation (112) we see that since $c_{AB}(\omega,x,y)$ is zero for points outside Q_{AB}, the output spectrum contains information only about that part of the spectrum $t(\omega,x,y)$ which lies within Q_{AB}. This being the case, we can define

$$t_{AB}(\omega,x,y) = \frac{r_{AB}(\omega,x,y)}{4\pi^2\, c_{AB}(\omega,x,y)}, \quad \text{for } (\omega,x,y) \in Q_{AB},$$

$$= 0, \text{ otherwise,} \tag{113}$$

where $(\omega,x,y) \in Q_{AB}$ means that the point with coordinates (ω,x,y) belongs to the point set Q_{AB}.

The Fourier transform of $t_{AB}(\omega,x,y)$ is the <u>principal solution</u>

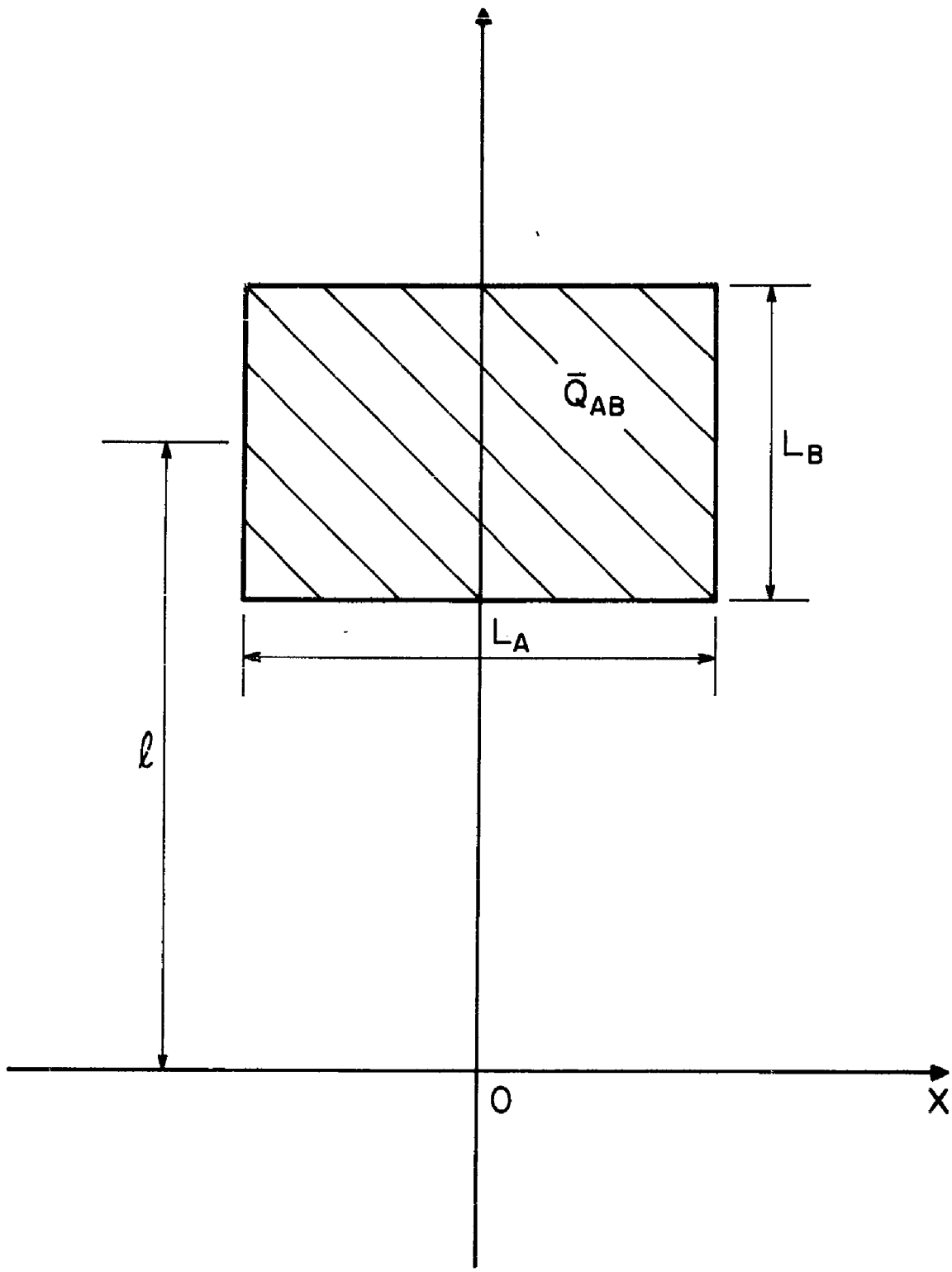

Figure 3. Spatial Frequency Plane of the Cross-Correlation Antenna System with the "Aperture" $\bar{Q}_{AB}$ Shown Hatched.

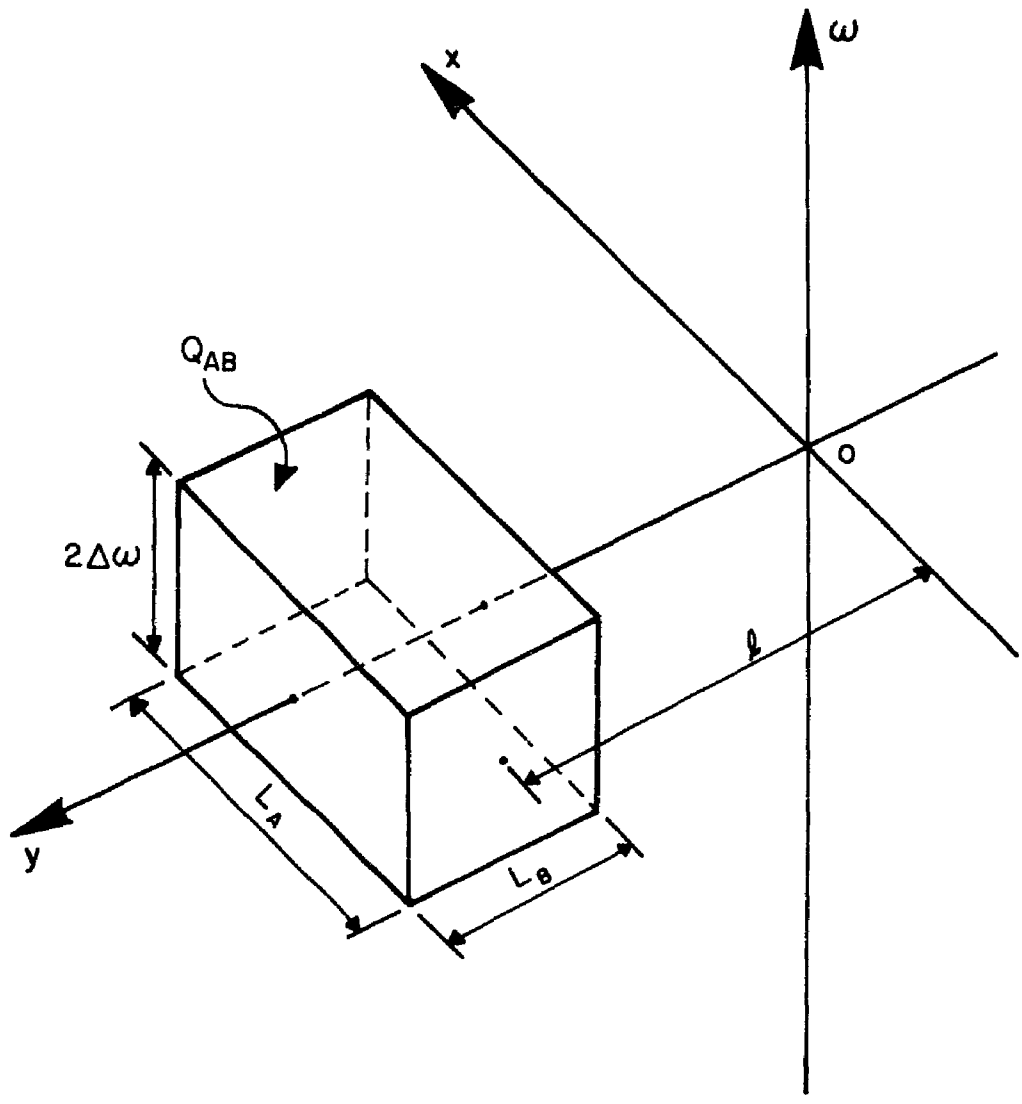

Figure 4. Combined Spatio-Temporal Frequency Space for the Cross-Correlation System in which the Region Q_{AB} is Shown as a Rectangular Parallelpiped.

$$T_{AB}(\tau,u,v) = \frac{1}{(2\pi)^{3/2}} \int_{-\infty}^{\infty}\int_{-\infty}^{\infty}\int_{-\infty}^{\infty} t_{AB}(\omega,x,y)\, e^{j[\omega\tau-xu+yv]}\, d\omega dx dy . \qquad (114)$$

It is a filtered version of the true distribution $T(\tau,u,v)$ with no components of frequency which lie outside the region Q_{AB}. However, those components which are present are identical to those of the true source distribution.

5.5 Direct Measurement of the Principal Solution

Equation (109) indicates that the output spectrum $r_{AB}(\omega,x,y)$ is generally a distorted version of the true spectrum $t(\omega,x,y)$. Because the system characteristics $F_A(\omega)$, $F_B(\omega)$, $a(x)$, and $b(y)$ are not only zero outside of Q_{AB} but can also take on arbitrary values inside the region, it was necessary to divide the output spectrum by the system spectrum (see Equation (113)) to recover the principal solution spectrum $t_{AB}(\omega,x,y)$.

However, if the system characteristics were all uniform within Q_{AB}, i.e., if

$$c_{AB}(\omega,x,y) = q_{AB}(\omega,x,y) = \frac{1}{4\pi^2} , \text{ for } (\omega,x,y) \in Q_{AB}, \qquad (115)$$

$$= 0 , \text{ otherwise,}$$

where $q_{AB}(\omega,x,y)$ is defined as the system function which is uniform in Q_{AB}, then from Equation (113) we have

$$r_{AB}(\omega,x,y) = t(\omega,x,y), \quad \text{for} \quad (\omega,x,y) \in Q_{AB}, \tag{116}$$

$$= 0 \quad , \quad \text{otherwise.}$$

The Fourier transform of $q(\omega,x,y)$ is

$$Q_{AB}(\tau,u,v) = \Delta\omega^2 L_A L_B \operatorname{sinc}\left(\frac{\Delta\omega\tau}{\pi}\right) \operatorname{sinc}\left(\frac{L_A u}{2\pi}\right) \operatorname{sinc}\left(\frac{L_B v}{2\pi}\right) e^{j\ell v} \tag{117}$$

where we have used the "sinc" notation of Woodward[48],

$$\operatorname{sinc} x = \frac{\sin \pi x}{\pi x} .$$

Comparing Equations (106) and (117) we see that

$$f_{AB}(\tau) = \frac{2}{\pi} \Delta\omega^2 \operatorname{sinc}\left(\frac{\Delta\omega\tau}{\pi}\right) \tag{118}$$

and

$$f_A(t) = f_B(t) = \sqrt{\frac{2}{\pi}} \Delta\omega \operatorname{sinc}\left(\frac{\Delta\omega t}{\pi}\right) . \tag{119}$$

The responses $f_A(t)$ and $f_B(t)$ are physically unrealizable* since they are non-zero for $t < 0$. However, if we are willing to accept a delay of τ_1 seconds, with $\tau_1 \gg \frac{2\pi}{\Delta\omega}$, between the input and the desired output, then to a good degree of approximation the response functions

*See, for example, Davenport and Root[43], p. 174.

$$f_A(t-\tau_1) = f_B(t-\tau_1) = A\sqrt{\frac{2}{\pi}}\,\Delta\omega\ \mathrm{sinc}\left[\frac{\Delta\omega}{\pi}\,(t-\tau_1)\right] \qquad (119.a)$$

can be synthesized. The two types of response $f_A(t)$ and $f_A(t-\tau_1)$ are shown in Figure 5. Since $f_A(t-\tau_1) \simeq 0$ for $t < 0$ there is usually negligible error in having the actual response envelope identically zero for $t < 0$.

Consequently, if the system impulse response envelopes and patterns are given by Equations (117), then the spectrum becomes (approximately)

$$4\pi^2 F_A(\omega)\ F_B^*(\omega)\ a(x)\ b(y) = 4\pi^2\,\frac{e^{j\omega(\tau_1-\tau_1)}}{4\pi^2} \simeq 1, \text{for } (\omega,x,y) \in Q_{AB},$$

$$= 0\ , \quad \text{otherwise}. \qquad (120)$$

The phase factor $e^{j\omega\tau_1}$ is due to the time delay necessary to insure a physically realizable system. Since we have the Hermitian product of the two filter spectra, $F_A(\omega)e^{j\omega\tau_1}$ and $F_B^*(\omega)e^{-j\omega\tau_1}$, this phase factor cancels out in the final result (a rather fortunate occurrence). It is interesting to note that the analogous condition of physical realizability does not obtain in the space domain. The antenna pattern's reverse, $\overset{\vee}{A}(u)$, is actually the response to a point source (spatial impulse) in the $u = 0$ direction. Since most patterns are real and have even symmetry, it is clear that $\overset{\vee}{A}(u) \neq 0$ for $u < 0$. Physically, we might "explain" this by saying that we can go forward and backward in space but only forward in time. However in practice there is a very important physical condition that must be satisfied in the spatial domain, namely, the antenna must be of finite length. In a sense this is an even more stringent

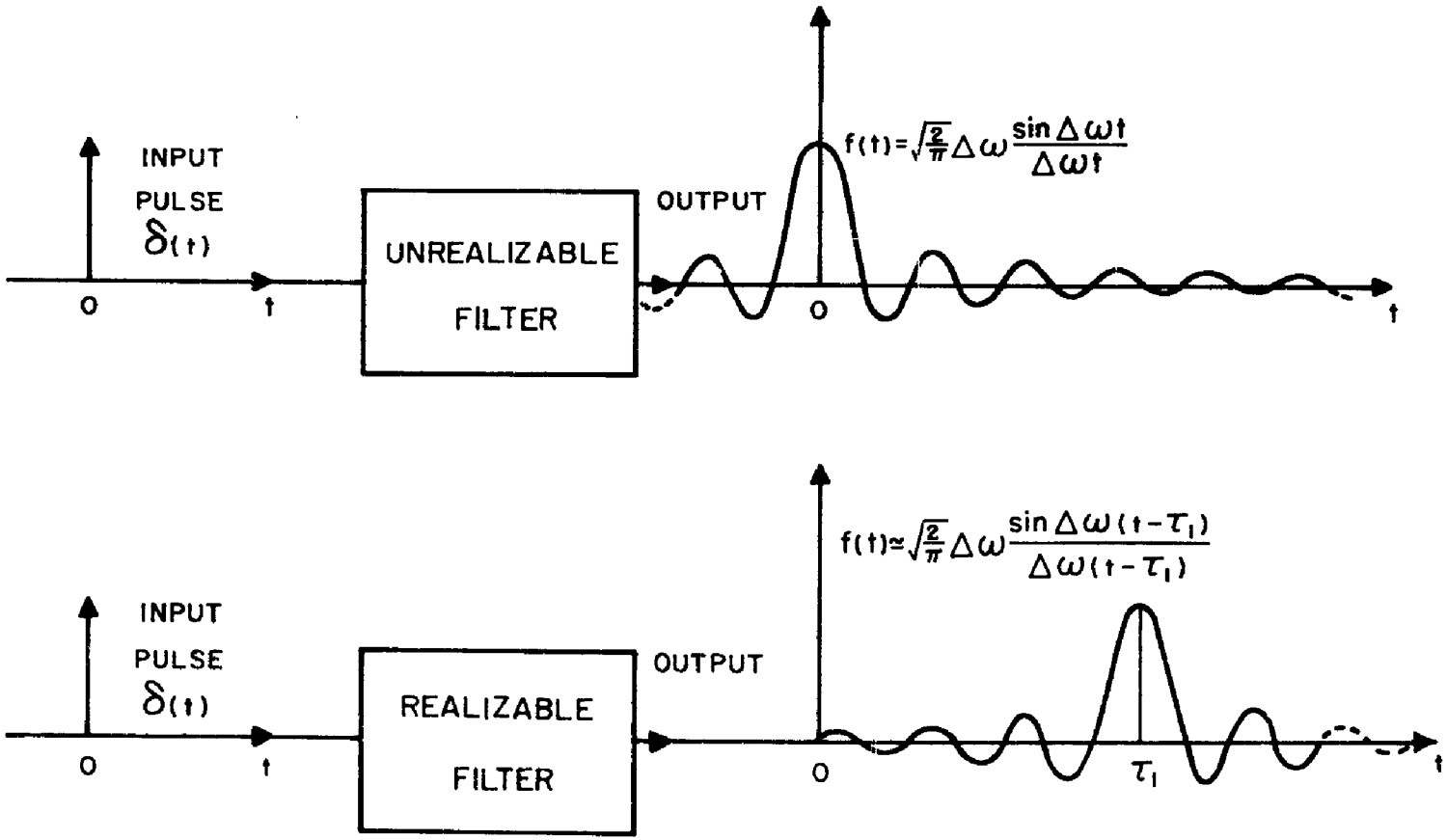

Figure 5. Impulse Responses of Realizable and Unrealizable Time-Domain Filters.

condition than that in the time domain. It allows the aperture function to be non-zero only over a finite region (e.g., $|x| \leq L_A/2$), whereas the impulse response of a time filter can be non-zero over the semi-infinite region $t \geq 0$.

Returning to the system with a uniform frequency response in the region Q_{AB} we see that to a good degree of approximation (if $\tau_1 \gg \frac{2\pi}{\Delta\omega}$)

$$R_{AB}(\tau,u,v) = T_{AB}(\tau,u,v)$$
$$= T(\tau,u,v) * Q_{AB}(\tau,u,v) \tag{121}$$

which is the principal solution.

5.6 Cross-Correlation System Outputs for Coherent and Incoherent Source Distributions

In Equation (28) in Chapter 3 it was indicated that a coherent quasi-monochromatic source distribution has the following mutual coherence function,

$$T(\tau,u,v) = V(u)\, V^*(v), \text{ for } \tau \ll 2\pi/\Delta\omega,$$

where $\Delta\omega$ is the bandwidth of the signals and satisfies the inequality $\Delta\omega \ll \omega_o$. Equation (29) indicates that the spatial frequency spectrum of the above function is

$$\overline{\overline{t}}\,(\tau,x,y) = v(x)\, v^*(y), \text{ for } \tau \ll 2\pi/\Delta\omega \,.$$

Both the mutual coherence function and its spatial frequency spectrum are factorable for small τ.

Now the system output in the presence of such a distribution is

$$R_{AB}(\tau,u,v)\Big|_{\tau \ll \frac{2\pi}{\Delta\omega}} = V(u)\, V^*(v) * f_{AB}(\tau)\, \check{A}(u)\, \check{B}^*(v) \tag{122}$$

$$= K\, V(u) * A(u)\quad V^*(v) * B^*(v) \tag{123}$$

where K is a constant. The output function is independent of τ and separable (for $\tau \ll 2\pi/\Delta\omega$).

Consequently we can write the spatial frequency spectrum of the output as

$$\overline{\overline{r}}_{AB}(\tau,x,y)\Big|_{\tau \ll 2\pi/\Delta\omega} = K\, 2\pi\, v(x)\, a(x)\, v^*(y)\, b^*(y) \tag{124}$$

i.e., this spectrum is also separable and independent of τ for small τ.

If the source distribution is incoherent then we can write (see Chapter 3, Equation (30)),

$$T(\tau,u,v) = T(\tau,u,u)\quad \delta(u-v)$$

as its mutual coherence function. The corresponding spectral density function is

$$t(\omega, x, y) = \frac{1}{(2\pi)^{3/2}} \int_{-\infty}^{\infty}\int_{-\infty}^{\infty}\int_{-\infty}^{\infty} T(\tau, u, v) \quad \delta(u-v) e^{-j(\omega\tau - ux + vy)} d\tau du dv$$

or

$$t(\omega, x-y) = \frac{1}{(2\pi)^{3/2}} \int_{-\infty}^{\infty}\int_{-\infty}^{\infty} T(\tau, u, u)\ e^{-j[\omega\tau - u(x-y)]} \tag{125}$$

which is a function only of the difference, (x-y), of the spatial frequency coordinates. If the system has a uniform weighting function in the region Q_{AB}, then its output spectrum, and the principal solution spectrum, will be

$$r_{AB}(\omega, x-y) = t(\omega, x-y), \text{ for } (\omega, x, y) \in Q_{AB},$$

$$= 0 \quad , \text{ otherwise,} \tag{126}$$

which also is a function of the difference, x-y, of the spatial frequency coordinates.

Combining both the coherent and incoherent cases we can make the following statements:

a) If the source distribution is coherent the spatial frequency power spectrum is separable for $\tau \ll {}^{2\pi}/_{\Delta\omega}$.

b) If the source distribution is incoherent the spatial frequency power spectrum is a function only of the difference, (x-y), of the spatial frequency coordinates.

In practice one can observe the spectrum only in the "aperture" Q_{AB}. Although $t(\omega,x,y)$ is an analytic function, and in theory can be extended to points outside Q_{AB} by analytic continuation, it has been shown[49] that in the presence of measurement errors very little meaningful continuation is possible. Consequently even if $t(\omega,x,y)$ is experimentally observed to be "coherent" or "incoherent" within Q_{AB} one cannot be sure that it will continue to be so outside the aperture. However from a practical point of view, if the spectrum, when measured within Q_{AB}, satisfies either of the above conditions, it is reasonable to infer that the sources are coherent or incoherent as the case may be.

5.7 Simplification of the Cross-Correlation System for the Case of Incoherent Sources

If the sources in different directions are incoherent, it is of no use to point the patterns of the two antennas in different directions. Only when the two beams are pointed in the same direction will there be appreciable output from the system. Thus if we set $u = v$ and substitute Equation (30) into Equation (105) we can write

$$R_{AB}(\tau,u,v)\Big|_{u=v} = T(\tau,u,u) * C_{AB}(\tau,u,u)$$

$$= \int_{-\infty}^{\infty}\int_{-\infty}^{\infty}\int_{-\infty}^{\infty} T(\tau-t,u_1,v_1)\,\delta(u_1-v_1) f_{AB}(t)\,\underset{\sim}{A}(u-u_1)\underset{\sim}{B}^{*}(u-v_1)\,dt\,du_1\,dv_1$$

$$= \int_{-\infty}^{\infty}\int_{-\infty}^{\infty} T(\tau-t,\ u_1,u_1)\ f_{AB}(t)\ \overset{\vee}{A}(u-u_1)\ \overset{\vee *}{B}(u-u_1)\ dtdu_1 \cdot \qquad (127)$$

Using Equation (34), and letting $R_{AB}(\tau,u,u) = \sqrt{2\pi}\ R_{AB}(\tau,u)$ we obtain

$$R_{AB}(\tau,u) = T(\tau,u) * f_{AB}(\tau)\ \overset{\vee}{A}(u)\ \overset{\vee *}{B}(u) \qquad (128)$$

as the two-dimensional cross-correlation output for the case of an incoherent source distribution.

We define the spatio-temporal frequency spectrum of this output to be

$$r_{AB}(\omega,z) = 2\pi\ t(\omega,z)\ F_A(\omega)\ F_B^{*}(\omega)\ a(z) * \overset{\vee *}{b}(z) \qquad (129)$$

where $z = x-y$, (see Equation (33)). Since the system's pattern is now in the form of a <u>product</u> of the individual field strength patterns $\overset{\vee}{A}(u)$ and $\overset{\vee *}{B}(u)$, the spatial frequency spectrum is in the form of the <u>convolution</u> of the aperture weighting functions $a(z)$ and $\overset{\vee *}{b}(z)$. Consequently, if the aperture functions are uniform for $|z| \leq \frac{L_A}{2}$ and $|z-\ell| \leq \frac{L_B}{2}$, as is shown in Figure 6a, then the spatial frequency spectrum $a(z) * \overset{\vee *}{b}(z)$ is shown in Figure 6b. The spectrum is a trapezoidal function and weights

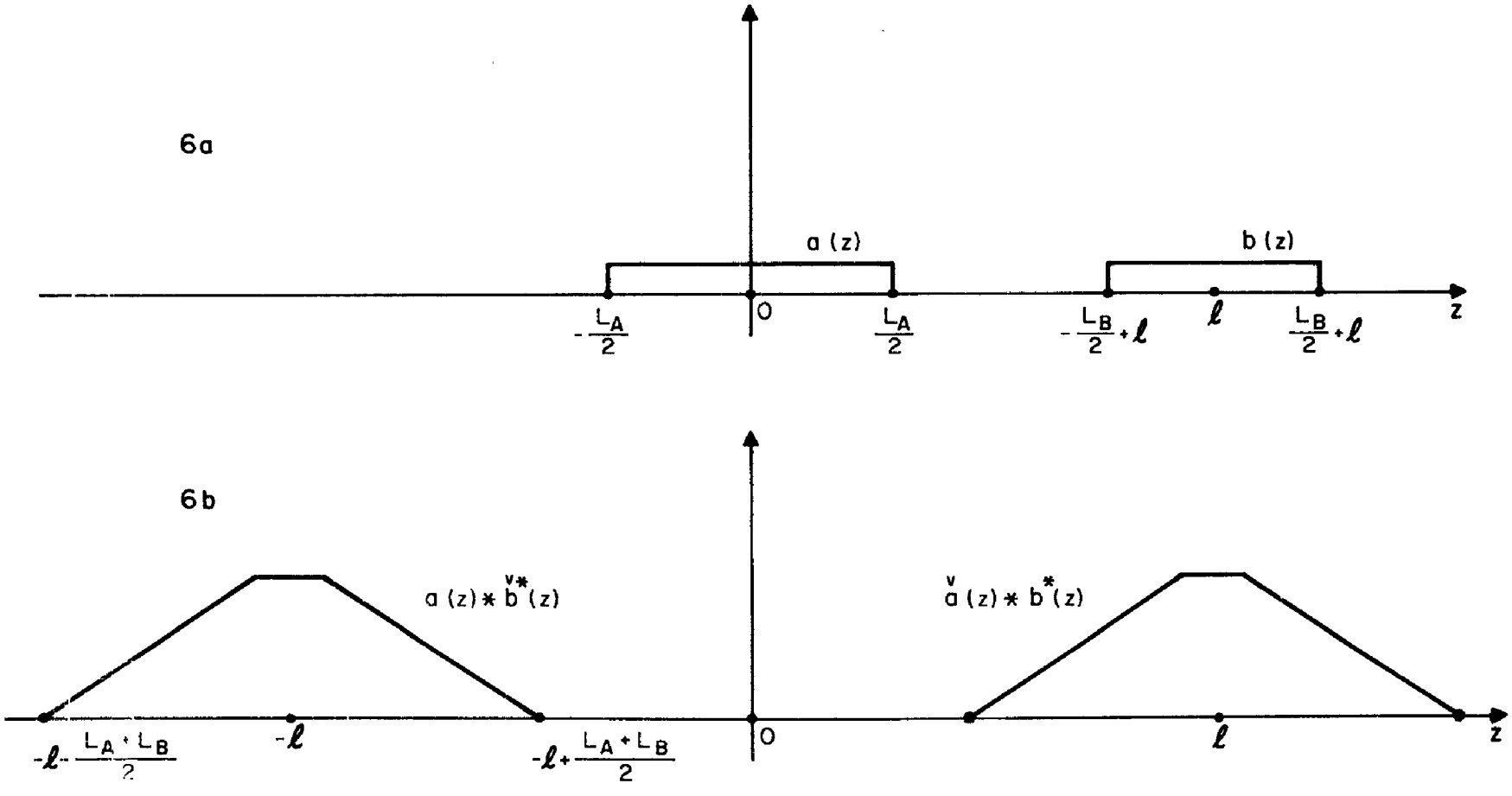

Figure 6. Aperture Distributions and Spatial Frequency Spectrum (for Incoherent Sources) of Two Uniformly Weighted Apertures.

more heavily the spatial frequencies near the center of its "aperture" than those near the edges. This results in a distortion of the source spectrum as "seen" at the system's output. Note also that the width of the "aperture" of the system is given by the sum, $L_A + L_B$, of the aperture widths of the individual antennas and is centered at $z = -\ell$.

In order to obtain a uniform spatial frequency spectrum one must use a compound interferometer[22]. A diagram of the weighting functions and associated spectrum of the system is shown in Figure 7. Instead of two uniformly weighted apertures the compound interferometer consists of just one uniformly weighted aperture and a simple interferometer. The two isotropic elements of the interferometer are located at the end points of the second aperture. Mathematically, they can be represented by Dirac deltas and their convolution with the other aperture function results in the uniform spectrum shown in part b of the diagram. The width of the "aperture" is also given by $L_A + L_B$ and its center is located at $z = -\ell$.

In Chapter 3 it was shown that in the incoherent case $T(\tau, u)$ is a real function. Consequently, its spectrum is complex symmetric, i.e., $t(\omega, z) = t^*(-\omega, -z)$. This means that by measuring $t(\omega, z)$ on the interval $2|z+\ell| \leq L_A + L_B$, we can automatically deduce its values on the interval $2|z-\ell| \leq L_A + L_B$. This region is also shown in Figures 6b and 7b.

Finally, we can define a system "aperture" Q'_{AB} for the incoherent case which is analogous to the more general Q_{AB} of the partially coherent case. Thus in Figure 8 is shown the combined spatio-temporal frequency plane for the incoherent case with the region Q'_{AB} indicated by cross-hatching.

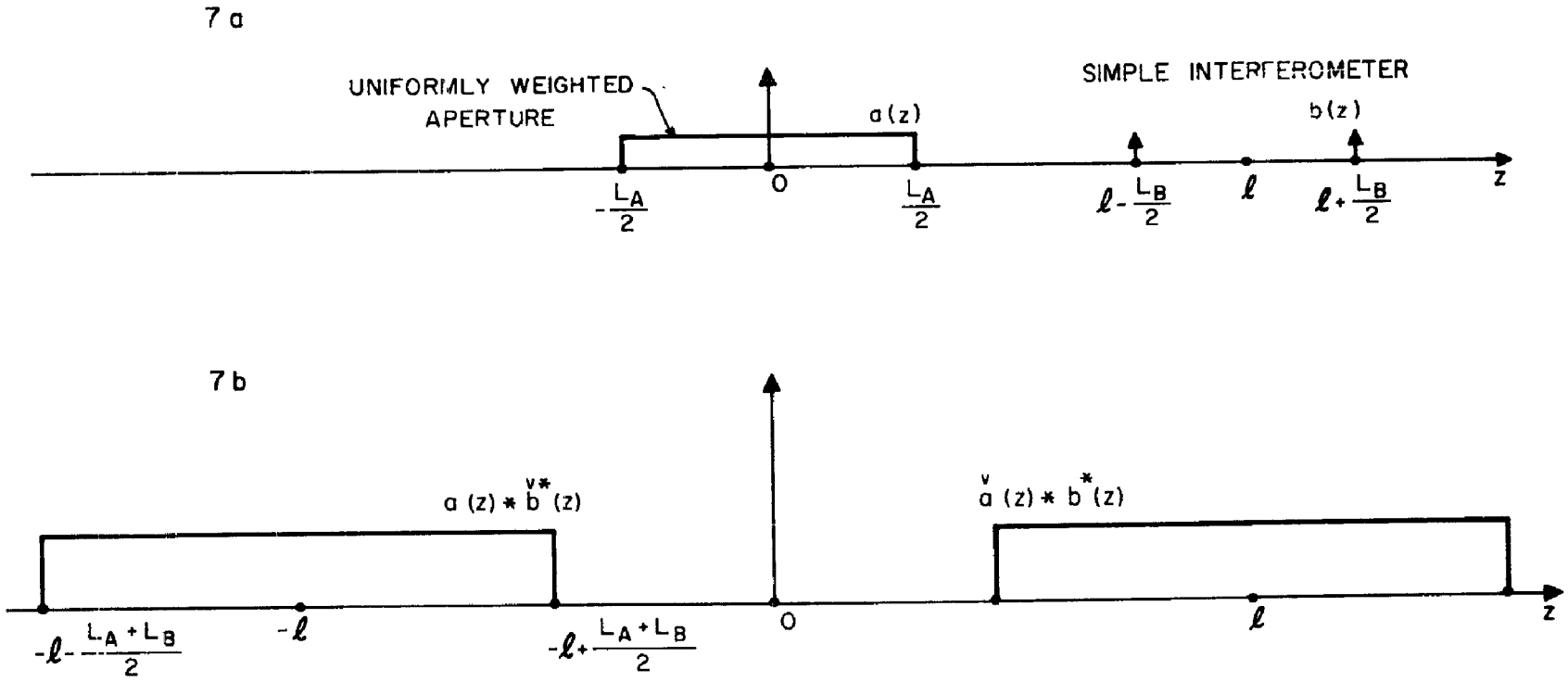

Figure 7. Aperture Distributions and Spacial Frequency Spectrum of the Compound Interferometer in the Presence of Incoherent Sources.

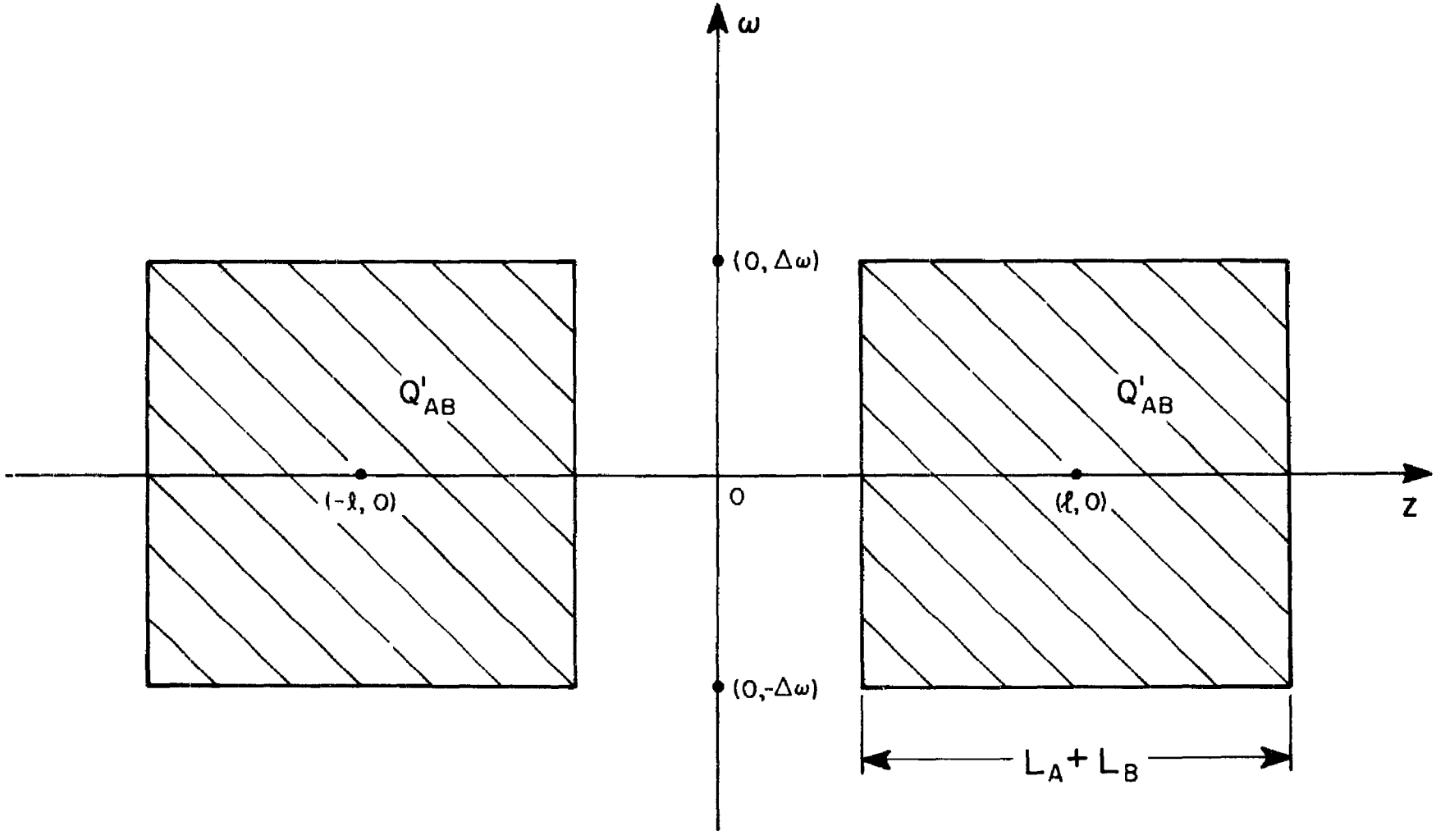

Figure 8. Spatio-Temporal Frequency Plane for the Case of an Incoherent Source Distribution with the Region Q'_{AB} Shown Hatched.

In summary, we can say that an incoherent source distribution has a principal solution spectrum which is a function only of the difference $z = x-y$ of the spatial frequency coordinates. Consequently, the problem reduces from three dimensions to two and by pointing both antenna patterns in the same direction ($u = v$) the system output also reduces to a function of two dimensions, delay τ, and beam direction u. A principal solution can be defined whose frequency spectrum is complex symmetric $\left(t(\omega, z) = t^*(-\omega, -z)\right)$, and for the above antenna system is identically zero for $|z-|\ell|| > \frac{L_A + L_B}{2}$ and $|\omega| < \Delta\omega$. Indeed, it was this type of principal solution which was first defined by Bracewell and Roberts[18] in connection with the mapping of the incoherent sources which are encountered in radio astronomy.

6. THE CORRELATION MATRIX OF THE ANTENNA SYSTEM

It will be recalled that in Section 4.4 we introduced the correlation matrix $R(\tau)$ which is associated with the complex envelopes, A(t) and B(t), of the narrow-band voltages a(t) and b(t). We will now show that for the two-antenna correlation system we can obtain a correlation matrix $R(\tau,u,v)$ which yields considerably more information about the source distribution than the original cross-correlation function $R_{AB}(\tau,u,v)$.

6.1 Cross-Correlation of Signals from Two Coincident Antennas

Let us consider one of the antennas, for example antenna A. If the signal from each of its elements is divided into two parts, with predetermined weighting coefficients, one obtains two sets of signals which can be combined additively to form two distinct output voltages from the antenna aperture. In effect they are the signals from two coincident antennas, A_1 and A_2, whose patterns can be independently scanned in the u and v directions respectively. These signals, after each has passed through an RF filter, can be cross-correlated in the same fashion as the signals from the distinct apertures A and B. The complex cross-correlation function that results is

$$R_{AA}(\tau,u,v) = T(\tau,u,v) * C_{AA}(\tau,u,v) \tag{130}$$

where

$$C_{AA}(\tau,u,v) = f_{A_1}(\tau) * \overset{\vee *}{f}_{A_2}(\tau)\ \overset{\vee}{A}_1(u)\ \overset{\vee *}{A}_2(v). \tag{131}$$

A similar cross-correlation function of two outputs from antenna B can be obtained and it is given by

$$R_{BB}(\tau,u,v) = T(\tau,u,v) * C_{BB}(\tau,u,v) \tag{132}$$

where

$$C_{BB}(\tau,u,v) = f_{B_1}(\tau) * \overset{\vee}{f}{}^{*}_{B_2}(\tau)\, B_1(u)\, B_2{}^{*}(v)\,. \tag{133}$$

6.2 The Correlation Matrix of the Two-Antenna System

By analogy with Equation (67) we can define the correlation matrix of the antenna system to be

$$R(\tau,u,v) = \begin{bmatrix} R_{AA}(\tau,u,v) & R_{AB}(\tau,u,v) \\ R_{BA}(\tau,u,v) & R_{BB}(\tau,u,v) \end{bmatrix}. \tag{134}$$

As before the cross-correlation function $R_{BA}(\tau,u,v)$ is related to $R_{AB}(\tau,u,v)$ by the formula

$$R_{BA}(\tau,u,v) = R_{AB}{}^{*}(-\tau,v,u)\,. \tag{135}$$

Now just as in the case of $R_{AB}(\tau,u,v)$, we can take the Fourier transform of this correlation matrix and we obtain

$$r(\omega,x,y) = \begin{bmatrix} r_{AA}(\omega,x,y) & r_{AB}(\omega,x,y) \\ r_{BA}(\omega,x,y) & r_{BB}(\omega,x,y) \end{bmatrix} \tag{136}$$

where

$$r_{AA}(\omega,x,y) = 4\pi^2\, t(\omega,x,y)\, F_{A_1}(\omega)\, F_{A_2}^{*}(\omega)\, a_1(x)\, a_2^{*}(y) \tag{137}$$

$$r_{BB}(\omega,x,y) = 4\pi^2 t(\omega,x,y)\, F_{B_1}(\omega)\, F_{B_2}^{*}(\omega)\, b_1(x)\, b_2^{*}(y) \tag{138}$$

$$r_{AB}(\omega,x,y) = 4\pi^2 t(\omega,x,y)\, F_{A}(\omega)\, F_{B}^{*}(\omega)\, a(x)\, b^{*}(y) \tag{139}$$

$$= r_{BA}^{*}(\omega,y,x). \tag{140}$$

Each of the elements of the frequency domain correlation matrix can be non-zero only where the corresponding system function, e.g., $F_{B_1}(\omega)F_{B_2}^{*}(\omega)b_1(x)b_2(y)$, is non-zero. Let us assume that the temporal frequency pass-bands are all equal in size. We can then turn our attention to the spatial frequency domain. Figure 9 shows the regions in the xy plane where the four distinct system functions are non-zero. Note that $\bar{Q}_{AB}$ is the "aperture" of the original cross-correlation system (see Figure 3). The three other regions, $\bar{Q}_{AA}$, $\bar{Q}_{BB}$, and $\bar{Q}_{BA}$, indicate the additional "apertures" of the system.

6.3 Principal Solution

By analogy with the principal solution for the original cross-correlation system given by Equation (114), we can define a principal solution

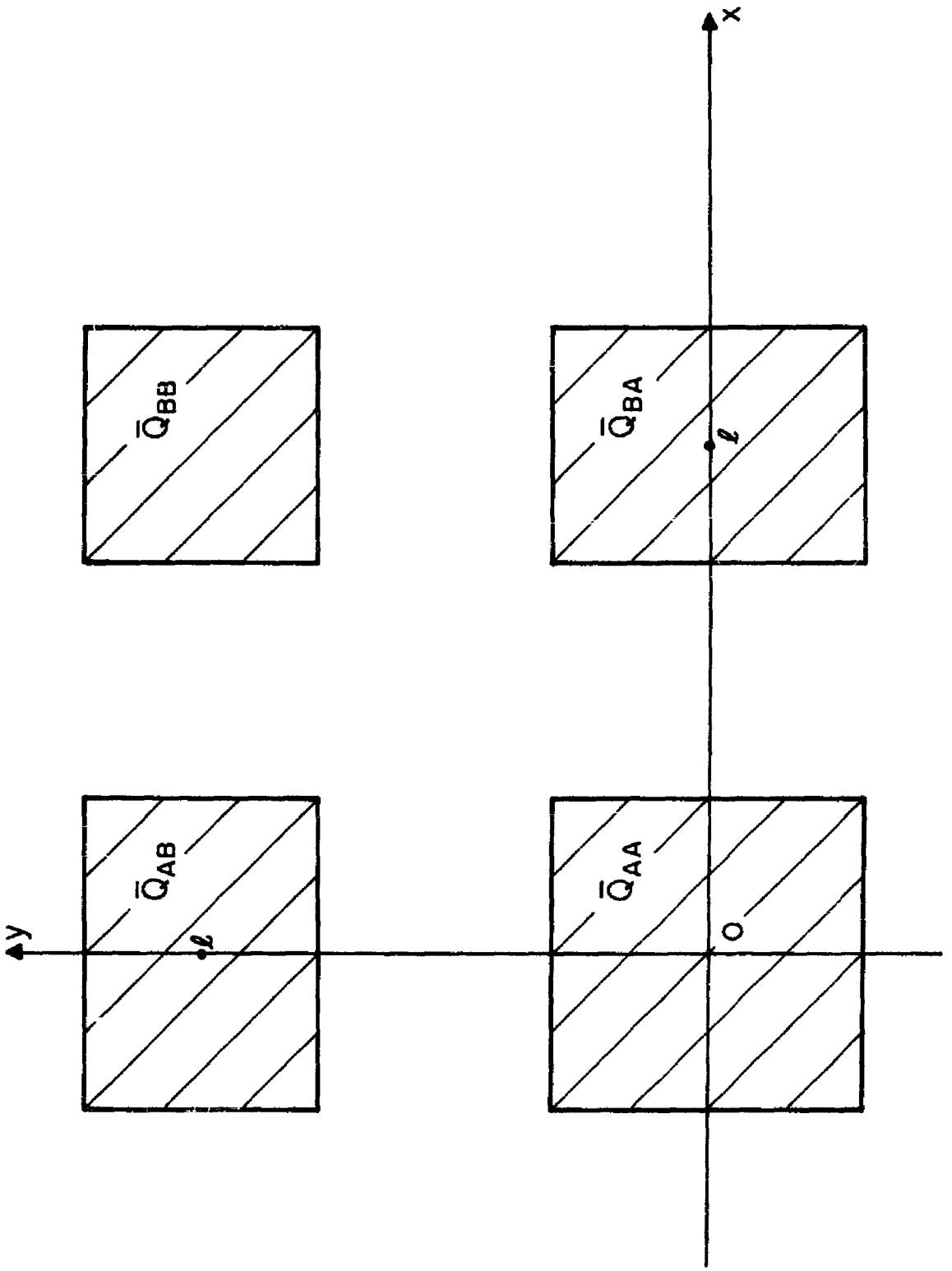

Figure 9. Spatial Frequency Plane on which the Cross-Correlation System's "Apertures" $\bar{Q}_{AA}$, $\bar{Q}_{AB}$, $\bar{Q}_{BA}$, and $\bar{Q}_{BB}$ are Shown Hatched.

for the correlation system as a whole to be the Fourier transform of

$$t_o(\omega,x,y) = t_{AA}(\omega,x,y) + t_{AB}(\omega,x,y)$$

$$+ t_{BA}(\omega,x,y) + t_{BB}(\omega,x,y) \tag{141}$$

where

$$t_{AA}(\omega,x,y) = \frac{r_{AA}(\omega,x,y)}{4\pi^2 F_{A_1}(\omega) F^*_{A_2}(\omega) a_1(x) a^*_2(y)} \quad , \quad \text{if } (\omega,x,y) \in Q_{AA},$$

$$= 0, \qquad \text{otherwise.} \tag{142}$$

Similar formulas obtain for $t_{AB}(\omega,x,y)$, $t_{BA}(\omega,x,y)$, and $t_{BB}(\omega,x,y)$. Thus

$$T_o(\tau,u,v) = \int_{-\infty}^{\infty}\int_{-\infty}^{\infty}\int_{-\infty}^{\infty} t_o(\omega,x,y)\, e^{\,j(\omega\tau - xu + yv)}\, d\omega dx dy \tag{143}$$

is the principal solution for the correlation system as a whole. Clearly this solution gives us much more information about the source distribution than does the cross-correlation system's principal solution as given by Equation (114).

The special cases of coherent and incoherent distributions give rise to the same type of outputs for this more general system as for the one described previously.

Finally, it should be noted that if the two apertures A and B are considered as parts of a single aperture C, and if two distinct signals from this larger aperture are cross-correlated, as described in Section 6.1, then the output from this system will have a spatial frequency "aperture" which is the same as that of the correlation matrix. Consequently, the principal solution for the aperture C is the same as the system solution given by Equation (143). Therefore, when mapping a source distribution, it is sufficient to obtain a cross-correlation function from the total available aperture. There is nothing available in the cross-correlation of signals from parts of an aperture that is not present in a cross-correlation of the signals from the entire aperture.

7. COMPARISON OF THE CROSS-CORRELATION AND THE CONVENTIONAL ANTENNA SYSTEM

In this chapter it will be shown that when the terminal voltage of a conventional linear antenna is square-law detected and time-averaged, the resulting output is just a special case of a cross-correlation antenna system. This means that a comparison of a linear and a cross-correlation system should be made between the square-law detected output of the former and the cross-correlated output of the latter system.

7.1 A Linear Antenna with Square-Law Detection

A diagram of a conventional linear antenna with a square-law detection system is shown in Figure 10. After being passed through the RF filter the antenna voltage can be written as

$$d(t,u) = D(t,u)\, e^{j\omega_o t} \tag{144}$$

where by analogy with Equations (96) and (97) of Chapter 5, we have

$$D(t,u) = V(t,u) * f_D(t) \overset{V}{D}(u) . \tag{145}$$

The antenna's pattern is D(u) and the filter response envelope is $f_D(t)$. This filtered signal is fed into a square-law device whose output is

$$d_{SL}(t,u) = \frac{1}{2} \mathrm{Re} \left\{ D^2(t,u)\, e^{j2\omega_o t} \right\} + \frac{1}{2} |D(t,u)|^2 . \tag{146}$$

This signal is then time-averaged. Since the double frequency component of the square-law detector output has a zero average we obtain

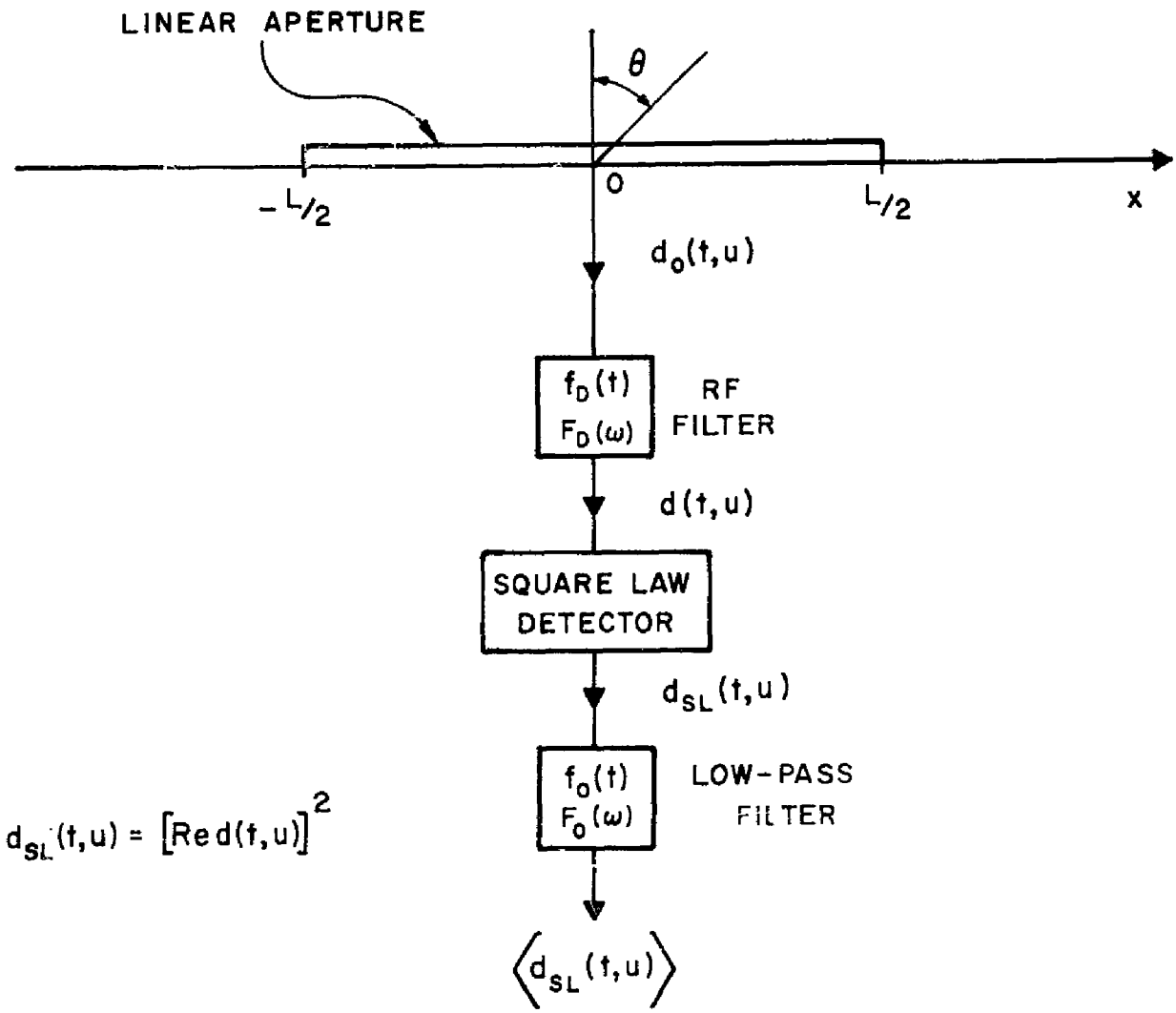

Figure 10. A Conventional Linear Antenna which Uses Square-Law Detection.

$$\left\langle d_{SL}(t,u) \right\rangle = \frac{1}{2} \left\langle |D(t,u)|^2 \right\rangle \quad . \tag{147}$$

Now it will be recalled that the cross-correlation's complex output is

$$R_{AB}(\tau,u,v) = \left\langle A(t,u)\, B^*(t-\tau,v) \right\rangle \quad . \tag{148}$$

Comparing these two results we see that except for the constant factor 1/2, the output from the square-law detection system is simply a degenerate case of the cross-correlator output which occurs when $A(t,u) = B(t,u) = D(t,u)$. It is half the Autocorrelation function of the signal from antenna D evaluated at $\tau = 0$.

$$2 \left\langle d_{SL}(t,u) \right\rangle = T(\tau,u,v) * f_{DD}(\tau)\, \overset{\vee}{D}(u)\, \overset{\vee}{D}^*(v) \Big|_{\substack{\tau=0 \\ u=v}} \tag{149}$$

where

$$f_{DD}(\tau) = f_D(\tau) * \overset{\vee}{f}_D^*(\tau) \tag{150}$$

7.2 Disadvantages of the Conventional System

Since the input to the square-law detector is the terminal voltage of only one antenna with only one scan parameter u, we see that when the source distribution is partially coherent, it is impossible to obtain the three-dimensional mapping of the mutual coherent function of the source distribution. As indicated by Equation (149) one can only

obtain the values of the antenna voltage's autocorrelation function along the single line, $\tau = 0$, $u = v$, whereas the cross-correlation system employing a single aperture yields the values of the filtered function for all points in the three-dimensional output space of the system.

In the case of incoherent sources the problem is not nearly as serious since even with the correlation system it is only the $u = v$ plane that is considered when the source distribution is scanned. (See Chapter 5, Section 7). Indeed the only difference in the space domain between the two outputs is that the power pattern of the conventional system is $|D(u)|^2$ and that of the cross-correlation system is $A(u)\,B^*(u)$ (compare Equations (103) and (149)). The latter pattern is clearly more flexible since it is the product of two distinct field strength patterns. It degenerates to the conventional power pattern when the two field strength patterns are identical, $(A(u) = B(u) = D(u))$.

7.3 Comparison of the Two Systems for The Case of Dolph-Chebyshev Array Synthesis

Let us first consider a conventional system whose antenna is in the form of a linear array. It was shown by Dolph[40] that the optimum array pattern is given by

$$D(\psi) = T_n(\psi) \tag{151}$$

where $\psi = \psi_o \cos(\beta \ell \sin\theta)$,

ℓ = element spacing,

θ = angle measured from the normal to the array,

$n+1$ = number of elements in the array,

$T_n(\psi)$ is the Chebyshev polynomial* of degree n.

The value of ψ_o is related to the sidelobe level ρ of the pattern by the formula

$$\rho = 20 \log_{10} T_n(\psi_o) . \tag{152}$$

The pattern is optimum in the sense that for a given array, of all patterns with an arbitrary sidelobe level ρ, the Chebyshev pattern has the narrowest beamwidth, or conversely, of all patterns with a given beamwidth it has the lowest sidelobes.

However, if the terminal voltage of such an optimum array is square-law detected, then the detector output for a point source in the direction ψ_s is proportional to

$$|D(\psi-\psi_s)|^2 = T_n^2(\psi-\psi_s) . \tag{153}$$

This output is a polynomial of degree 2n but is not the Chebyshev polynomial of that degree, $T_{2n}(\psi-\psi_s)$. Thus when the <u>power pattern</u> is considered the conventional Dolph-Chebyshev design is not optimum.

Let us now turn our attention to the cross-correlation system shown in Figure 11. The array is given the weighting coefficients necessary to produce the conventional field strength pattern $T_n(\psi)$. However, the center element of the array has its signal split into two parts; the first is given the amplitude $\frac{1}{2}\left(1 - \frac{1}{\sqrt{2}}\right)$ and the second the amplitude $\frac{1}{2}\left(1 + \frac{1}{\sqrt{2}}\right)$. The signals from the other n elements are combined in the

*For a discussion of the properties of these orthogonal functions, see Courant and Hilbert[30], pp. 88-90.

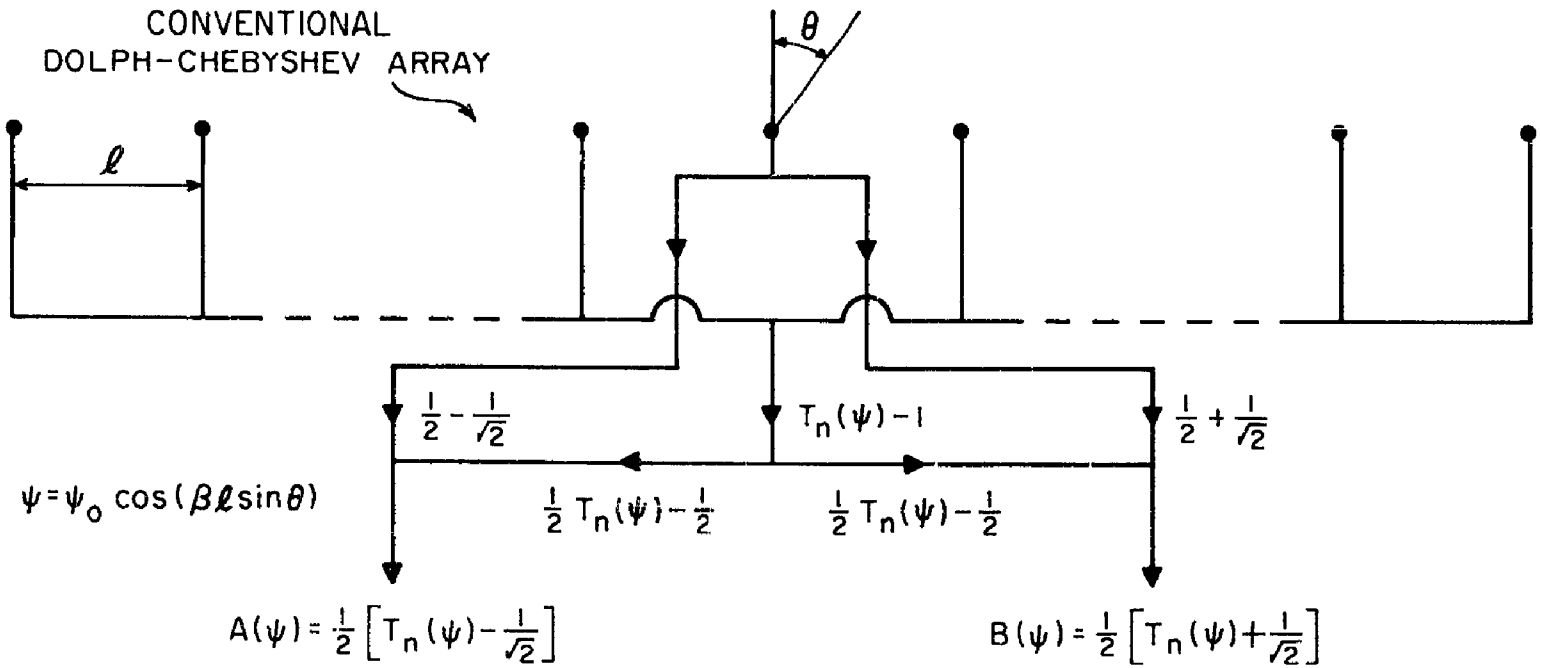

Figure 11. System Used to Obtain the Optimum Factor Patterns for the Dolph-Chebyshev Product Array.

usual way to form $T_n(\psi)$; however, since the central element's signal (normalized to 1) is missing we actually obtain $T_n(\psi) - 1$. This signal is split in two halves and to one half is added the first part of the center element's signal to form

$$A(\psi) = \frac{1}{2}\left(T_n(\psi) - \frac{1}{\sqrt{2}}\right) . \tag{154}$$

Likewise $B(\psi)$ is formed by adding the remaining two signals.

$$B(\psi) = \frac{1}{2}\left(T_n(\psi) + \frac{1}{\sqrt{2}}\right) . \tag{155}$$

Now if we note of the following identity

$$T_{2n}(\psi) = 2T_n^{\,2}(\psi) - 1 \quad , \tag{156}$$

and if the above pair of combined signals are cross-correlated with zero time delay it is easy to see that except for a constant factor we obtain the following product pattern

$$R(\psi) = A(\psi)\, B^*(\psi) = T_{2n}(\psi) \tag{157}$$

For the point source in the direction ψ_s we have

$$R(\psi) = T_{2n}(\psi - \psi_s) \tag{158}$$

as the system output. This method, due to Price[36], yields the desired

result. The system output is a Chebyshev polynomial of degree 2n and as such it has the lowest sidelobes of any possible pattern of the array when a certain beamwidth is specified. In particular, the improvement in the sidelobe level of this cross-correlation pattern over that of the conventional Dolph-Chebyshev pattern (i.e., Equation (153)) is shown in Figure 12. Both patterns have the same beamwidths measured to the first null and the element spacing is $\lambda/2$. The improvement, plotted as a function of the sidelobe level of the conventional pattern, is about 6 db but is slightly higher for small arrays and relatively high sidelobe levels.

It is worth remarking that the method of synthesizing the product pattern $T_{2n}(\psi)$, which we have just described, is not unique! To show this we note that we can write

$$T_{2n}(\psi) = 2^{2n-1} \prod_{k=1}^{2n} (\psi - \psi_k) \tag{159}$$

where ψ_k, the kth zero of the polynomial, is given by

$$\psi_k = \cos\left[\frac{2k-1}{4n}\pi\right], \quad k = 1, 2, \ldots, 2n. \tag{160}$$

The 2n zeros determine the polynomial. They can be arranged in two groups of n zeros in

$$W = \frac{1}{2}\frac{(2n)!}{(n!)^2} \tag{161}$$

ways.

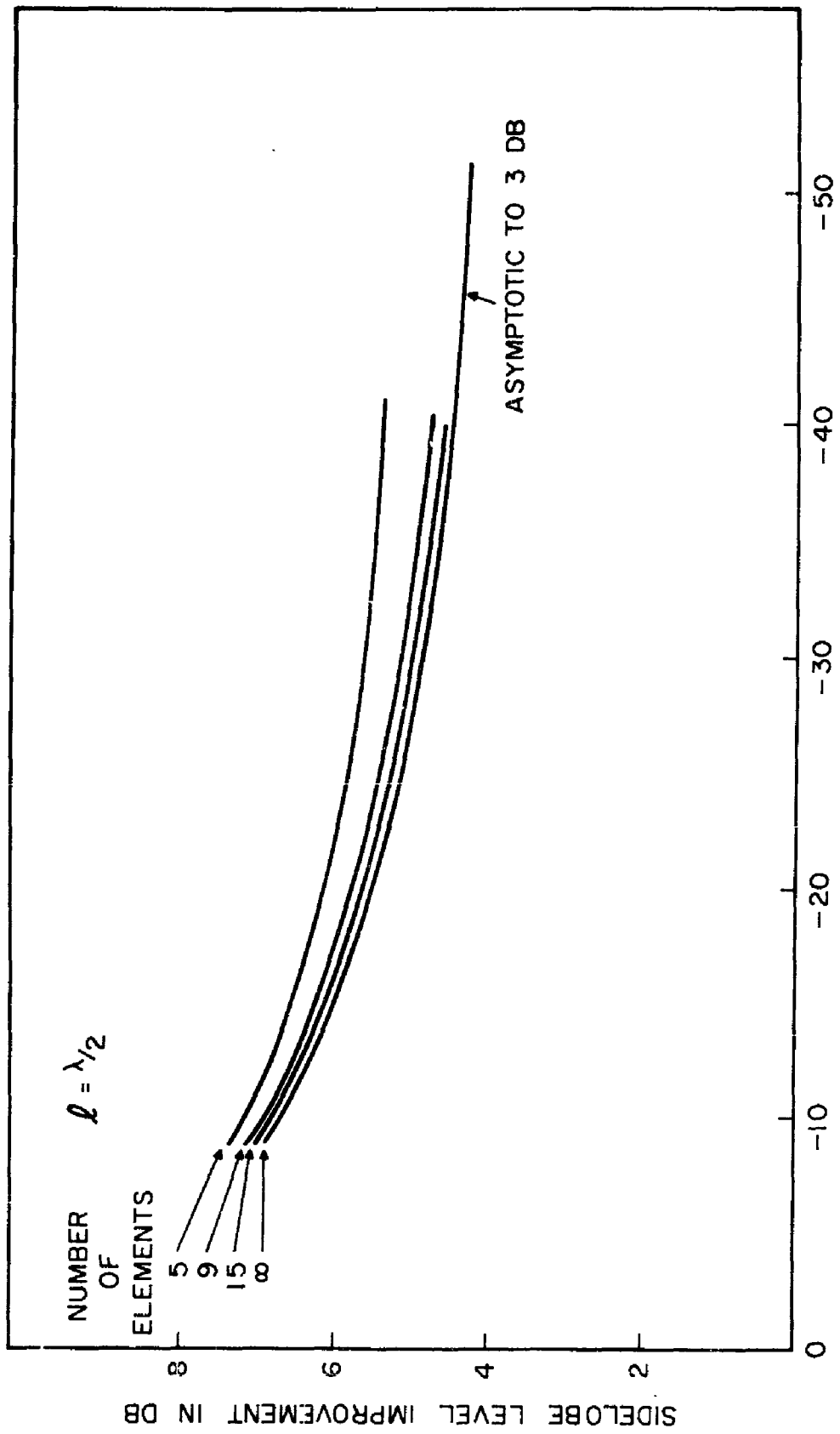

Figure 12. Sidelobe Level Improvement of the Dolph-Chebyshev Cross-Correlation Array Over the Conventional Array when Both Have the Same Beamwidths Measured to the First Null.

Since one group of n zeros will determine say $A(\psi)$, and the other will specify $B(\psi)$, we see that there are W possible ways to synthesize the product pattern $T_{2n}(\psi) = A(\psi)\, B^*(\psi)$. It is natural to ask if there is an optimum factorization of $T_{2n}(\psi)$, i.e., which of the W possible pairs of factor patterns $A(\psi)$ and $B(\psi)$ is best in some way.

If the system is being used to receive a signal from some known direction, and if there is a distribution of incoherent noise sources in addition to the signal, then the system output will be

$$R_{S+N}(\tau,\psi) = [S_o(\tau)\delta(\psi-\psi_s) + N(\tau,\psi)] * f_{AB}(\tau)\, A(\psi)\, B^*(\psi) \quad (162)$$

where $S_o(\tau)\ \delta(\psi-\psi_s)$ and $N(\tau,\psi)$ are the signal and noise coherence functions respectively. It is clear that it does not matter how the zeros of $T_{2n}(\psi)$ are shared between $A(\psi)$ and $B(\psi)$ since these patterns enter the output expression simply as the product $A(\psi)\, B^*(\psi) = T_{2n}(\psi)$. Consequently the W possible ways of producing the optimum product pattern are all equivalent when the sources are incoherent.

This is not the case for coherent and partially coherent sources, In particular, let us consider the case of a desired signal incident from the direction ψ_s and a coherent interfering signal from an arbitrary direction ψ_c. In practice this situation occurs when there are two distinct paths between a transmitting and a receiving antenna (multipath propagation). It has been shown elsewhere[51] that if the relative amplitudes of the desired and interfering signals are 1 and $Se^{j\xi}$ respectively (ξ is the relative phase), then the real system output, when $\tau = 0$ and both patterns are beamed in the ψ_s direction, is proportional to

$$\bar{R}'(0,\psi_s) = 1 + 2S \frac{A_o(\psi_s - \psi_c) + B_o(\psi_s - \psi_c)}{2} \cos \xi$$

$$+ S^2 A_o(\psi_s - \psi_c) B_o(\psi_s - \psi_c) \qquad (163)$$

where

$$A_o(\psi) = \frac{A(\psi)}{A(0)} , \quad B_o(\psi) = \frac{B(\psi)}{B(0)} , \qquad (164)$$

are the normalized, real, factor patterns of $T_{2n}(\psi)$. Notice that the second term in the above expression, which is due to the cross-product of the desired and interfering signals, is proportional to the sum of the two factor patterns. If the interfering signal is low level ($S \ll 1$), the interference rejection will depend on this sum pattern. Now if we select the factor patterns in the manner of Figure 11 then we have

$$\frac{1}{2}\left[A_o(\psi_s-\psi_c) + B_o(\psi_s-\psi_c)\right] = \frac{1}{2}\left[\frac{T_n(\psi_s-\psi_c) - \frac{1}{\sqrt{2}}}{T_n(0) - \frac{1}{\sqrt{2}}} + \frac{T_n(\psi_s-\psi_c) + \frac{1}{\sqrt{2}}}{T_n(0) + \frac{1}{\sqrt{2}}}\right] \qquad (165)$$

$$= \frac{T_n(\psi_s-\psi_c) - \frac{1}{2T_n(0)}}{T_n(0) - \frac{1}{2T_n(0)}} . \qquad (166)$$

If, as is usually the case, $T_n(0) \gg 1$, we can write the sum pattern to a good degree of approximation as

$$\frac{1}{2}\left[A_o(\psi_s-\psi_c) + B_o(\psi_s-\psi_c)\right] = \frac{T_n(\psi_s-\psi_c)}{T_n(0)} \qquad (167)$$

Consequently, the output is

$$\bar{R}'(0,\psi_s) = 1 + 2S\,\frac{T_n(\psi_s - \psi_c)}{T_n(0)}\,\cos\xi + S^2\,\frac{T_{2n}(\psi_s - \psi_c)}{T_{2n}(0)} \quad (168)$$

and we see that not only does the system reject the self-product of the interfering signal in the optimum Chebyshev fashion ($T_{2n}(\psi_s-\psi_c)$), but the cross-product of the two signals is also rejected in the optimum fashion ($T_n(\psi_s-\psi_c)$). This occurs only if the factor patterns $A(\psi)$ and $B(\psi)$ are given by Equations (154) and (155) respectively. In this sense, then, this factorization is the optimum one.

Finally we should note that since the pattern of any uniformly spaced linear array can be represented as a polynomial,[52] we can synthesize a product pattern of any form by simply determining the zeros of the pattern and distributing them equally between its two factor patterns.[37,51] The manner in which the distribution is made could be determined from considerations of interference rejection as in the Chebyshev case. The patterns of two coincident arrays of n+1 elements will each be a polynomial of degree n. Their product pattern will be a polynomial of degree 2n with 2n distinct zeros. On the other hand the power pattern of a conventional array of n+1 elements will also be a polynomial of degree 2n but will have only n distinct zeros. Consequently we can say that the product pattern has twice as many degrees of freedom as the conventional power pattern.

8. MULTIPLE CROSS-CORRELATION

Having studied in some detail the cross-correlation of the signals of two antennas we now will consider the effect of multiple cross-correlation of the signals from an arbitrary number of antennas. By now it is well-known that when used for mapping the temperature distribution of remote sources these systems are basically nonlinear.[20, 31] The output of a four-antenna system, for example, will contain cross-product terms due to sources in different directions even when their signals are mutually incoherent. The explanation for the failure of such systems is simple. The temperature distribution is a distribution of average power and as such, is determined by a second moment of the probability distribution of the field phasor V(t,u), i.e.,

$$T(\tau,u,v) = \iint V_{\tau,u}\ V^*_{t-\tau,v}\ p\left\{V_{t,u}, V^*_{t-\tau,v}\right\} dV_{t,u} dV^*_{t-\tau,v} \qquad (169)$$

where $p\,[V_{t,u}, V^*_{t-\tau,v}]$ is the joint probability distribution of the field from the source in the u direction at time t and the field from the source in the v direction at time $t-\tau$. To emphasize the fact that t, τ, u, and v are essentially parameters in the above integral, we have for example, let $V_{t,u}$ be the value of V(t,u) at time t and for the direction u. The integration, of course, is over all values of the complex amplitudes $V_{t,u}$ and $V^*_{t-\tau,v}$.

Now by going to a higher order of cross-correlation we are no longer dealing with second moments and hence by definition with temperature brightness. All temperature information about the distribution is contained in the mutual coherence function $T(\tau,u,v)$. The information in the higher order

correlations clearly concerns the higher order moments and hence can be used to specify the joint probability distribution of the sources, e.g., $p\left\{V_{t-\tau_1,u_1}, V^*_{t-\tau_2,u_2}, V_{t-\tau_3,u_3}, \ldots, V^*_{t-\tau_n,u_n}\right\}$. Conversely, if the probability distribution is known, all of the moments can be determined from it including the second or temperature moment. However, it will be shown in Section 8.3 that the higher order moments of a gaussian distribution are completely determined by the first and second moments.

8.1 A Multiple Cross-Correlation Antenna System

A diagram of the system, whereby the terminal voltages of N antennas are cross-correlated, is shown in Figure 13. In Appendix B a detailed analysis shows that the complex system output has an expected value of

$$R_{A_1A_2\ldots A_N}(\tau_1, \tau_2, \ldots, \tau_N, u_1, u_2, \ldots, u_N)$$

$$= T^{(N)}(\tau_1,\tau_2,\ldots\tau_N,..,u_1,u_2,..,u_n) * \overset{\vee}{f}_1(\tau_1)\ldots\overset{\vee *}{f}_2(\tau_2)\ \overset{\vee}{f}_3(\tau_3)\ \overset{\vee *}{f}_4(\tau_4)$$

$$\ldots\overset{\vee *}{f}_N(\tau_N)\ \overset{\vee}{A}_1(u_1)\ \overset{\vee *}{A}_2(u_2)\ \overset{\vee}{A}_3(u_3)\ \overset{\vee *}{A}_4(u_4)\ldots\ \overset{\vee *}{A}_N(u_N) \qquad (170)$$

where

$$T^{(N)}(\tau_1,\tau_2,\ldots,\tau_N, u_1, u_2\ldots,u_N) =$$

$$E\left\{V(t-\tau_1,u_1)\ V^*(t-\tau_2,u_2)\ V(t-\tau_3,u_3)\ldots\ldots V^*(t-\tau_N,u_N)\right\} \qquad (171)$$

with τ_k and u_k being the time delay and beam direction of the kth antenna whose pattern is $A_k(u)$ and filter response envelope is $f_k(t)$

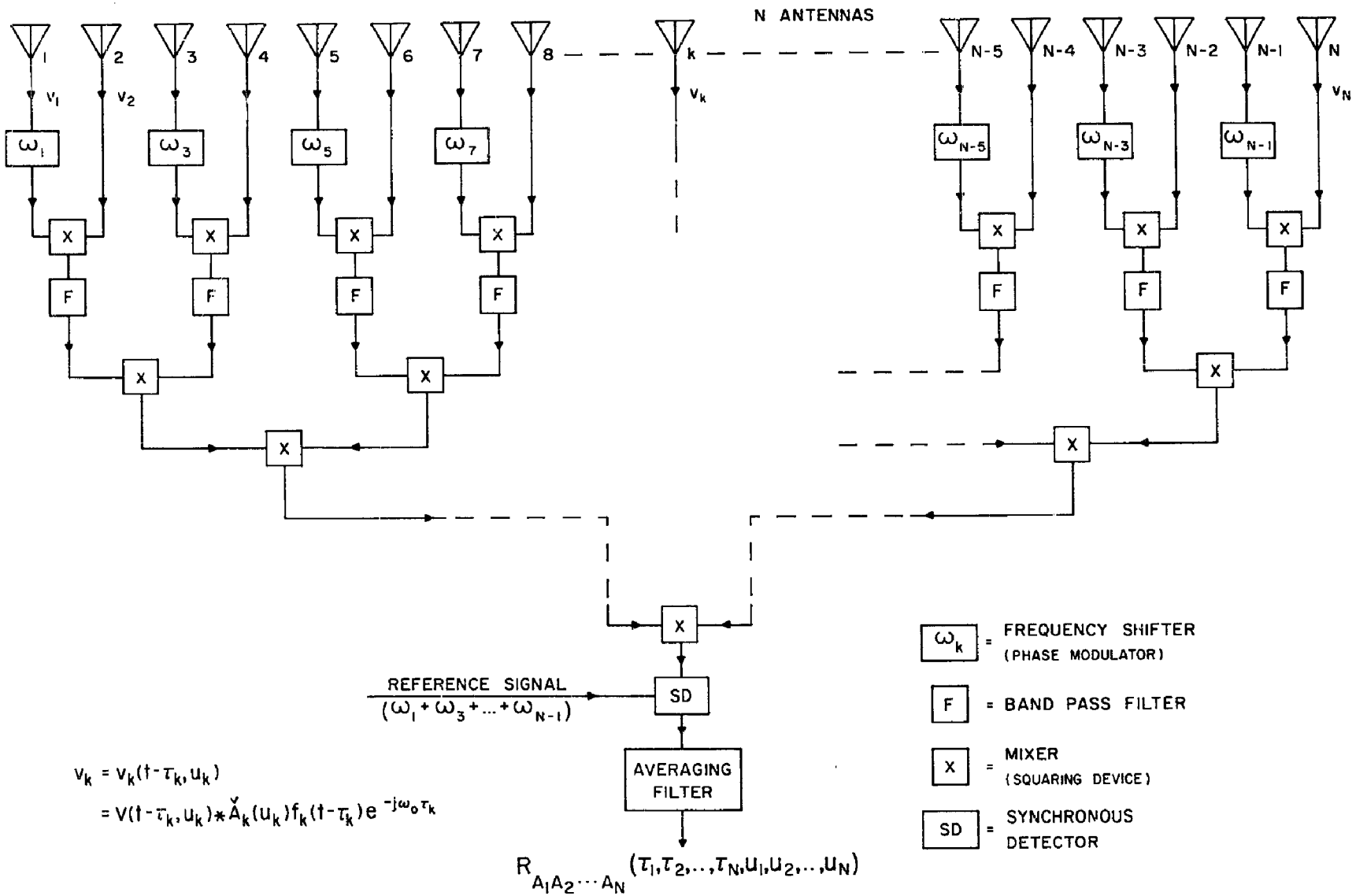

Figure 13. System for Cross-Correlating the Voltages of N Antennas.

It is clear from Equation (170) that a Fourier analysis of the output will be simply a generalization to 2N dimensions of the analysis for the case of a single cross-correlation. Thus the system output spectrum is

$$r_{A_1A_2\ldots\ldots A_N}(\omega_1, \omega_2, \ldots, \omega_N, x_1, x_2, \ldots, x_N)$$

$$= (2\pi)^N \, t^{(N)}(\omega_1,\omega_2,..,\omega_N, x_1,..,x_N) \, a_1(x_1) \, a_2^*(x_2) \, a_3(x_3)\ldots.$$

$$\ldots\ldots a_N^*(x_N) \, \overset{\vee}{F}_1(\omega_1) \, \overset{\vee *}{F}_2(\omega_2)\ldots\ldots \overset{\vee *}{F}_N(\omega_N) \qquad (172)$$

where

$$r_{A_1\ldots A_N}(\omega_1,\omega_2,\ldots,\omega_N, x_1,\ldots, x_N), \; t^{(N)}(\omega_1,\omega_2,\ldots, \omega_N,x_1,.., x_N),$$

$a_k(x_k)$, and $F_k(\omega_k)$, are the inverse Fourier transforms of

$$R_{A_1\ldots A_n}(\tau_1,\tau_2,\ldots,\tau_N, u_1,\ldots, u_N), \; T^{(N)}(\tau_1\tau_2,\ldots,\tau_N,u_1,u_2,..,u_N),$$

$A_k(u_k)$, and $f_k(\tau)$,

respectively.

Letting $Q_{12\ldots N}$ be the support of the system function $a_1(x_1) \, a_2^*(x_2)\ldots. a_N^*(x_N) \, \overset{\vee}{F}_1(\omega_1) \, \overset{\vee *}{F}_2(\omega_2)\ldots\ldots\ldots \overset{\vee *}{F}_N(\omega_N)$, we define the principal solution for the Nth order correlation system as the Fourier transform of

$$t^{(N)}_{A_1\ldots A_N}(\omega_1,\ldots,\omega_N,x_1,\ldots,x_N) = \frac{r_{A_1\ldots A_N}(\omega_1,\ldots,\omega_N,x_1,\ldots,x_N)}{(2\pi)^N F_1(\omega_1)\ldots F_N^*(\omega_N)a_1(x_1)\ldots a_N^*(x_N)},$$

$$\text{if } (\omega_1\ldots,\omega_N,x_1,\ldots,x_N)\in Q_{123\ldots N}, \tag{173}$$

$$= 0, \quad \text{otherwise}.$$

Thus the principal solution is

$$T^{(N)}_{A_1\ldots A_N}(\tau_1,\tau_2,\ldots,\tau_N,u_1,u_2,\ldots,u_N) =$$

$$\frac{1}{(2\pi)^N}\int_{-\infty}^{\infty}\int_{-\infty}^{\infty}\cdots\int_{-\infty}^{\infty} t^{(N)}_{A_1\ldots A_N}(\omega_1,\omega_2,\ldots,\omega_N,x_1,x_2,\ldots,x_N)$$

$$e^{j(\omega_1\tau_1-\omega_2\tau_2+\ldots-\omega_N\tau_N-x_1u_1+x_2u_2-x_3u_3+\ldots+x_Nu_N)}$$

$$d\omega_1\ldots d\omega_N dx_1\ldots dx_N \tag{174}$$

which is a filtered version of the following Nth moment of the joint probability distribution

$$T^{(N)}(\tau_1,\tau_2,\ldots,\tau_N,u_1,u_2,\ldots,u_N) = \int_{-\infty}^{\infty}\int_{-\infty}^{\infty}\cdots\int_{-\infty}^{\infty} V_{\tau_1,u_1}V^*_{\tau_2,u_2}V_{\tau_3,u_3}\ldots V^*_{\tau_N,u_N}$$

$$p\left(V_{\tau_1,u_1},V^*_{\tau_2,u_2},V_{\tau_3,u_3},\ldots,V^*_{\tau_N,u_N}\right)dV_{\tau_1,u_1}dV^*_{\tau_2,u_2}\ldots\ldots dV^*_{\tau_N,u_N}. \tag{175}$$

Note that for N even, $\tau_1 = \tau_2 = \tau_3 = \ldots = \tau_N = 0$ and $u_1 = u_2 = u_3 = \ldots\ldots = u_N = u$ we get

$$T^{(N)}(0,0,\ldots,0,u,u,\ldots.u) = E\left\{\left|V_{t,u}\right|^N\right\} = \int \left|V_{t,u}\right|^N p\left\{V_{t,u}\right\} dV_{t,u} \tag{176}$$

which is the Nth moment of the probability distribution of the source in the u direction.

It should be remarked that for the above results we have tacitly assumed that N was even. If N is odd the output in most practical cases will be zero since most sources have even probability distributions (e.g., gaussian). However, more general distributions are possible and their odd moments can be measured by using an odd number of antennas. In Appendix B we give the modification of the correlation system that will perform a correlation of an odd number of signals.

8.2 Generalized Correlation Matrix

Just as it was shown in Chapter 6 that a cross-correlation of the voltages of two antennas yields only a part of the available information from the system, so in the generalized case it can be shown that the multiple correlation output $R_{A_1\ldots A_N}(\tau_1,\tau_2,\ldots,\tau_N,u_1,u_2,\ldots,u_N)$ is only one of N^N possible outputs, all of which are distinct functions of the delay and scan variables. For example, we could form N distinct outputs from a single antenna and obtain an N-dimensional cross-correlation just as we obtained a two-dimensional cross-correlation of the signals from antenna A, (see Chapter 6). By analogy with that output we could let $R_{A_1A_1\ldots A_1}(\tau_1,\ldots,\tau_N,u_1,\ldots,u_N)$ be its N-dimensional counterpart. The 2 x 2

correlation matrix will also have counterpart and the typical element of this generalized correlation "matrix" is

$$R_{A_k A_\ell A_m \cdots A_q}(\tau_1,\tau_2,\ldots,\tau_N,u_1,u_2,\ldots,u_N) =$$

$$T^{(N)}(\tau_1,\tau_2,\ldots,\tau_N,u_1,\ldots,u_N) * \overset{\vee}{f}_k(\tau_1)\ \overset{\vee *}{f}_\ell(\tau_2)\ \overset{\vee}{f}_m(\tau_3)\ldots.$$

$$\ldots\ldots\overset{\vee *}{f}_q(\tau_N)\ \overset{\vee}{A}_k(u_1)\ \overset{\vee *}{A}_\ell(u_2)\ \overset{\vee}{A}_m(u_3)\ \ldots\ldots\overset{\vee *}{A}_q(u_N) \qquad (177)$$

where each of the N indices, k, ℓ, m,..., q, assume values from 1 to N.

Each element, $R_{A_k A_\ell \ldots\ldots A_q}(\tau_1,\tau_2,\ldots,\tau_N,u_1,\ldots,u_N)$, of the generalized correlation matrix has a principal solution, $T^{(N)}_{A_k \ldots A_q}(\tau_1,\ldots,u_N)$, associated with it. We define the principal solution of the Nth order correlation system as a whole to be the sum of these N^N principal solutions, i.e.,

$$T_o^{(N)}(\tau_1,\tau_2,\ldots,\tau_N,u_1,\ldots,u_N) =$$

$$\sum_{k=\ell}^{N}\ \sum_{\ell=1}^{N}\ \ldots\ldots\ \sum_{q=1}^{N} T^{(N)}_{A_k A_\ell \ldots A_q}(\tau_1,\ldots,\tau_N,\ u_1,\ldots,u_N) \qquad (178)$$

where

$$T^{(N)}_{A_k A_\ell \ldots\ldots A_q}(\tau_1,\tau_2,\ldots,\tau_N,u_1,u_2,\ldots,u_N)$$

is the Fourier transform of

$$t^{(N)}_{A_k A_\ell \ldots A_q}(\omega_1,\ldots,\omega_N,x_1\ldots,x_N) = \frac{r_{A_k A_\ell \ldots A_q}(\omega_1,\ldots,\omega_N,x_1,\ldots,x_N)}{(2\pi)^N \overset{\vee}{F}_k(\omega_1)\ldots\overset{\vee *}{F}_q(\omega_N)a_k(x_1)\ldots a^*_q(x_N)}$$

$$\text{if } (\omega_1,\ldots,x_N) \in Q_{k\ell\ldots q},$$

$$= 0, \quad \text{otherwise,} \tag{179}$$

and $r_{A_k\ldots A_q}(\omega_1,\ldots,x_N)$ is the inverse Fourier transform of the output cross-correlation function $R_{A_k\ldots A_q}(\tau_1,\ldots,u_N)$.

8.3 Sources with Gaussian Statistics

If the sources have a gaussian joint probability distribution with zero means it can be shown[54] that

$$E\left\{V(t-\tau_1,u_1)\ V^*(t-\tau_2,u_2)\ V(t-\tau_3,u_3)\ldots V^*(t-\tau_N,u_N)\right\}$$

$$= \sum_{\text{a.d.p.}} \prod_{\substack{i=1 \\ \neq j}}^{N/2} E\left\{V'(t-\tau_i,u_i)\ V'(t-\tau_j,u_j)\right\}, \text{ if N is even,}$$

$$= 0, \text{ if N is odd,} \tag{180}$$

where a.d.p. means all distinct pairs and

$$V'(t-\tau_i,u_i) = V(t-\tau_i,u_i), \text{for i odd,}$$

$$= V^*(t-\tau_i,u_i), \text{for i even} \tag{181}$$

Thus the higher order moments of a gaussian distribution are all expressible in terms of the sum of products of second order moments. For example if N = 4 we can write

$$E\left\{ V(t-\tau_1,u_1)\ \ V^*(t-\tau_2,u_2)\ \ V(t-\tau_3,u_3)\ V^*(t-\tau_4,u_4)\right\}$$

$$= \ T(\tau_2-\tau_1,\ u_1,\ u_2)\ T\ (\tau_4-\tau_3,\ u_3,\ u_4)$$

$$+\ T(\tau_4-\tau_1,\ u_1,\ u_4)\ T\ (\tau_2-\tau_3,\ u_3,\ u_2)$$

$$+\ T'(-\tau_1+\tau_3,\ u_1,\ u_3)\ T'(-\tau_2+\tau_4,\ u_2,\ u_4) \qquad (182)$$

where $T(\tau,u,v)$ is given by Equation (19) and

$$T'\ (\tau,u,v) = E\left\{V(t,\ u)\ V\ (t-\tau,v)\right\}\ . \qquad (183)$$

If the complex signals have zero-mean statistically independent real and imaginary components and the covariances of the components are the same, then $T'(\tau,u,v) = 0$. Such signals represent circular complex gaussian processes[47].

This result is simply a generalization of the well-known fact that if the mean and variance (first and second moments) of a gaussian random variable are known, then all higher moments can be deduced from them*. We can infer that if such is the case no further information about the source distribution is available in the higher order correlations. Consequently, if we knew a priori that the sources had gaussian statistics a single cross-correlation of the signals would be sufficient.

*See, for example, Davenport and Root[13], pp. 146-147.

Conversely, if the measured higher order correlations are related to the measured second order correlations in the manner indicated by Equation (180), then one can infer that the source distribution has gaussian statistics.

9. THE APPLICATION OF CROSS-CORRELATION ANTENNA SYSTEMS TO RADAR

In this chapter it will be shown that antenna cross-correlation techniques can be used to advantage in radar systems. In the radar case, since one is both transmitting and receiving signals, it is possible to use two antennas for transmitting as well as two for receiving, four antennas in all. To distinguish the two transmitted signals, one is shifted in frequency by the amount ω_1, with $\omega_1 \ll\ll \omega_o$. The receiving antenna system is designed to respond only to the cross-product of these two signals which return after striking the targets.

Such a cross-correlation radar system has distinct advantages over the conventional system. It will be shown that the directivity for a given side lobe level can be increased by extending the Dolph-Chebyshev synthesis technique to the composite pattern of the four antennas. Furthermore, since the system is designed to respond to the cross-product of the two returning signals, it will be shown that the effect of remote active noise sources is virtually eliminated in the time-averaged system output.

9.1 The Cross-Correlation Radar System

A diagram of the system is shown in Figure 14. There are four antennas, two of which are used for transmitting (A_1 and A_2), and two of which are used for receiving, (B_1 and B_2). The pulsed transmitter signal is split in two equal parts and that part which is fed to antenna A_2 is tagged with an additional frequency ω_1, i.e., the carrier frequency is shifted from ω_o to $\omega_o + \omega_1$, with $\omega_o \gg\gg \omega_1$. This distinguishes the two signals which are transmitted by the antennas.

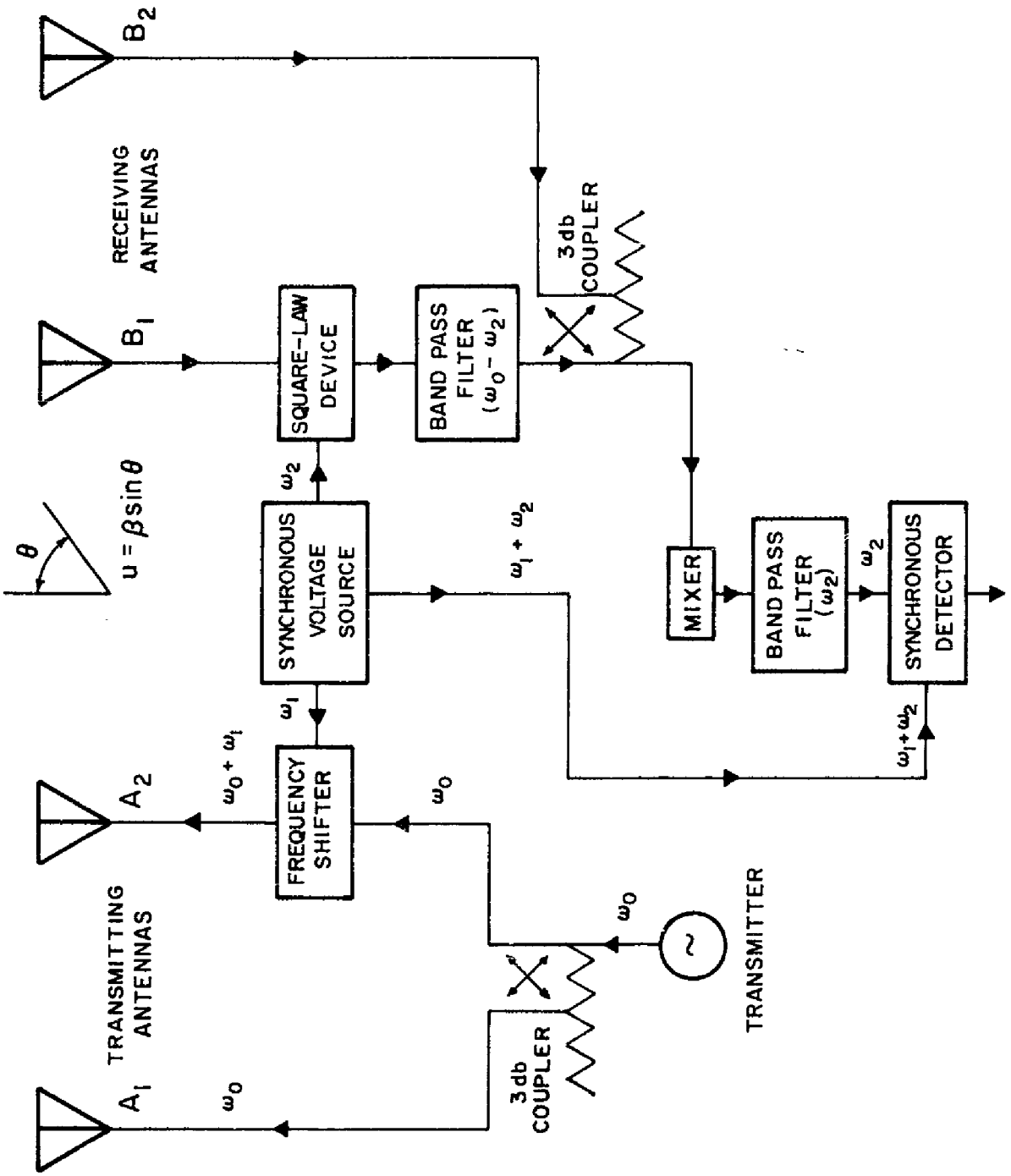

Figure 14. Cross-Correlation Radar System.

After striking the target (or targets) the signals return and are received by the other pair of antennas, B_1 and B_2. In practice of course the four antennas need not be physically separated. One could use four coincident antennas which share the same aperture (see Section 9.2). The cross-correlation of the terminal voltages of these antennas is, in principle, the same as with any correlation system, except that the various filters used must be wide-band in order to pass the video pulses of the radar.* A detailed analysis of the processing is given in Appendix C.

The system output in the radar case is usually displayed on an oscilloscope. Thus, a saw-tooth wave, synchronized with the pulse repetition rate, is used to produce a repeating image on the 'scope. The abscissa of the display is usually the range coordinate s, while the vertical deflection, at each s, is proportional to the system output and hence to the strength of the return from the target at that range. In the appendix it is shown that for a target at the range r and in direction v, the average deflection on the 'scope, as a function of antenna beam direction u and range coordinate s, is

---

*For simplicity of analysis we have assumed in what follows that the filters' frequency characteristics are uniform in the band $|\omega-\omega_o| < \Delta\omega$. We also have tacitly assumed the case of $\tau = 0$.

$$R(s,u) = P_o(s-r) \left\{ A_1(v-u)B_1(v-u)A_2^*(v-u)B_2^*(v-u)e^{j2\omega_1 r/c} \right\} \qquad (184)$$

where

$$P_o(s) = | P(2 s/c)|^2 \qquad (185)$$

is equal to the absolute square of the video pulse, $P(2s/c)$, and $A_1(u)$, $A_2(u)$, $B_1(u)$, and $B_2(u)$ are the field strength patterns of the four antennas.

The phase factor $e^{j2\omega_1 r/c}$ depends on the target distance, but for all targets within the maximum practical range r_{max}, one can choose ω_1 low enough so that this factor is almost unity. Consequently, we can rewrite Equation (184), to a good degree of approximation, as

$$R(s,u) = P_o(s-r) \left\{ A_1(v-u)B_1(v-u)A_2^*(v-u)B_2^*(v-u) \right\} . \qquad (186)$$

Now with a conventional radar system, where quite often the signals are transmitted and received on the same antenna*, the analogous output is

$$D(s,u) = P_o(s-r) \; | \; D(v-u) \; |^4 \qquad (187)$$

*A duplexer is used to isolate the transmitted and received pulses.

where D(u) is the antenna's field strength pattern and we have assumed that square-law detection is used. Comparing Equations (186) and (187) we see that mathematically, the latter is just a degenerate case of the former which occurs when

$$A_1(u) = A_2(u) = B_1(u) = B_2(u) = D(u). \tag{188}$$

Clearly the cross-correlation system is preferrable since its four distinct patterns can be specified independently; in a sense, this system has four times as many "degrees of freedom" as the conventional one. We will now consider the implications of this in the design of optimum Dolph-Chebyshev systems.

9.2 Optimum Dolph-Chebyshev Design

We recall from Section 7.3 that the pattern of an optimum Dolph-Chebyshev array is given by Equation (151) shown below

$$D(\psi) = T_n(\psi).$$

However, when such an array is used for radar, the system output is proportional to

$$D(s,\psi) = P_o(s-r)\ T_n^4\ (\psi_o-\psi) \tag{189}$$

where, by analogy with Equation (187), we have assumed a point target at

range r and in the direction ψ_o. As a function of $\psi_o - \psi$ the system output is a polynomial of degree 4n but is not the desired Chebyshev polynomial of that degree, $T_{4n}(\psi_o - \psi)$.

Now let us consider the special case of the cross-correlation radar system when the four antennas A_1, A_2, B_1, and B_2 are in the form of coincident linear arrays. This is indicated in Figure 15 where an aperture weighting network is shown which takes the signals to and from the elements of the array and combines them in a predetermined way to produce the four distinct patterns $A_1(\psi)$, $A_2(\psi)$, $B_1(\psi)$, and $B_2(\psi)$. In particular, if we let

$$
\begin{aligned}
A_1(\psi) &= T_n(\psi) + \left(\frac{1}{2} + \frac{1}{2\sqrt{2}}\right)^{\frac{1}{2}} \\
A_2(\psi) &= T_n(\psi) + \left(\frac{1}{2} - \frac{1}{2\sqrt{2}}\right)^{\frac{1}{2}} \\
B_1(\psi) &= T_n(\psi) - \left(\frac{1}{2} + \frac{1}{2\sqrt{2}}\right)^{\frac{1}{2}} \\
B_2(\psi) &= T_n(\psi) - \left(\frac{1}{2} - \frac{1}{2\sqrt{2}}\right)^{\frac{1}{2}}
\end{aligned}
\tag{190}
$$

then, except for a constant factor, we can show that the correlation system output is

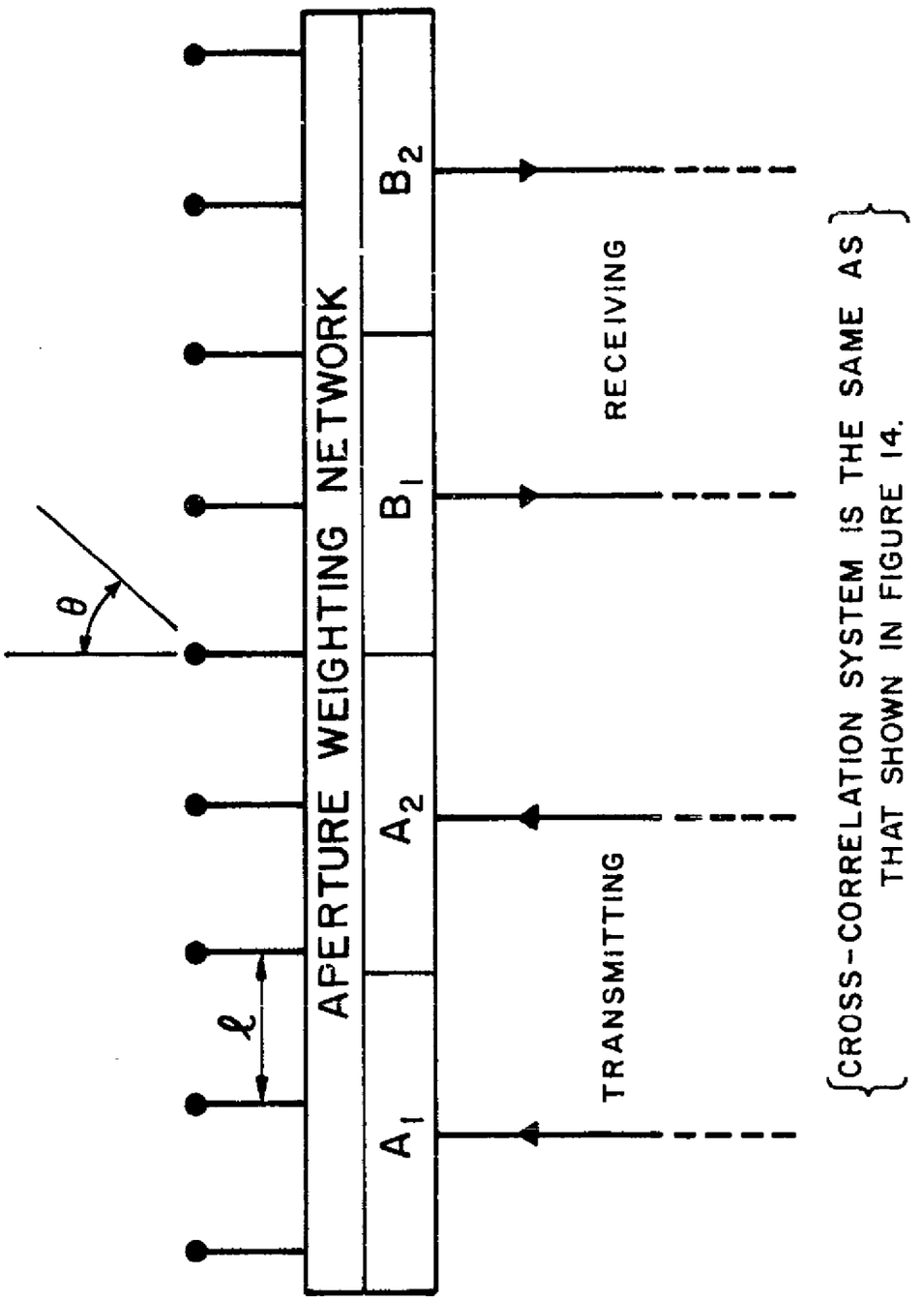

Figure 15. The Aperture Weighting Network Associated with the Four Coincident Radar Arrays.

$$R(s,\psi) = P_o(s-r)\ T_{4n}(\psi_o - \psi)\ . \tag{191}$$

This is the desired output since the system's over-all pattern is given by the Chebyshev polynomial of degree 4n.

A quantitative analysis of the sidelobe level of this pattern and of that of the conventional case, as given in Equation (189), shows that if both have the same beamwidth measured to the first null, then for large arrays (e.g., $\ell = \frac{\lambda}{2}$,, $n > 9$), the cross-correlation pattern's sidelobe level is about 7 or 8 db lower than that of the conventional pattern. This is shown in Figure 16 where the sidelobe level improvement in db is plotted as a function of the conventional pattern's sidelobe level, also in db. The second curve, indicated by "Mattingly System", is the improvement obtained when two distinct antennas are used, one for transmitting and one for receiving. If the two patterns are given by

$$A(\psi) = T_n(\psi) - \frac{1}{\sqrt{2}} \tag{192}$$

$$B(\psi) = T_n\ \psi + \frac{1}{\sqrt{2}} \tag{193}$$

then the system output, corresponding to Equations (189) and (191), is

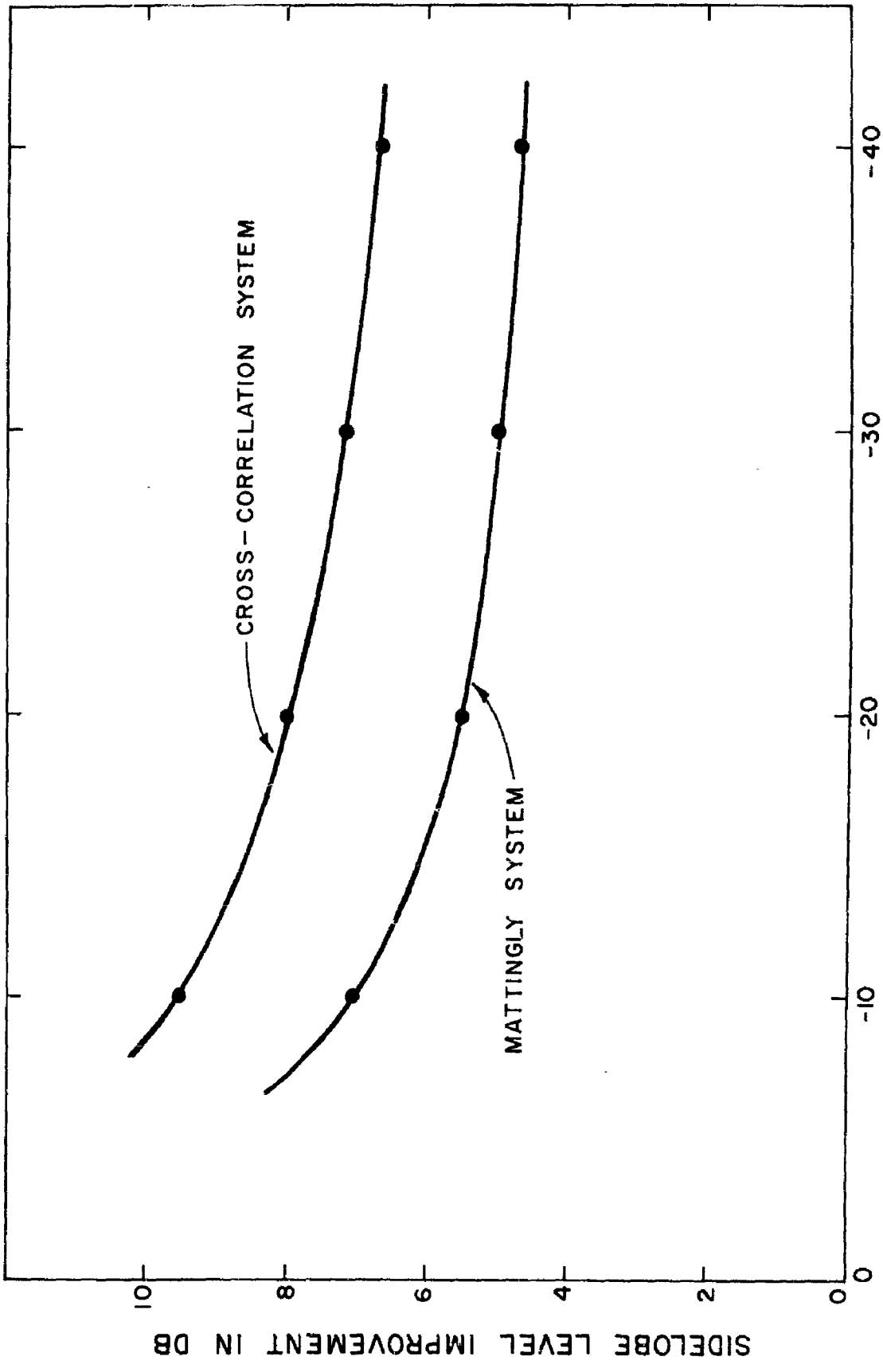

Figure 16. Sidelobe Level Improvement of the Mattingly and Cross-Correlation Radar Patterns as a Function of the Conventional Dolph-Chebyshev Sidelobe Level.

$$R_M(s,\psi) = P_o(s-r)\ T_{2n}^2(\psi_o - \psi) \qquad (194)$$

and the pattern is better than that of the conventional system in that its sidelobes are lower by about 5 or 6 db as indicated in Figure 16. This system was first proposed by R. L. Mattingly in 1960[53].

It can be concluded that the conventional radar antenna system employing a Dolph-Chebyshev design is inadequate due to the multiplicative effect of the transmitting and receiving patterns and of the square-law detection. Thus, instead of the optimum Chebyshev polynomial $T_{4n}(\psi)$, one obtains $T_n^4(\psi)$. It was shown that by properly selecting the four individual patterns of the cross-correlation system, (Equation (190)), one can synthesize the over-all pattern $T_{4n}(\psi)$ which of course is optimum in the sense mentioned above.

9.3 Noise Suppression

Since the transmitted and hence the received signals are in the form of two distinct pulse trains whose carrier frequencies differ by the fixed amount ω_1, the receiving section of the system has been designed to respond to the cross-product of these signals (it therefore is a true cross-correlation system).

On the other hand, given a background distribution of active noise sources, the random noise due to this distribution, which is incident on the receiving antennas, will in general not have such a dual nature. The noise distribution can be given mathematically by $N(t_i u)$ which gives the field at the origin of the antenna coordinate system at time t due to the

noise source in the direction u. The terminal voltages of the two antennas, due to the noise, can be written as $N_{B_1}(t)$ and $N_{B_2}(t)$ where

$$N_{B_k}(t) = \int_{-\beta}^{\beta} N(t,u)\, B_k(u)\,du \tag{195}$$

for k = 1, 2.

Since the noise and signals are uncorrelated, the time-averaged effect of cross-products of noise and signals in the cross-correlator output will reduce to zero. In Appendix C it is shown that the "self-product" of the noise in the output can be written as

$$n_o(t) = N_{B_1}(t)\, N^*_{B_2}(t)\, e^{-j\omega_1 t} . \tag{196}$$

The average value of $n_o(t)$ sampled at $t = \frac{2s}{c} + k\,\tau_o$ for N samples is

$$n_{o,N}(s) = \left\{ \frac{1}{N} \sum_{k=0}^{N-1} N_{B_1}\left(\frac{2s}{c} + k\,\tau_o\right) N^*_{B_2}\left(\frac{2s}{c} + k\,\tau_o\right) e^{-j\omega_1\left(\frac{2s}{c}+k\tau_o\right)} \right\} \tag{197}$$

where we have changed variables from time t to range s, with $t = \frac{2s}{c}$. This is proportional to the average vertical deflection of the oscilloscope

at range s and in the appendix it is shown that the expected value of this deflection is

$$E\left\{n_{o,N}(s)\right\} = \left\{N_{B_1B_2} \quad \frac{\sin N\omega_1\tau_o}{N \sin \omega_1\tau_o} \; e^{-j\omega_1(\frac{2s}{c} + \frac{N-1}{2}\tau_o)}\right\} \tag{198}$$

where

$$N_{B_1B_2} = E\left\{N_{B_1}(\frac{2s}{c} + k\,\tau_o)\; N^*_{B_2}\;(\frac{2s}{c} + k\,\tau_o)\right\} . \tag{199}$$

But

$$\left|E\left\{n_{o,N}(s)\right\}\right| \leq |\, N_{B_1B_2}\,| \left|\frac{\sin N\,\omega_1\tau_o}{N \sin \omega_1\tau_o}\right| \tag{200}$$

and

$$\lim_{N\to\infty}\left|E\left\{n_{o,N}(s)\right\}\right| \leq \lim_{N\to\infty} |\, N_{B_1B_2}\,| \left|\frac{\sin N\,\omega_1\tau_o}{N \sin \omega_1\tau_o}\right| = 0 \tag{201}$$

except for $\omega_1 \tau_o = 2q\pi$, with q integral. Consequently, the time-averaged output due to the noise is inversely proportional to the number of pulse repetitions N, and in the limit as N approaches infinity, the noise output's average value approaches zero. We can explain this by noting that the system is designed to respond to a pair of signals with a fixed frequency difference ω_1. Since the noise does not have this dual nature its effect in the system output averages to zero. The special cases $\omega_1 \tau_o = 2q\pi$ need not concern us since we can always design our system to avoid these values.

This result contrasts with the noise output of a conventional system employing square-law detection. In such a situation the part of the terminal voltage of the antenna which is due to the noise is

$$N_D(t) = \int_{-\infty}^{\infty} N(t,u)\ D(u)\ du \tag{202}$$

where D(u) is the antenna's field strength pattern. The low-frequency output of the square-law detector due to this noise voltage is

$$n_{SL}(t) = \tfrac{1}{2} \mid N_D(t) \mid^2 \tag{203}$$

This output has a positive average which we define as

$$\langle n_{SL}(t) \rangle = \bar{N}_D \cdot \tag{204}$$

Consequently, in the presence of background noise the conventional system's display will have a positive vertical deflection whose average value is independent of range and is proportional to the average noise power $\bar{N}_D$. However, if the antenna is scanned this averaged noise output will vary with scan angle (except in the rather unrealistic case when the noise sources are uniformly distributed). On the other hand, the cross-correlation system output due to the noise sources has a time-average of zero which in general is independent of both range and scan angle.

9.4 Suppression of Jamming Signals

In some situations there might be, in addition to the target echoes, a series of jamming pulses which are received by the antenna. They will be from the directions of the jamming transmitter (or transmitters) and of any targets which can reflect these jamming pulses towards the receiving antenna. If the carrier frequency ω_o and pulse repetition rate τ_o of this interference is the same as that of the desired echoes, a conventional system has no choice but to accept both the signal and the jamming noise.

The cross-correlation system differs from this since it is designed to respond only to a pair of target echoes at frequencies ω_o and $\omega_o + \omega_1$. Therefore unless the jamming signals are also in this dual form the time-average of the interference will approach zero as the number of pulse repetitions increases. The proof of this statement is essentially the same as that for the suppression of random background noise of Section 9.3.

10. THE MAPPING OF A TARGET DISTRIBUTION WITH A CROSS-CORRELATION RADAR SYSTEM

An arbitrary distribution of radar targets will generally produce echoes which are partially coherent. In this chapter a general theory of mapping such a target distribution is presented. One must use a cross-correlation system the details of which are described in Chapter 9. The resolution of the system is limited in two ways. First, the non-zero beamwidths of the antenna patterns smooth the observed target distribution, as the patterns are scanned. Second, due to the transmitted pulses not being infinitety sharp, the measurement of the range of the targets will also be a smoothed version of the true range distribution.

Let us consider a system which uses just one aperture of length L. Its four patterns, $A_1(u)$, $A_2(v)$, $B_1(u)$, and $B_2(v)$ are generated by the aperture weighting network of Figure 15. We will assume that the radar pulses have a spectrum of width $\Delta\omega$. Under these restrictions, an aperture of length L and a bandwidth of $\Delta\omega$, it is pertinent to ask what is the best one can do in mapping the target distribution. We will now show that we can obtain a principal solution which is similar to the one described in Chapter 5 for active sources.

10.1 Description of the Target Distribution

The targets are assumed to be located within the range of the system and also in the far-field of the antennas ($2L^2/\lambda \leq r \ll r_{max}$). We associate with the target in the u direction and at range r, the complex number $g(t,u,r)e^{j\omega_o r/c}$. Note that it is a function of time; this allows for target scintillation, rotation, and translation as time progresses. The

phase factor $e^{j\omega_o r/c}$ is present because our reference point is located at the center of antenna aperture. Thus $g(t,u,r)e^{j\omega_o r/c}$ represents the target distribution as observed from the antenna.

10.2 System Output in the Presence of the Target Distribution

Let us suppose that we are interested in the amount of correlation between the echoes from the targets at (u,ℓ) and (v,r). If we beam one of the transmitting antenna patterns in the u direction and the other in the v direction and if we delay the set of pulses sent to the nearer target by $s/c = (\ell-r)/c$ seconds, then the two targets will be struck simultaneously by the pulses. The delay of the pulses sent to the nearer target compensates for the delay imposed by the extra distance s on the pulses sent to the other target. Since the returning echoes also have a different distance to travel, the output signals will also have a relative delay, i.e., the signals from the more distant target is delayed in returning by an additional s/c seconds. Accordingly the output of the receiving antenna whose pattern is beamed at the nearer target is delayed by the same relative amount. This will insure that the echoes from the two targets enter the cross-correlator at the same time.

The two transmitted signals are

$$A_1(t-\ell/c,\ u_1-u) = \sum_{k=0}^{N-1} P(t-\ell/c - 2kT_o)\ A_1(u_1-u)e^{j\omega_o \ell/c} \qquad (205)$$

$$A_2(t+r/c,\ u-v) = \sum_{k=o}^{N-1} P(t+r/c\ -2k\tau_o)\ A_2(u_1-v)e^{j\left[\left(\omega_o + \omega_1\right) r/c + \omega_1 t\right]}. \qquad (206)$$

We have advanced one signal by r/c seconds and the other by ℓ/c seconds. The second signal is tagged with the constant phase modulation ω_1. Note that the pulse repetition rate is $2\tau_o$ where $\tau_o = 2r_{max}/c$. This permits a delay of one pulse relative to the other of as much as τ_o with practically no interference from preceding or succeeding pulses.

After striking the targets the pulses return and are received by antennas B_1 and B_2. Their two output voltages are

$$B_1(t,\ell,r,u,v) = \int_{-\infty}^{\infty}\int_{-\infty}^{\infty} \sum_{k=0}^{N-1} \left\{ P\left(t-\frac{2(\ell-r_1)}{c} - 2k\tau_o\right)e^{j\frac{2\omega_o}{c}(\ell-r_1)} A_1(u_1-u) + \right.$$

$$\left. P\left(t+\frac{\ell+r}{c} - \frac{2r_1}{c} - 2k\tau_o\right)e^{j\left[\frac{\omega_o}{c}(\ell+r-2r_1) + \omega_1\left(t+\frac{\ell+r-2r_1}{c}\right)\right]} A_2(u_1-v) \right\}$$

$$B_1(u_1-u)\ g\left(t+\frac{\ell-r_1}{c},\ u_1, r_1\right)\ e^{j\frac{2\omega_o r_1}{c}}\ du_1 dr_1 \qquad (207)$$

$$B_2(t,\ell,r,u,v) = \int_{-\infty}^{\infty}\int_{-\infty}^{\infty}\sum_{k=o}^{N-1}\left\{P\left(t+\frac{\ell+r}{c}-\frac{2r_2}{c}-2k\tau_o\right)e^{\frac{j\omega_o}{c}(\ell+r-2r_2)}A_1(u_2-u)+\right.$$

$$\left.P\left(t+\frac{2(r-r_2)}{c}-2k\tau_o\right)e^{j\left[\frac{2\omega_o}{c}(r-r_2)+\omega\left(t+2\frac{r-r_2}{c}\right)\right]}A_2(u_2-v)\right\}B_2(u_2-v)$$

$$g\left(t-\frac{r-r_2}{c},u_2,r_2\right)e^{j\frac{2\omega_o}{c}r_2}\,du_2dr_2. \qquad (208)$$

Note that the voltage $B_1(t,\ell,r,u,v)$ has been advanced by the amount ℓ/c and $B_2(t,\ell,r,u,v)$ has been advanced by r/c. In Appendix D it is shown that when these signals are cross-correlated with $\tau=0$, the system output can be written as

$$R(\ell,r,u,v) = G(o,\ell,r,u,v) * \overset{V}{C}_1(u)\overset{V*}{C}_2(v)\ \overline{P}(\ell)\overline{P}^*(r) \qquad (209)$$

where

$$C_1(u) = A_1(u)B_1(u) \qquad (210)$$

$$C_2(v) = A_2(v)B_2(v) \qquad (211)$$

$$\overline{P}(r) = P(2r/c) \qquad (212)$$

and

$$G(\tau,\ell,r,u,v) = \left\langle g(t,u,\ell)\ g^{*}(t-\tau,v,r) \right\rangle \qquad (213)$$

is the mutual coherence function of the target distribution.

Equations (210) and (211) show that in effect we have two independent radar systems each of which uses distinct patterns for transmitting and receiving. One system beams its two-way pattern in the u direction and the other system beams its pattern in the v direction. Equation (212) indicates the role of the pulse shape in the mapping of the target distribution. $\bar{P}(r-r_o) = P\left[\frac{2}{c}(r-r_o)\right]$ is the response, as a function of range r, to a point target at r_o. The pulses P(t) in the radar system correspond to the RF filter response functions $f_A(t)$ and $f_B(t)$ in the cross-correlation receiving system described in Chapter 5.

10.3 Fourier Analysis of the System Output

The system output $R(\ell,r,u,v)$ is a smoothed version of the mutual coherence function of the target distribution (evaluated at $\tau=0$). If we take the 4-dimensional inverse Fourier transform of Equation (209), the convolution theorem can be used to obtain

$$r(\xi,\eta,x,y) = (2\pi)^2\ g(o,\xi,\eta,x,y)\ \bar{p}(\xi)\ \bar{p}^{*}(\eta)c(x).\ c^{*}(y)) \qquad (214)$$

where $r(\xi,\eta,x,y)$, $g(o,\xi,\eta,x,y)$, $\bar{p}(\xi)$, $\bar{p}(\eta)$, $c_1(x)$, and $c_2(y)$ are the

inverse Fourier transforms of $R(\ell, r, u, v)$, $G(o, \ell, r, u, v)$, $\bar{P}(\ell)$, $\bar{P}(r)$, $C_1(u)$, and $C_2(v)$ respectively. Now since in Equation (210)

$$C_1(u) = A_1(u)\, B_1(u)$$

we can again invoke the convolution theorem to obtain

$$c_1(x) = (2\pi)^{\frac{1}{2}}\, a_1(x) * b_1(x) \tag{215}$$

where $a_1(x)$ and $b_1(x)$ are the inverse Fourier transforms of $A_1(u)$ and $B_1(u)$ respectively. In a similar fashion we can write

$$c_2(y) = (2\pi)^{\frac{1}{2}}\, a_2(y) * b_2(y). \tag{216}$$

$c_1(x)$ and $c_2(y)$ can be thought of as the spatial frequency spectra of the radar system's composite patterns $C_1(u)$ and $C_2(v)$, respectively.

Since the four apertures coincide and are all of length L, it follows that

$$\begin{aligned} c_1(x) &\equiv 0, \quad \text{for} \quad |x| > L, \\ c_2(y) &\equiv 0, \quad \text{for} \quad |y| > L. \end{aligned} \tag{217}$$

Thus the system has a spatial frequency response which is non-zero only within the region of the xy plane for which $|x| \lesssim L$ and $|y| \lesssim L$.

Similarly we define $\bar{p}(\xi)$ as the spatial frequency spectrum of the system's response in the radial direction ℓ. This spectrum is related to the temporal spectrum of the transmitted signal pulse. Thus if

$$P(t) = \frac{1}{\sqrt{2\pi}} \int_{-\infty}^{\infty} p(\omega) e^{j\omega t} d\omega \tag{218}$$

then

$$\bar{P}(\ell) = \frac{c}{2\sqrt{2\pi}} \int_{-\infty}^{\infty} p\left(\frac{c}{2}\xi\right) e^{j\xi\ell} d\xi \tag{219}$$

and

$$\bar{p}\ (\xi) = \frac{c}{2}\ p\ \left(\frac{c}{2}\xi\right) . \tag{220}$$

But we stipulated that $p(\omega)$ was practically zero for $|\omega| > \Delta\omega$ (see page 110); consequently we have

$$\bar{p}(\xi) \overset{\omega}{\approx} 0, \quad \text{for } |\xi| > \frac{2\Delta\omega}{c} . \tag{221}$$

Thus the antenna system will reject those radial spatial frequencies which lie outside the interval $|\xi| \leq \frac{2\Delta\omega}{c}$. Clearly it will also reject those frequencies η such that $|\eta| > \frac{2\Delta\omega}{c}$.

It has been shown, therefore, that the correlation antenna system acts as a low-pass filter of the spatial frequencies x and y which correspond to the bearing directions u and v and it acts as a low-pass filter of the spatial frequencies ξ and η which correspond to range coordinates ℓ and r. The "aperture" of the system is a four-dimensional region centered at the origin and with boundaries given by the hyperplanes $\xi = \pm \frac{2\Delta\omega}{c}$, $\eta = \pm \frac{2\Delta\omega}{c}$, $x = \pm L$, $y = \pm L$. Furthermore, within this region the system function weights the target spectrum in a more or less arbitrary fashion which depends on the pattern and pulse spectra. The output spectrum is usually a distorted version of the target spectrum because of this.

However we can use Equation (214) to define

$$g_o(o,\xi,\eta,x,y) = \frac{r(\xi,\eta,x,y)}{(2\pi)^2 c_1(x) c_2^*(y)\ \bar{p}(\xi)\ \bar{p}^*(\eta)}, \quad \text{for } (\xi,\eta,x,y) \in Q, \tag{222}$$

$$= 0, \qquad \text{otherwise,}$$

where we have defined the four-dimensional point set Q to be that for which $|c_1(x)\ c_2^*(y)\ \bar{p}(\xi)\ \bar{p}^*(\eta)| \not\equiv 0$. In our case it is the above-mentioned four-dimensional volume with center at the origin. The Fourier transform of

$g_o(o,\xi,\eta,x,y)$ will be defined as the principal solution, $G_o(o,\ell,r,u,v)$. The spatial frequency spectrum, $g_o(o,\xi,\eta,x,y)$, is identical to that of the required mutual coherence function $G(o,\ell,r,u,v)$, but only over the region Q. For points outside of Q it is, by definition, equal to zero. Consequently $G_o(o,\ell,r,u,v)$ is a smoothed version of $G(o,\ell,r,u,v)$ whose non-zero spatial frequency components are identical to those of $G(\phi,\ell,r,u\ v)$. In this sense then, $G_o(o,\ell,r,u,v)$ is the best or principal solution to the problem of mapping a stationary target distribution with a finite antenna and a finite bandwidth.

11. CONCLUSIONS

In this thesis we have considered the application of cross-correlation techniques to linear antenna arrays. Probably the most important result of this work was the demonstration that a two-antenna cross-correlation system can be used to measure a source distribution's mutual coherence function. Since coherent and partially coherent signals are not uncommon in practice, e.g., radar, multipath propagation, and scattering from nearly objects, the results obtained here should be of interest to the antenna engineer. The demonstration that a conventional antenna system with square-law detection is just a special case of the cross-correlation system makes it possible to evaluate in a straightforward manner the relative merits of a conventional and a cross-correlation system. An interesting result is that the analysis of multiple correlation systems is quite simple (at least in theory) since their outputs are ammenable to Fourier analysis just as in the two-antenna case. Finally, it is felt that the new cross-correlation radar system, in spite of its involved circuitry, has a number of advantages over the conventional system which should recommend it in some applications.

REFERENCES

1. Pearson, Karl, "On the General Theory of Skew Correlation and Non-Linear Regression," Drapers Company Research Memoirs, Biometric Series II, pp. 9-10, 1904.

2. Chuprov, A. A., (Tschuprow), "Principles of the Mathematical Theory of Correlation," English Translation, William Hodge and Company Ltd., 1939.

3. Wiener, N., "Generalized Harmonic Analysis," Acta Mathematica, Vol. 55, 1930.

4. Wiener, N., "Extrapolation, Interpolation, and Smoothing of Stationary Time Series," John Wiley and Sons, 1949.

5. Born and Wolf, "Principles of Optics," Chapter 10, Pergamon Press, 1959.

6. Verdet, E., Ann. Scientif. l'Ecole Normale Superieure, Vol. 2, p. 291, 1865. (Paris, L'Imprimerie Imperiale), Vol. 1, p. 106, 1869.

7. Von Laue, M., Ann.d.Physik, Vol. 23, No. 4, p. 1, 1907.

8. Van Cittert, P. H., Physica, Vol 1, p. 201, 1934.

9. Zernike, F., Physica, Vol. 5, p. 785, 1938.

10. Wolf, E., Il Nuovo Cimento, Vol. 12, p. 884, 1954.

11. Wolf, E., Proc. Roy. Soc., A Vol. 230, p. 246, 1955.

12. Wolf, E., Proc. Phys. Soc., Vol. 71, p. 257, 1958.

13. Blanc-Lapierre, A., and Dumontet P., Rev. D'Optique, Vol. 34, p. 1, 1955.

14. Beran, M. J., Optica Acta, Vol. 5, p. 88, 1955.

15. Parrent, Jr., G. B., "Studies in the Theory of Partial Coherence," Optica Acta, Vol. 6, No. 3, p. 285, July 1959.

16. Parrent, Jr., G. B., "On the Propagation of Correlation in Radio Fields," Proc. Radio Wave Propagation Symposium, Academic Press, Ltd., London.

17. Bracewell, R. N., "Antennas and Data Processing," IRE Trans., PGAP, AP-10, No. 2, pp. 108-111, March 1962.

18. Bracewell, R. N., and Roberts, J. A., "Aerial Smoothing in Radio Astronomy," Australian Journal of Physics, Vol. 7, pp. 615-640, December 1954.

19. Drane, C. J., "Phase Modulated Antennas," Air Force Cambridge Research Center, Technical Report No. AFCRC-TR-59-138 (AD 215 374), April 1959.

20. Ksienski, A. A., "Signal Processing Antennas - Part I," The Microwave Journal, Vol. 4, No. 10, pp. 77-85, October 1961.

21. Mills, B. Y., and Little, A. G., "A High Resolution Aerial System of A New Type," Australian Journal of Physics, Vol. 6, p. 272, 1953.

22. Covington, A. E., and Broten, N. W., "An Interferometer for Radio Astronomy with a Single-Lobed Radiation Pattern," Trans. IRE, PGAP, Vol. AP-5, No. 3, pp. 247-255, July 1957.

23. Arsac, J., "Application of Mathematical Theories of Approximation to Aerial Smoothing in Radio Astronomy," Australian Journal of Physics, Vol. 10, p. 16, 1957.

24. Barber, N. F., "Correlation and Phase Methods of Direction Finding," N. Z. Journal of Science and Technology, pp. 416-424, March 1957.

25. Barber, N. F., "Optimum Arrays for Direction Finding," N. Z. Journal of Science, Vol. 1, p. 35, March 1958.

26. Berman, A., and Clay, C. S., "Theory of Time-Averaged Product Arrays," J. Acoust. Soc. of America, Vol. 29, No. 7, pp. 805-812, July 1957.

27. Drane, C. J., and Parrent, Jr., G. B., "Selection of Optimum Antenna Arrays," AFCRC Antenna Laboratory Technical Report, ASTIA Document No. AD 117 103, May 1957.

28. Drane, C. J., and Parrent, Jr., G. B., "On the Mapping of Extended Sources with Nonlinear Correlation Antennas," IRE Trans., PGAP, Vol. AP-10, No. 2, pp. 126-130, March 1962.

29. Hanbury Brown, R., and Twiss, R. Q., "A New Type of Interferometer for Use in Radio Astronomy," Phil. Mag. (7), Vol. 45, pp. 663-682, 1954.

30. Hanbury Brown, R., and Twiss, R. Q., "A Test of a New Type of Stellar Interferometer on Sirius," Nature, Vol. 178, p. 1046, 1956.

31. Linder, I. W., "Resolution Characteristics of Correlation Arrays," J. of Research, Sec. D., National Bureau of Standards, Vol. 65D No. 3, pp. 245-252, May-June 1961.

32. MacPhie, R. H., "Comments on 'Multiple Target Response of Data Processing Systems'", IRE Trans., PGAP, Vol. AP-10, No. 5, pp. 642-643, September 1962.

33. MacPhie, R. H., "Optimum Cross-Correlation Radar System," Proc. IRE, Vol. 50, No. 12, pp. 2508-2509, December 1962.

34. MacPhie, R. H., "On the Mapping by a Cross-Correlation Antenna System of Partially Coherent Radio Sources," Technical Report No. 62, Antenna Laboratory, University of Illinois, Urbana, Illinois, October 1962.

35. Pedinoff, M. E., and Ksienski, A. A., "Multiple Target Response of Data-Processing Systems," IRE Trans., PGAP, AP-10, No. 2, pp. 112-125, March 1962.

36. Price, O. R., "Reduction of Sidelobe Level and Beamwidth for Recciving Antennas," IRE Proc., Vol. 48, No. 6, pp. 1177-1178, June 1960.

37. Welsby, V. G., and Tucker, D. G., "Multiplicative Receiving Arrays," J. Brit. IRE, Vol. 19, pp. 369-382, June 1959.

38. White, W. D., Ball, C. O., and Deckett, M., "Final Report on Nonlinear Antenna Study," Contract No. AF30(602)-1873, RADC-TR-59-179, ASTIA No. 228 886, September 1959.

39. Young, A. O., and Ksienski, A. A., "Signal and Data Processing Antennas," IRE Trans. on Military Electronics, Vol. MIL-5, No. 2. pp. 91-102, April 1961.

40. Dolph, C. L., "A Current Distribution for Broadside Arrays Which Optimizes the Relationship Between Beamwidth and Sidelobe Level," Proc. IRE, Vol. 34, No. 6, pp. 335-348, 1946.

41. Jasik, H., "Antenna Engineering Handbook," Chapter 2, p. 25, McGraw-Hill, 1961.

42. Korn, G. A., and Korn, T. M., "Mathematical Handbook for Scientists and Engineers," p. 576, McGraw-Hill, 1961.

43. Davenport, Jr., W. B., and Root, W. L., "An Introduction to the Theory of Random Signals and Noise," Chapter 8, McGraw-Hill, 1958.

44. Schwartz, Laurent, "Theorie des Distributions," Tome I, Actualities Scientifiques et Industrielles, 1091, p. 17, 1950.

45. Arsac, J., "Transformation de Fourier et Théorie des Distributions," Dunod, Paris, 1961.

46. Erdelyi, Arthur, "Modern Mathematics for the Engineer," E. F. Bechenbach, Editor, p. 30, McGraw-Hill, 1961.

47. Reed, I. S., "On a Moment Theorem for Complex Gaussian Processes," IRE Trans., PGIT, Vol. IT-8, No. 3, pp. 194-195, April 1962.

48. Woodward, P. M., "Probability and Information Theory, with Applications to Radar," Pergamon Press Ltd., p. 29, 1953.

49. MacPhie, R. H., "On Increasing the Effective Aperture of Antennas by Data Processing," Technical Report No. 58, Antenna Laboratory, University of Illinois, July 1962.

50. Courant, R., and Hilbert, D., "Methods of Mathematical Physics," Vol. I, Interscience, 1953.

51. MacPhie, R. H., "Synthesis of Antenna Product Patterns Obtained from a Single Array," Technical Report No. 50, p. 6, University of Illinois, Antenna Laboratory, January 1961.

52. Schelkunoff, S. A., "A Mathematical Theory of Linear Arrays," B.S.T.J., Vol. 22, No. 1, pp. 80-107, 1943.

53. Mattingly, R. L., "Nonreciprocal Radar Antennas," Proc. IRE, Vol. 48, No. 4, pp. 795-796, 1960.

54. Nuttall, Albert H., "High-Order Covariance Functions for Complex Gaussian Processes," Trans. IRE, PGIT, Vol. IT-8, No. 3, pp. 225-256, April 1962.

APPENDIX A

THE CASE OF TWO-DIMENSIONAL SOURCE DISTRIBUTIONS AND PLANAR ANTENNAS

In the main body of this thesis we considered a one-dimensional source distribution. More realistically, the direction of a remote radio source can be specified as a point on a sphere of "infinite" radius with the antenna at its center. This leads to a two-dimensional source distribution which can be measured by a planar antenna system. We will now outline this generalization from one to two dimensions. At the same time we will consider the practical problem resulting from the directive properties of the elements of the array. Then the problem of changing variables from the (u,v) domain to the (θ,ϕ) domain will be studied. Finally we will show that for electromagnetic fields the Fourier transform relation between the far-field pattern and the aperture distribution is a valid relation when the far electric field and the aperture current density are considered. The relation between the far electric field and the aperture electric field is not as simple.

A.1 The Output of a Planar Antenna Cross-Correlation System and the Effect of Element Pattern

Let us consider a planar antenna located in the $z = 0$ plane. The total pattern of the antenna can be written as

$$A(u,v) = E(u,v)\ A_a(u,v) \tag{A.1}$$

where

$$u = \beta \sin\theta \cos\varphi \qquad v = \beta \sin\theta \sin\varphi \tag{A.2}$$

and $E(u,v)$ is the element pattern which as a function of u and v varies much more slowly than the array pattern $A_a(u,v)$. The terminal voltage of the array, in the presence of the source distribution $V(t,u,v)$, is

$$A(t,u,v) = \iint V(t,u',v') \; E(u',v') \; A_a(u'-u, v'-v) \; du' \, dv'. \tag{A.3}$$

Note that the array pattern can be scanned but the individual elements' pattern cannot be scanned.

If we let

$$V_E(t,u,v) = V(t,u,v) \; E(u,v) \tag{A.4}$$

then Equation (A.3) becomes

$$A(t,u,v) = \iint V_E(t,u',v')\, A_a(u'-u,\ v'-v)\, du'\, dv' \tag{A.5}$$

$$= V_E(t\ u,v) * A_a(u,v) \tag{A.6}$$

From Equation (A.6) we see that the effect of the element pattern is to change the source distribution as "observed" by the array. This change is given by Equation (A.2). It can be easily shown that the mutual coherence function of the "observed" source distribution is

$$T_E(\tau,u_1,v_1,u_2,v_2) = \left\langle V_E(t,u_1,v_1)\ V_E^*(t-\tau,u_2,v_2) \right\rangle \tag{A.7}$$

$$= E(u_1,v_1)\ E^*(u_2,v_2)\ T(\tau,u_1,v_1,\ u_2,v_2) \tag{A.8}$$

where $T(\tau,u_1,v_1,u_2,v_2)$ is the true mutual coherence function.

The output from a second planar array can be written as

$$B(t,u,v) = V_E(t,u,v) \quad * \quad B_a(u,v) \tag{A.9}$$

and when the two output voltages are filtered and cross-correlated we obtain

$$R(\tau, u_1, v_1, u_2, v_2) = T_E(\tau, u_1, v_1, u_2, v_2) * f_{AB}(\tau)\ \check{A}(u_1, v_1)\ \check{B}^*(u_2, v_2). \quad (A.10)$$

Equation (A.10) indicates that the cross-correlated output of the system is a filtered version of $T_E(\tau, u_1, v_1, u_2, v_2)$ and not of the true mutual coherence function $T(\tau, u_1, v_1, u_2, v_2)$.

The inverse Fourier transform of $R(\tau, u_1, v_1, u_2, v_2)$ is

$$r(\omega, x_1, y_1, x_2, y_2) = t_E(\omega, x_1, y_1, x_2, y_2)\ c_{AB}(\omega, x_1, y_1, x_2, y_2) \quad (A.11)$$

where

$$c_{AB}(\omega, x_1, y_1, x_2, y_2,) = F_A(\omega)\ F_B^*(\omega)\ a(x_1, y_1)\ b^*(x_2, y_2) \quad (A.12)$$

We define

$$t_{EAB}(\omega, x_1, y_1, x_2, y_2) = \frac{r(\omega, x_1, y_1, x_2, y_2)}{c_{AB}(\omega, x_1, y_1, x_2, y_2)}, \text{if } (\omega, x_1, y_1, x_2, y_2) \in Q_{AB} \quad (A.13)$$

$$= 0 \quad , \quad \text{otherwise.}$$

The Fourier transform of $t_{EAB}(\omega, x_1, y_1, x_2, y_2)$ is the principal solution. But in view of Equation (A.8) we can write the principal solution as

$$T_{EAB}(\tau, u_1, v_1, u_2, v_2) = T(\tau, u_1, v_1, u_2, v_2)\ E(u_1, v_1)\ E^*(u_2, v_2) * Q(\tau, u_1, v_1, u_2, v_2) \tag{A.14}$$

where, by analogy with Equation (117), $Q(\tau, u_1, v_1, u_2, v_2)$ is the Fourier transform of a system function which is uniform within Q_{AB}, the system's "aperture".

Note that the element patterns are included in the convolution integral of Equation (A.14) and strictly speaking cannot be separated from the desired mutual coherence function $T(\tau, u_1, v_1, u_2, v_2)$. However, in most cases the antenna elements are much smaller than the array itself and the element patterns are slowly varying functions when compared to $Q(\tau, u_1, v_1, u_2, v_2)$. If this is the case we can write

$$T_{EAB}(\tau, u_1, v_1, u_2, v_2) = E(u_1, v_1)\ E^*(u_2, v_2) \left\{ T(\tau, u_1, v_1, u_2, v_2) * Q(\tau, u_1, v_1, u_2, v_2) \right\} \tag{A.15}$$

to a good degree of approximation. Consequently we obtain

$$T_{AB}(\tau, u_1, v_1, u_2, v_2) = \frac{T_{EAB}(\tau, u_1, v_1, u_2, v_2)}{E(u_1, v_1)\ E^*(u_2, v_2)} \tag{A.16}$$

as the principal solution corrected for the effect of element pattern. This result is valid only in regions where $|E(u,v)|$ is non-zero.

A.2 The Mutual Coherence Function in the Angular Domain

In practice it is more meaningful to express the mutual coherence function as a function of the angular variables θ and φ rather than of $u = \beta\sin\theta\cos\varphi$ and $v = \beta\sin\theta\sin\varphi$. Since $T(\tau, u_1, v_1, u_2, v_2)$ is a power density function we know that $T(0, u_1, v_1, u_2, v_2)\ du_1 dv_1 du_2 dv_2$ is the cross-power incident on the antenna system from the elementary regions located at (u_1, v_1) and (u_2, v_2). Transforming this element of cross-power from the (u,v) to the (θ, φ) domain, we write

$$T(0, u_1, v_1, u_2, v_2)\ du_1 dv_1 du_2 dv_2 =$$

$$T(0,\ \beta\sin\theta_1\cos\varphi_1, \beta\sin\theta_1\sin\varphi_1, \beta\sin\theta_2\cos\varphi_2, \beta\sin\theta_2\sin\varphi_2)$$

$$\frac{\partial(u_1, v_1, u_2, v_2)}{\partial(\theta_1, \varphi_1, \theta_2, \varphi_2)}\ d\theta_1\ d\varphi_1\ d\theta_2\ d\varphi_2 \tag{A.17}$$

where

$$\frac{\partial(u_1, v_1, u_2, v_2)}{\partial(\theta_1, \varphi_1, \theta_2, \varphi_2)} = \beta^4 \cos\theta_1 \cos\theta_2 \sin\theta_1 \sin\theta_2 \qquad (A.18)$$

is the Jacobian of the transformation.

Now let us define the mutual coherence function in the angular domain to be $\dot{T}(\tau, \theta_1, \varphi_1, \theta_2, \varphi_2)$. The cross-power incident on the system from the elementary regions located at (θ_1, φ_1) and (θ_2, φ_2) is

$$T'(0, \theta_1, \varphi_1, \theta_2, \varphi_2) \sin\theta_1 \sin\theta_2 \, d\varphi_1 \, d\varphi_2 \, d\theta_1 \, d\theta_2 \qquad (A.19)$$

If we equate this with the cross-power given by Equation (A.17) we obtain

$$T'(0, \theta_1, \varphi_1, \theta_2, \varphi_2) = \beta^4 \cos\theta_1 \cos\theta_2, \; T(0, \beta\sin\theta_1 \cos\varphi_1, \beta\sin\theta_1 \sin\varphi_1, \beta\sin\theta_2 \cos\varphi_2, \beta\sin\theta_2 \sin\varphi_2) \qquad (A.20)$$

as the relation between the mutual coherence functions in the (u,v) and

(θ,φ) domains.

This result also applies when we consider the source distribution to be weighted by the antenna element pattern.

$$T'_E(\tau,\theta_1,\varphi_1,\theta_2,\varphi_2) = \beta^2\cos\theta_1\cos\theta_2\ E\left\{\beta\sin\theta_1\cos\varphi_1,\beta\sin\theta_1\sin\varphi_1\right\}$$

$$E^*\left\{\beta\sin\theta_2\cos\varphi_2,\beta\sin\theta_2\sin\varphi_2\right\}\ T(\tau,\beta\sin\theta_1\cos\varphi_1,\beta\sin\theta_1\sin\varphi_1,\beta\sin\theta_2\cos\varphi_2,$$

$$\beta\sin\theta_2\sin\varphi_2) \qquad \text{(A.21)}$$

and if the element patterns are slowly varying we can write

$$T'_{AB}\ (\tau,\theta_1,\varphi_1,\theta_2,\varphi_2) = \frac{T'_{EAB}\ (\tau,\theta_1,\varphi_1,\theta_2,\varphi_2)}{E(\beta\sin\theta_1\cos\varphi_1,\beta\sin\theta_1\sin\varphi_1)\ E^*(\beta\sin\theta_2\cos\varphi_2,\beta\sin\theta_2\sin\varphi_2)}. \qquad \text{(A.22)}$$

A.3 Fourier Analysis for Electromagnetic Fields

Let us assume that the electromagnetic field is known on the plane $z = o$. This plane can be thought of as the extended aperture of an antenna.

Any electromagnetic field in the plane can be decomposed as the sum of two modes, the TE and TM modes, each of which can be represented by a scalar function. In particular let us consider the TE mode and a field which varies only in the x direction. This is analogous to the one-dimensional apertures which were considered in the thesis. The electric component is

$$\vec{E}(x,z) = \hat{y}\, E_y(x,z)\,. \tag{A.23}$$

The scalar field $E_y(x,o)$ in the aperture plane has as Fourier transform $\tilde{E}_y(\beta\sin\theta)$, which represents a spectrum of plane waves. Considering just one of these plane waves we can write

$$\hat{y}\, \tilde{E}_y(\beta\sin\theta)\, e^{-j\vec{\beta}\cdot\vec{r}} = \hat{y}\, \tilde{E}_y(\beta\sin\theta)\, e^{-j[\beta\sin\theta\, x + \beta\cos\theta\, z]} \tag{A.24}$$

which represents the field at any point (x,z) due to the plane wave. The total field is the integral of all such plane waves over all possible directions.

$$E_y(x,z) = \int_{-\infty}^{\infty} \tilde{E}_y(\beta\sin\theta)\, e^{-j[\beta\sin\theta\, x + \beta\cos\theta\, z]}\, d\beta\sin\theta. \qquad (A.25)$$

The field at any point can be recovered from its plane wave expansion on the plane $z = o$.

Equivalent Current Sheet

If we again consider the plane wave given by Equation (A.24) we can use Maxwell's Equation

$$\vec{H}(x,z) = -\frac{1}{j\omega_o\mu}\ \text{curl}\ \vec{E}(x,z) \qquad (A.26)$$

to write

$$\tilde{H}_x(\beta\sin\theta) = \frac{-\beta\cos\theta}{j\omega_o\mu}\,\tilde{E}(\beta\sin\theta) \qquad (A.27)$$

as the x component of the plane wave's magnetic field. But it also follows from Maxwell's Equations that

$$H_x(x,o) = \frac{1}{2}\ J_y(x) \qquad (A.28)$$

where $J_y(x)$ is the density function of an equivalent sheet of electric current flowing in the z = o plane. Taking Fourier transforms of both sides of Equation (A.28) gives

$$\tilde{H}_x(\beta\sin\theta) = \frac{1}{2}\ \tilde{J}_y(\beta\sin\theta) \tag{A.29}$$

and in view of Equation (A.27) we can write

$$\tilde{J}_y(\beta\sin\theta) = \frac{-2\beta\cos\theta}{j\omega_o\mu}\ \tilde{E}(\beta\sin\theta). \tag{A.30}$$

Substituting this result into Equation (A.25) gives

$$E_y(x,z) = \frac{-j\omega_o\mu}{2} \int_{-\infty}^{\infty} \tilde{J}_y(\beta\sin\theta)\ e^{-j[\beta\sin\theta\ x\ +\ \beta\cos\theta\ z]}d\theta \tag{A.31}$$

which represents the electric field at any point in terms of the spectrum of the current density in the aperture plane.

Far-Field Approximation

Let us rewrite Equation (A.31) as

$$E_y(r_o,\theta_o) = \frac{-j\omega_o\mu}{2} \int_{-\infty}^{\infty} \tilde{J}_y(\beta\sin\theta)\, e^{-j\beta r_o \cos(\theta-\theta_o)}\, d\theta \qquad (A.32)$$

where

$$r_o^2 = x^2 + z^2 \quad \text{and} \quad \theta_o = \tan^{-1}\left(\frac{x}{z}\right).$$

If the observation point (r_o,θ_o) is in the far-field r_o is very large and the integral on the right side of Equation (A.32) can be evaluated by the method of stationary phase. We can write

$$E_y(r_o,\theta_o) \simeq -\frac{j\omega_o\mu}{2} J_y(\beta\sin\theta_o)\, e^{-j\beta r_o} \int_{-\infty}^{\infty} e^{-j\frac{\beta r_o}{2}(\theta-\theta_2)^2} d\theta$$

$$\simeq \frac{j\omega_o\mu\,\pi}{2} H_o^{(2)}(\beta r_o)\, \tilde{J}_y(\beta\sin\theta_o) \qquad (A\ 33)$$

where $H_o^{(2)}(\beta r_o)$ is the Hankel function of the second kind. Thus we see that the far electric field at a fixed radius r_o from the origin is proportional to the Fourier transform of the current density function in the aperture with the transform variables being $\beta\sin\theta$ and x. This is not the case for the relation between the aperture electric field and the far electric field. Starting with Equation (A.25) we can show that in the far field

$$E_y(r_o,\theta_o) \simeq \pi H_o^{(2)}(\beta r_o)\,\beta\cos\theta_o\,\tilde{E}_y(\beta\sin\theta_o)\,. \qquad (A.34)$$

Note the additional factor $\cos\theta_o$

APPENDIX B

OUTPUT OF THE MULTIPLE CROSS-CORRELATION SYSTEM

The signal from each of the N antennas is passed through an RF filter and delayed a certain amount. Thus the signal from the kth antenna after the filtering and the delay is

$$V_k(t-\tau_k, u_k) = A_k(t-\tau_k, u_k)\, e^{-j\omega_o \tau_k} \tag{B.1}$$

where

$$A_k(t, u_k) = \int_{-\beta}^{\beta} \int_{0}^{\infty} V(t-t_1, u)\, A_k(u-u_k)\, du\, f_k(t_1)\, dt_1 \tag{B.2}$$

$$= V(t, u_k) * f_k(t) \overset{\vee}{A}_k(u_k) .$$

As is shown in Figure 13, the signal from the first antenna is fed into a frequency shifter (phase modulator) which increases the carrier frequency from ω_o to $\omega_o + \omega_1$ with $\omega_o \ggg \omega_1$. Thus the signal can be written as

$$V_1(t-\tau_1, u_1, \omega_1) = A_1(t-\tau_1, u_1) e^{-j(\omega_o \tau_1 - \omega_1 t)} . \tag{B.3}$$

This signal is fed into a mixer (a squaring device) along with the signal from antenna 2, $V_2(t-\tau_2, u_2)$. There is a component in the mixer output at frequency ω_1 and it can be written as

$$p_{12}(t, \tau_1, \tau_2, u_1, u_2) = A_1(t-\tau_1, u_1)\, A_2^*(t-\tau_2, u_2)\, e^{-j\omega_o(\tau_1-\tau_2)}\, e^{j\omega_1 t} \tag{B.4}$$

In a similar fashion the signal from antenna 3 is passed through a frequency shifting device with modulation frequency ω_3 and after it is mixed with the signal from antenna 4 the mixer output contains a signal whose carrier is at frequency $\omega_3 \lll \omega_o$ It is given by

$$p_{34}(t,\tau_3,\tau_4,u_3,u_4) = A_3(t-\tau_3,u_3)\, A_4^*(t-\tau_4,u_4)\, e^{-j\omega_o(\tau_3-\tau_4)}\, e^{j\omega_3 t} \tag{B.5}$$

As can be seen in Figure 13 the signals of each adjacent pair of antennas are correlated in this manner and each mixer output has a distinct carrier frequency ω_k, with $k = 1,3,5,\ldots,N-1$.

If, after passing through a band-pass filter,* each of these single correlation outputs is mixed with the adjacent one, i.e., p_{12} with p_{34}, p_{56} with p_{78}, etc., and the process continued until a single output results, we can write the expression for the signal in the output at frequency $\omega_1 + \omega_3 + \ldots + \omega_{N-3} + \omega_{N-1}$ as follows

$$\begin{aligned} p_{123\ldots N}(t,\tau_1,\tau_2,\ldots,\tau_N,u_1,u_2,\ldots,u_N) = \\ A_1(t-\tau_1,u_1)A_2^*(t-\tau_2,u_2)A_3(t-\tau_3,u_3)\, A_4^*(t-\tau_4,u_4)\ldots\ldots \\ \ldots A_{N-1}(t-\tau_{N-1},u_{N-1})\, A_N^*(t-\tau_N,u_N) e^{-j\left\{\omega_o[\tau_1-\tau_2+\tau_3-\tau_4+\ldots-\tau_N]-[\omega_1+\omega_3+\ldots+\omega_{N-1}]t\right\}}. \end{aligned} \tag{B.6}$$

Then if the output is fed into a synchronous detector along with a reference signal at frequency $\omega_1+\omega_3+\ldots+\omega_{N-1}$, the detector output before time-averaging will be the following real voltage

*For simplicity of analysis we assume that the filter has no effect on the output signals in the narrow band $|\omega-\omega_k| \leq \Delta\omega$ and completely rejects the double frequency RF output signals and the signals in the low frequency band $|\omega| \leq \Delta\omega$.

$$\bar{R}'_{A_1A_2\ldots A_N}(t,\ \tau_1,\tau_2,\tau_3,\ldots,\tau_N,\ u_1,\ u_2,\ldots,u_N) = R_e\left\{A_1(t-\tau_1,u_1)\ A_2^*(t-\tau_2,u_2)\right.$$

$$\left.A_3(t-\tau_3,u_3)\ A_4^*(t-\tau_4,\ u_4)\ldots A_N^*(t-\tau_N,u_N)\ \cdot e^{-j\omega_o(\tau_1-\tau_2+\tau_3-\ldots-\tau_N)}\right\} \qquad (B.7)$$

If one of the signals, say $A_1(t-\tau_1,u_1)e^{j\omega_o(t-\tau_1)}$, is taken in phase quadrature then the above result becomes

$$\bar{R}''_{A_1A_2\ldots A_N}(t,\ \tau_1,\tau_2,\ldots,\tau_N,u_1,\ldots,u_N) = I_m\left\{A_1(t-\tau_1,u_1)\ A_2^*(t-\tau_2,u_2)\ldots.\right.$$

$$\left.\ldots A_N^*(t-\tau_N,\ u_N)\ e^{-j\omega_o[\tau_1-\tau_2+\tau_3-\ldots-\tau_N]}\right\}. \qquad (B.8)$$

Thus we define

$$R_{A_1A_2\ldots A_N}(t,\tau,\tau_2,\ldots,\tau_N,u_1,\ldots,u_N) =$$

$$e^{j\omega_o[\tau_1-\tau_2+\ldots-\tau_N]}\left[\bar{R}'_{A_1\ldots A_N}(t,\tau_1,\ldots,u_N)\ +\ j\ \bar{R}''_{A_1\ldots A_N}(t,\tau_1,\ldots,u_N)\right] \qquad (B.9)$$

as the complex system output for the case of N correlations. Using Equation (B.2) we can write the expected value of the time-average of this output as

$$R_{A_1A_2\ldots A_N}(\tau_1,\ldots,\tau_N,u_1,\ldots,u_N) = E\left\{\int_{-\beta}^{\beta}\int_{-\beta}^{\beta}\ldots\int_{-\beta}^{\beta}\int_{0}^{\infty}\int_{0}^{\infty}\ldots\int_{0}^{\infty} V(t-\tau_1-t_1,u_1')\cdot\right.$$

$$\cdot V^*(t-\tau_2-t_2,u_2')\ V(t-\tau_3-t_3,u_3')\ V^*(t-\tau_4-t_4,u_4')\ldots V^*(t-\tau_N-t_N,u_N')\cdot$$

$$\left.A_1(u_1'-u_1)\ A_2^*(u_2'-u_2)\ldots A_N^*(u_N'-u_N)\ f_1(t_1)\ f_2^*(t_2)\ \ldots f_N^*(t_N)du_1'du_2'\ldots du_N'dt_1\ldots dt_N\right\} \qquad (B.10)$$

$$= \int_{-\beta}^{\beta} \cdots \int_{-\beta}^{\beta} \int_{0}^{\infty} \cdots \int_{0}^{\infty} T^{(N)}(\tau_1+t_1, \tau_2+t_2, \ldots, \tau_N+t_N, u_1', u_2', \ldots, u_N')$$

$$\overset{\vee}{A}_1(u_1-u_1') \overset{\vee *}{A}_2(u_2-u_2') \cdots \overset{\vee *}{A}_N(u_N-u_N') \; f_1(t_1) \; f_2^*(t_2) \cdots f_N^*(t_N) du_1' \ldots du_N' \; dt \ldots dt_N \tag{B.11}$$

where

$$T^{(N)}(\tau_1, \tau_2, \ldots, \tau_N, u_1, \ldots, u_N) = E\left\{V(t-\tau_1, u_1) \; V^*(t-\tau_2, u_2) \cdots V^*(t-\tau_N, u_N)\right\}. \tag{B-12}$$

Since the source distribution is stationary, this function is independent of the exact time t at which the evaluation occurs. Inspection of the integrand of Equation (B-11) will reveal that we can write

$$R_{A_1 A_2 \ldots A_N}(\tau_1, \tau_2, \ldots, \tau_N, u_1, \ldots, u_N) = T^{(N)}(\tau_1, \tau_2, \ldots, \tau_N, u_1, \ldots, u_N)$$

$$* \left[\overset{\vee}{A}_1(u_1) \overset{\vee *}{A}_2(u_2) \overset{\vee}{A}_3(u_3) \cdots \overset{\vee *}{A}_N(u_N) \; \overset{\vee}{f}_1(\tau_1) \; \overset{\vee *}{f}_2(\tau_2) \; \overset{\vee}{f}_3(\tau_3) \cdots \overset{\vee *}{f}_N(\tau_N)\right] \tag{B-13}$$

which is the convolution of $T^{(N)}(\tau_1, \tau_2, \ldots, \tau_N, u_1, \ldots, u_N)$ by the reverse of the system function $A_1(u_1) \; A_2^*(u_2) \cdots A_N^*(u_N) \; f_1(\tau_1) f_2^*(\tau_2) f_3(\tau_3) \cdots f_N^*(\tau_N)$.

In the above derivation we have assumed that N was even. In most practical cases this will be the only pertinent situation since most of the source distributions will have even probability distributions, e.g., gaussian, and hence all odd moments will be zero. However, this will not always be the case and in order to measure the odd moments of a distribution we must use an odd number of antennas The process is the same as for an

even number except that the last antenna signal is shifted in frequency by $\omega_N - \omega_o$ rather than by ω_N. It is then mixed directly with the output signal resulting from the mixing of the signals from antennas N-2 and N-1. The rest of the process is the same as before.

Finally we note that the two-antenna system is just a special case of the above. The output of the single mixer is fed immediately into the synchronous detector along with a signal at frequency ω_1. The output is $R_{A_1A_2}(\tau_1,\tau_2,u_1,u_2)$ and if we let $\tau_1 = 0$, $\tau_2 = \tau$, $u_1 = u$, $u_2 = v$, $A_1 = A$, and $A_2 = B$, we have

$$R^{(2)}_{A_1A_2}(\tau_1,\tau_2,u_1,u_2) = R_{AB}(\tau,u,v) \tag{B.14}$$

APPENDIX C

CORRELATION RADAR SYSTEM

A diagram of the system is shown in Figure 14. The pulsed transmitter signal is divided into two equal parts, one of which is shifted in frequency from ω_o to $\omega_o + \omega_1$, with $\omega_o \ggg \omega_1$. This slight change in frequency can be accomplished by inserting in the feed line a rotary phase shifter whose phase change is at the constant rate of ω_1 radians per second.

These two distinct signals are then fed to antennas A_1 and A_2 and the far fields of the two antennas can be written as

$$A_1(t,v) = \sum_{k=o}^{N-1} P(t-k\,\tau_o)A_1(v) \qquad (C.1)$$

$$A_2(t,v,\omega_1) = \sum_{k=o}^{N-1} P(t-k\,\tau_o)\,A_2(v)e^{j\omega_1 t} \qquad (C.2)$$

where P(t) is the video pulse, and τ_o is the pulse repetition period. We have assumed that the transmitter is turned on at t = 0 and the pulse is repeated N-1 times. $A_1(v)$ and $A_2(v)$ are the far-field patterns of antennas A_1 and A_2 respectively. The absence of RF filters in the

feed lines of the transmitting and receiving antennas of Figure 14 is due to our assuming, for simplicity, that the actual filters have uniform pass-bands and hence pass the signals unaltered.

Now for simplicity let us consider the case of a single target in the v direction and at a range r. The returning echoes are received by the other two antennas, B_1 and B_2. The terminal voltage of antenna B_1 can be written as

$$b_1(t) = \sum_{k=o}^{N-1} P(t - \frac{2r}{c} - k\tau_o)\left[A_1(v) + A_2(v)e^{j\omega_1(t-\frac{2r}{c})}\right]B_1(v)e^{j\omega_o(t-\frac{2r}{c})} \tag{C.3}$$

Note the time delay term $\frac{2r}{c}$, where c is the velocity of light in the medium. This is the time required for the pulses to reach the target and after reflection to return to the antenna. It is common practice to choose the pulse repetition period τ_o so that if the maximum practical target distance is r_{max}, then $\tau_o = \frac{2r_{max}}{c}$. Thus all echoes due to one pulse will have returned before the succeeding pulse is transmitted. This avoids any ambiguity in range measurement. If for the present we assume that the target is stationary, each pulse will return at the same time relative to its corresponding transmitted pulse. Consequently, we can, for simplicity of notation, consider the time interval $0 \leq t < \tau_o$ knowing that the returns of succeeding intervals will be identical to the first whose response, with the carrier frequency factor suppressed, can be written as

$$B_1(t) = P(t-t_r)\left[A_1(v) + A_2(v)e^{j\omega_1(t-t_r)}\right]B_1(v)e^{-j\omega_o t_r} \qquad (C.4)$$

for $0 \leq t \leq \tau_o$,

and where we have let

$$t_r = \frac{2r}{c} . \qquad (C.5)$$

The voltage of antenna B_2 is

$$B_2(t) = P(t-t_r)\left[A_1(v) + A_2(v)e^{j\omega_1(t-t_r)}\right]B_2(v)e^{-j\omega_o t_r} \qquad (C.6)$$

for $0 \leq t < \tau_o$, where $B_2(v)$ is the receiving field strength pattern of antenna B_2.

Now in order to distinguish the two output voltages, $b_1(t)$ is shifted in frequency; it is fed into a square-law device along with a second signal at frequency ω_2. The frequency ω_2 is chosen to be much larger than the RMS spectral width, $\Delta\omega$, of the pulse P(t), while ω_1 is very much smaller. For example, if the operating frequency, $\frac{\omega_o}{2\pi}$, of the radar is 10 Gc, and the pulses are one microsecond in length then $\frac{\Delta\omega}{2\pi} = 1$ Mc, and we could let $\frac{\omega_1}{2\pi} = .1$Kc, and $\frac{\omega_2}{2\pi} = 1$ Gc. A filter is located at the frequency shifter's output which passes only the signal at the difference frequency, $\omega_o - \omega_2$.

This can be written as

$$\bar{B}_1(t) = P(t-t_r)\left[A_1(v) + A_2(v)e^{j\omega_1(t-t_r)}\right] B_1(v)e^{j[\omega_o(t-t_r)-\omega_2 t]} . \qquad (C.7)$$

This voltage, along with $B_2(t)$, is fed into a mixer which forms the square of their sum, i.e.,

$$\left[R_e\left(\bar{B}_1(t) + B_2(t)\right)\right]^2 =$$

$$\left[R_e\left\{P(t-t_r)\left[A_1(v) + A_2(v)e^{j\omega_1(t-t_r)}\right] B_1(v)e^{j[\omega_o(t-t_r)-\omega_2 t]}\right\}\right. \qquad (C.8)$$

$$\left. + R_e\left\{P(t-t_r)\left[A_1(v) + A_2(v)e^{j\omega_1(t-t_r)}\right] B_2(v)e^{j\omega_o(t-t_r)}\right\}\right]^2 .$$

If an RF filter, whose passband is centered at frequency ω_2, is located at the mixer output it will pass the following RF signal

$$C(t) = |P(t-t_r)|^2 \left[|A_1(v)|^2 + |A_2(v)|^2 \right.$$

$$\left. + A_1(v)A_2^*(v)e^{-j\omega_1(t-t_r)} + A_1^*(v)\, A_2(v)e^{j\omega_1(t-t_r)} \right] B_1(v)B_2^*(v)e^{-j\omega_2 t} . \qquad (C.9)$$

If this signal is fed into a synchronous (phase) detector along with a reference voltage at frequency $\omega_2 + \omega_1$, the detector output can be written as

$$r(t) = |P(t-t_r)|^2 \left\{ C_o(v)e^{j\omega_1 t_r} + C_1(v)e^{j\omega_1 t} + C_2(v)e^{j2\omega_1\left(t-\frac{t_r}{2}\right)} \right\} \qquad (C.10)$$

where

$$C_o(v) = A_1(v)\, B_1(v)\, A_2^*(v)\, B_2^*(v)$$

$$C_1(v) = \left(|A_1(v)|^2 + |A_2(v)|^2 \right) B_1(v)\, B_2^*(v) \qquad (C.11)$$

$$C_2(v) = A_1^*(v)\, B_1(v)\, A_2(v)\, B_2^*(v)$$

As mentioned earlier, this result is valid for $0 \leq t < \tau_o$. The output for any value of t can be written

$$r_N(t) = \sum_{k=o}^{N-1} |P(t-t_r-k\,\tau_o)|^2 \left[C_o(v)e^{j\omega_1 t_r} + C_1(v)^{j\omega_1 t} + C_2(v)e^{j2\omega_1(t-\frac{t_r}{2})}\right] \qquad (C.12)$$

In practice, a linear saw-tooth voltage wave, synchronized with the pulse repetition rate, is often used to produce a visual display of this output on an oscilloscope. Thus, the abscissa of the display is the range coordinate s and the vertical deflection is proportional to the strength of the target return. For a given range s this deflection is given by the values of $r_N(t)$ sampled at $t = k\,\tau_o + \frac{2s}{c}$. The average value of this deflection after N-1 repetitions of the pulse is

$$R_N(s) = \frac{1}{N} P_o(s-r) \sum_{k=o}^{N-1} \left\{C_o(v)e^{j\omega_1 t_r} + C_1(v)e^{j\omega_1\left(\frac{2s}{c} + k\,\tau_o\right)} + C_2(v)e^{j2\omega_1\left(\frac{2s}{c} + k\,\tau_o - t_r\right)}\right\}$$

$$= P_o(s-r) \left\{ C_o(v)\, e^{j\omega_1 t_r} + C_1(v) \frac{\sin\left(N\,\omega_1 \frac{\tau_o}{2}\right)}{N \sin\left(\omega_1 \frac{\tau_o}{2}\right)} e^{j\omega_1 \left(\frac{N-1}{2}\,\tau_o + \frac{2s}{c}\right)} \right.$$

$$\left. + C_2(v) \frac{\sin\left(N\,\omega_1 \tau_o\right)}{N \sin\left(\omega_1 \tau_o\right)} e^{j\omega_1 \left[(N-1)\tau_o + \frac{4s+2r}{c}\right]} \right\} \qquad \text{(C.13)}$$

where, in changing variables from t to s, we have redefined the pulse function as

$$P_o(s) = \left| P\left(\frac{2s}{c}\right) \right|^2 . \qquad \text{(C.14)}$$

It will be shown later that it is to our advantage to require that $\omega_1 \tau_o$ be small, say 0.5 radians or less. If this is the case, $\sin \omega_1 \tau_o \cong \omega_1 \tau_o$, and the absolute value of the second and third terms of Equation (C.13) can be written as

$$P_o(s-r) \left| C_1(v) \frac{\sin\left(N\,\omega_1 \frac{\tau_o}{2}\right)}{N \sin\left(\omega_1 \frac{\tau_o}{2}\right)} e^{j\omega_1 \left[\left(\frac{N-1}{2}\right)\tau_o + \frac{2s}{c}\right]} \right.$$

(C.15)

$$\left. + C_2(v) \frac{\sin N\,\omega_1 \tau_o}{N \sin \omega_1 \tau_o}\, e^{j\omega_1 \left[(N-1)\tau_o + \frac{4s+2r}{c}\right]} \right| \leq \frac{P_o(s-r)}{\omega_1 \tau_o} \left\{ \frac{2|C_1(v)|}{N} + \frac{|C_2(v)|}{N} \right\}$$

Note that as N increases, the absolute value at these terms approaches zero and in the limit Equation (C.13) becomes

$$\lim_{N \to \infty} R_N(s) = P_o(s-r)\, C_o(v) e^{j\omega_1 t_r} \tag{C.16}$$

or

$$R(s) = P_o(s-r)\, A_1(v)\, B_1(v)\, A_2^*(v)\, B_2^*(v)\, e^{j\omega_1 t_r}. \tag{C.17}$$

A not uncommon case is when all the patterns are real, and one can write the actual real system output as

$$R(s) = P_o(s-r)\, A_1(v)\, B_1(v)\, A_2(v)\, B_2(v) \cos\left(\frac{2\omega_1 r}{c}\right). \tag{C.18}$$

But if $2\omega_1 r/c = \pi/2$ the output is zero, a rather undesirable result. The cos $(2\omega_1 r/c)$ factor is due to the time delay $2r/c$ between the transmitted pulse and that which is received. As a consequence the reference signal in the synchronous detector leads the desired signal by $2\omega_1 r/c$ radians. This, in general, will cause a reduction in the system output and for real

patterns it is given by cos $(2\omega_1 r/c)$. Now if we select ω_1 so that $\omega_1 \tau_o = .5$ radians, then the reduction in the system output will be to $\{\cos(.5)\}$ 100 = 88% of the maximum possible output. This will occur for targets at the range limit r_{max}. For targets which are closer, the reduction is less. A better and still rather simple scheme would be to set the reference signal with a delay so that it is exactly in phase with the response from targets in the center of the range at $r_{max}/2$. Then it would lead the responses from r_{max} and lag the responses from r=0, by 0.25 radians. The reduction in the output in these cases would be to 96.8% of the maximum possible value. Thus we see that by keeping the phase modulation frequency low enough we can, to a reasonable approximation, obtain the following average response at the position s on the oscilloscope's range coordinate

$$R(s) = P_o(s-r)\, A_1(v)\, A_2^*(v)\, B_1(v)\, B_2^*(v) \qquad (C.19)$$

However it can be shown that by introducing a continuously varying phase compensation in the reference voltage of the synchronous detector one can completely remove the phase factor $2\omega_1 r/c$ for all values of r. It can also be shown that in this case $\omega_1 \tau_o$ need not be restricted to small values and there is a certain value of $\omega_1 \tau_o$, namely $4\pi/3$, which will cause the other two terms of the detector output to average out to zero at a maximum rate. This scheme, however, is rather complicated and it might have no significant advantage over the one mentioned above in many practical situations.

For this simpler system it is clear that ω_1, τ_o, and r_{max} are not independent. In usual practice one is given the value of r_{max}, e.g., 150 kilometers. From this, one can use the delay formulas to obtain

$$\tau_o = \frac{2r_{max}}{c} \quad . \tag{C.20}$$

In this case $\tau_o = 2(150)/300,000 = 10^{-3}$ seconds. The pulses are repeated every millisecond. Finally, we require that $\omega_1 \tau_o = .5$; hence in this case $\omega_1 = .5/10^{-3} = 500$ radians per second which is approximately 80 cps.

If, as is commonly done, the composite patterns of the antenna system are scanned, then for a scan direction u, we can write the system output, as a function of u and s, as follows

$$R(s,u) = P_o(s-r)\ A_1(v-u)\ A_2^*(v-u)\ B_1(v-u)\ B_2^*(v-u) \, . \tag{C.21}$$

This is the system response to a point target in the v direction and at range r.

SUPPRESSION OF BACKGROUND NOISE

Let us suppose that in addition to the distribution of passive targets there is a background distribution of independent, active, noise sources.

If we assume that the antenna has an RF filter which passes only a narrow band of frequencies centered at ω_o we can give the following description of the noise as a function of time and direction

$$n(t,u) = N(t,u)e^{j\omega_o t} \tag{C.22}$$

where $N(t,u)$ is the narrow band complex noise phasor at time t due to the noise source in the u direction. It is a random function of time and we assume it is stationary; its statistical properties are invariant under a shift of the time origin.

The system output will contain components due to the target reflections alone (signals), the noise alone, and cross-products of the reflections and the noise. But since the noise is random and the reflections are not, these cross-products terms will average out to zero. It remains to investigate the output components due to the noise alone. The two output noise voltages are

$$\tilde{n}_{B_1}(t) = \int_{-\infty}^{\infty} N(t,u)\, B_1(u) du\, e^{j(\omega_o - \omega_2)t} \tag{C.23}$$

$$= N_{B_1}(t)\, e^{j(\omega_o - \omega_2)t}, \tag{C.24}$$

where

$$N_{B_1}(t) = \int_{-\infty}^{\infty} N(t,u)\, B_1(u)du \,, \tag{C.25}$$

and

$$n_{B_2}(t) = N_{B_2}(t)e^{j\omega_o t} \,, \tag{C.26}$$

where

$$N_{B_2}(t) = \int_{-\infty}^{\infty} N(t,u)\, B_2(u)du \,. \tag{C.27}$$

The mixer forms the product of the sum of these two voltages and the filter at the mixer output passes the component at frequency ω_2. It is given by

$$n_{\omega_2}(t) = \frac{1}{2}\left[N_{B_1}(t)\, N^*_{B_2}(t)\right] e^{-j\omega_2 t} \,. \tag{C.28}$$

The output of the synchronous detector corresponding to this voltage is proportional to

$$n_o(t) = N_{B_1}(t)\, N^*_{B_2}(t)\, e^{-j\omega_1 t} . \qquad (C.29)$$

The average value of this output, sampled at $t = 2s/c + k\,\tau_o$, for N samples, is given by

$$n_{o,N}(s) = \frac{1}{N} \sum_{k=o}^{N-1} N_{B_1}\left(\frac{2s}{c} + k\,\tau_o\right) N^*_{B_2}\left(\frac{2s}{c} + k\,\tau_o\right) e^{-j\omega_1\left(\frac{2s}{c} + k\,\tau_o\right)} . \qquad (C.30)$$

This is proportional to the oscilloscope's average vertical deflection at the position s of the horizontal range coordinate. Since the noise is stationary, and essentially uncorrelated between pulses, we can write the expected value of $n_{o,N}(s)$ as

$$E\left\{n_{o,N}(s)\right\} = \frac{1}{N} \sum_{k=o}^{N-1} E\left\{N_{B_1}\left(\frac{2s}{c} + k\,\tau_o\right) N^*_{B_2}\left(\frac{2s}{c} + k\,\tau_o\right)\right\} e^{-j\omega_1\left(\frac{2s}{c} + k\,\tau_o\right)}$$

$$= \frac{N_{B_1B_2}}{N}\, e^{-j\omega_1 \frac{2s}{c}} \sum_{k=0}^{N-1} e^{-jk\omega_1\tau_o}$$

$$= N_{B_1B_2}\, \frac{\sin N\omega_1\tau_o}{N \sin \omega_1\tau_o}\, e^{-j\omega_1\left(\frac{2s}{c} + \frac{N-1}{2}\,\tau_o\right)} \qquad (C.31)$$

where

$$N_{B_1 B_2} = E\left\{N_{B_1}\left(\frac{2s}{c} + k\,\tau\right)\, N^*_{B_2}\left(\frac{2s}{c} + k\,\tau\right)\right\} \tag{C.32}$$

is the mathematical expectation or statistical average of $N_{B_1}\left(\frac{2s}{c} + k\,\tau\right)$ $N^*_{B_2}\left(\frac{2s}{c} + k\,\tau\right)$, and due to stationarity, is independent of k. From Equation (C.31) we can write

$$\left| E\left\{n_{o,N}(s)\right\}\right| \leq |N_{B_1 B_2}| \left|\frac{\sin\left(N\,\omega_1\tau\right)}{N \sin\,\omega_1\tau}\right| \tag{C.33}$$

and except when $\omega_1\tau = 2q\pi$, for integral q, we have

$$\lim_{N\to\infty}\left| E\left\{n_{o,N}(s)\right\}\right| \leq \lim_{N\to\infty} |N_{B_1 B_2}| \left|\frac{\sin\left(N\,\omega_1\tau\right)}{N \sin\,\omega_1\tau}\right| \tag{C.34}$$

$$= 0 \,.$$

APPENDIX D

RADAR MAPPING OF A TARGET DISTRIBUTION

If the output voltage $B_1(t,\ell,r,u,v)$, as given by Equation (207) of Chapter 10, is first shifted in frequency to $\omega_o - \omega_2$, and then mixed with $B_2(t,\ell,r,u,v)$ as given by Equation (208), the output of the band-pass filter (at frequency ω_2) can be written as

$$m(t,\ell,r,u,v) = \int_{-\infty}^{\infty}\int_{-\infty}^{\infty} A_1(u_1-u)\, B_1(u_1-u)\, A_2^*(u_2-v)\, B_2^*(u_2-v) \int_{\sigma}^{\infty}\int_{\sigma}^{\infty} \sum_{k=o}^{N-1}\sum_{i=o}^{N-1}$$

$$P(t-\tfrac{2}{c}(\ell-r_1)-2k\tau_o)\; P^*(t-\tfrac{2}{c}(r-r_2)-2i\tau_o)\, e^{j\left\{\frac{2\omega_o}{c}\left[\ell-r\right]-\frac{2\omega_1}{c}(r-r_2)\right\}} g(t+\tfrac{\ell-r_1}{c},u_1,r_1)$$

$$g^*(t+\tfrac{r-r_2}{c},u_2,r_2)\,du_1\,du_2\,dr_1\,dr_2\, e^{-j(\omega_1+\omega_2)t} \qquad (D.1)$$

Note that the usual correlation delay τ, has not been introduced. Consequently the system output will be the cross-correlation of the two antenna voltages evaluated at $\tau = o$. We have also assumed that the RF filters of the system are capable of passing the video pulses of the radar with no distortion. However even with these simplifications the

mathematical analysis is still quite involved.

Letting the reference voltage be

$$v_{REF}(t) = e^{-j\left[(\omega_1+\omega_2)\,t \;+\; \frac{2\omega_1}{c}\left(r-\frac{r_{max}}{2}\right)\right]} \tag{D.2}$$

the output of the synchronous detector becomes

$$\bar{R}'_N(t,\ell,r,u,v) = \int_{-\infty}^{\infty}\int_{-\infty}^{\infty} \overset{\vee}{C}_1(u-u_1)\,\overset{\vee}{C}_2(v-u_1) \sum_{k=o}^{N-1}\sum_{i=o}^{N-1} \int_{-\infty}^{\infty}\int_{-\infty}^{\infty} P\left\{t+\frac{2}{c}(\ell-r_1)-2k\tau_o\right\} \tag{D.3}$$

$$P^*\left\{t+\frac{2}{c}(r-r_2)-2i\tau_o\right\} e^{j\frac{2\omega_o}{c}[\ell-r]}\, g\left(t+\frac{\ell-r_1}{c},u_1r_1\right) g^*\left(t+\frac{r-r_2}{c},u_2r_2\right) dr_1\,dr_2\,du_1\,du_2$$

where we have defined

$$C_1(u) = A_1(u)\;B_1(u) \tag{D.4}$$

$$C_2(v) = A_2(v)\ B_2(v)\ . \tag{D.5}$$

There are other terms in the output, just as in the single target case (see Equation C.10), but since they all have a zero time-average we have, for simplicity of presentation, omitted them in the above output expression. Since the pulses are essentially non-overlapping (orthogonal) we can write the output as

$$\bar{R}_N(s,\ell,r,u\ v) = \overset{\vee}{C}_1(u)\overset{\vee}{C}_2(v) * \sum_{k=0}^{N-1} \int_0^\infty\int_0^\infty \bar{P}\left(s+\ell-r_1-2kr_{max}\right) e^{j\frac{2\omega_o}{c}(s+\ell)}$$

$$\bar{P}^*\left(s+r-r_2-2kr_{max}\right) e^{j\frac{2\omega_o}{c}(s+r)}\ g\left(\frac{2s+\ell-r_1}{c},\ u, r_1\right) g^*\left(\frac{2s+r-r_2}{c},\ v, r_2\right) dr_1 dr_2 \tag{D.6}$$

where $s = ct/2$.

For a target at a given range, for example r_1, we will assume that its reflection coefficient, $g(t,u,r_1)$, is slowly varying compared to the pulse that strikes it. This occurs when

$$s = \ell - r_1 - 2kr_{max} = 0 \tag{D.7}$$

or

$$r_1 = s + \ell - 2kr_{max} \, . \tag{D.8}$$

Similarly the pulse strikes the relatively unchanging target at range r_2 when

$$r_2 = s + r - 2kr_{max} \, . \tag{D.9}$$

Substituting these results into Equation (D.6) gives

$$\bar{R}_N(s,\ell,r,u,v) = \overset{\vee}{C}_1(u)\,\overset{\vee}{C}{}_2^*(v) * \sum_{k=o}^{N-1} \int_o^\infty \int_o^\infty \bar{P}\left(s+\ell-r_1-2kr_{max}\right) \tag{D.10}$$

$$\bar{P}\left(s+r-r_2-2kr_{max}\right) e^{j\frac{2\omega_o}{c}(\ell-r)} g\left(\frac{s+2kr_{max}}{c}, u, r_1\right) g^*\left(\frac{s+2kr_{max}}{c}, v, r_2\right) dr_1 dr_2$$

$$= e^{j\frac{2\omega_o}{c}(\ell-r)}\left\{\overset{\vee}{C}_1(u)\ \overset{\vee *}{C}_2(v)\ \sum_{k=o}^{N-1}\ \overline{P}\left(s+\ell-2kr_{max}\right)\overline{P}^{*}\left(s+r-2kr_{max}\right)\right\}$$

$$* \left\{g\left(\frac{s+2kr_{max}}{c}, u, s+\ell-2kr_{max}\right) g^{*}\left(\frac{s+2kr_{max}}{c}, v, s+r-2kr_{max}\right)\right\} . \qquad (D.11)$$

Letting the output be sampled at $s = 2kr_{max}$ (i.e., at $t = 2kT_o$), the average output is given by

$$\overline{R}_N(\ell, r, u, v) = \frac{1}{N}\sum_{k=o}^{N-1} e^{j\frac{2\omega_o}{c}(\ell-r)}\left\{\overset{\vee}{C}_1(u)\ \overset{\vee *}{C}_2(v)\ \overline{P}(\ell)\ \overline{P}^{*}(r) *\right.$$

$$\left. g\left(\frac{4kr_{max}}{c}\ u, \ell\right) g^{*}\left(\frac{4kr_{max}}{c}, v, r\right)\right\} . \qquad (D.12)$$

Now if the target function $g(t,u,r)$ satisfies the ergodic hypothesis, then we have

$$E\left\{g(t,u,\ell)\ g^{*}(t-\tau,v,r)\right\} = G\ (\tau,\ell,r,u,v) \tag{D.13}$$

where $G(\tau,\ell,r,u,v)$ is the mutual coherence function of the target distribution.

The expected value of the system output after N pulses is

$$E\left\{\bar{R}_N(\ell,r,u,v)\right\} = \frac{1}{N}\sum_{k=o}^{N} e^{j\frac{2\omega_o}{c}(\ell-r)}\left\{\underset{\sim}{C}_1(u)\ \underset{\sim}{C}_2^{*}(v)\ \bar{P}(\ell)\ \bar{P}^{*}(r)\right.$$

$$\left.* G\ (o,\ell,r,u,v)\right\} \tag{D.14}$$

or

$$\bar{R}(\ell,r,u,v) = e^{j\frac{2\omega_o}{c}(\ell-r)}\ \underset{\sim}{C}_i(u)\ \underset{\sim}{C}_2^{*}(v)\ \bar{P}(\ell)\ \bar{P}^{*}(r) * G(o,\ell,r,u,v)\ . \tag{D.15}$$

Multiplying both sides of the above equation by $e^{-j\frac{2\omega_c}{c}(\ell-r)}$ gives

$$R(\ell, r, u, v) = e^{-j\frac{2\omega_o}{c}(\ell - r)} \bar{R}(\ell, r, u, v) \tag{D.16}$$

$$= \overset{\vee}{C}_1(u)\, \overset{\vee *}{C}_2(v)\, \bar{P}(\ell)\, \bar{P}^*(r) * G(o, \ell, r, u, v) \tag{D.17}$$

as the required system output.

AF 33(657)-10474

DISTRIBUTION LIST

One copy each unless otherwise indicated

Armed Services Technical Information Agency
Attn: TIP-DR
Arlington Hall Station
Arlington 12, Virginia (20 copies)

Air Force Systems Command (SCSE)
Andrews Air Force Base
Washington 25, D. C.

Aeronautical Systems Divsion
Attn: ASRNCF-3
Wright-Patterson Air Force Base
Ohio (5 copies)

Aeronautical Systems Division
Attn: ASNSED, Mr. Mulligan
Wright-Patterson Air Force Base
Ohio

Aeronautical Systems Division
Attn: ASAPRL
Wright-Patterson Air Force Base
Ohio

Aeronautical Systems Division
Attn: ASRSA - Library
Wright-Patterson Air Force Base
Ohio

Aeronautical Systems Division
Attn: ASNPRS
Wright-Patterson Air Force Base
Ohio

Commander
Air Force Systems Command
Aeronautical Systems Division
Wright-Patterson Air Force Base
Ohio
Attn: ASNCSO

Commander
Air Force Systems Command
Attn: ASNPOT, Mr. Finocharo
Aeronautical Systems Division
Wright-Patterson Air Force Base
Ohio

Commander
Foreign Technology Division
Attn: TD-El
Wright-Patterson Air Force Base
Ohio

Air Force Cambridge Research Laboratory
Attn: CRRD
Laurence G. Hanscom Field
Bedford, Massachusetts

Commander
Air Force Missile Test Center
Technical Library
Patrick Air Force Base
Florida

Commander
Air Force Missile Development Center
Attn: Technical Library
Holloman Air Force Base
New Mexico

Air Force Ballistic Missile Division
Attn: Technical Library, Air Force Unite Post Office
Los Angeles, California

Commanding Officer
USARDVL
Attn: SIGRA/SL-NAI
Ft. Monmouth, New Jersey

Chief, Bureau of Ships
Attn: Code 312
Main Navy Building
Washington 25, D. C.

Commander
Air Proving Ground Center (AFSC)
Headquarters 3208th Test Group
Eglin Air Force Base, Florida

Director
Ballistics Research Laboratory
Attn: Ballistics Measurement Lab.
Aberdeen Proving Ground, Maryland

National Aeronautics & Space Adm.
Attn: Librarian
Langley Field, Virginia

Rome Air Development Center
Attn. RALTM
Griffiss Air Force Base
New York

Rome Air Development Center
Attn: RAWED, Mr. R. F. Davis
Griffiss Air Force Base
New York

Commander
Research & Technology Division
Attn: RTHR, Maj. J. Gregory
Bolling Air Force Base
Washington 25, D. C.

Office of Chief Signal Officer
Engineering & Technical Division
Attn: SIGNET-5
Washington 25, D. C.

Commanding Officer
U. S. Army Electronics R&D Activity
Attn: SELWS-ED
White Sands, Missile Range, New Mexico

Director
Surveillance Department
Evans Area
Attn: Technical Document Center
Belman, New Jersey

Commander
U. S. Naval Air Test Center
Attn: WST-54, Antenna Section
Patuxent River, Maryland

Material Laboratory, Code 932
New York Naval Shipyard
Brooklyn 1, New York

Director
Naval Research Laboratory
Attn: Code 5200
Washington 25, D. C.

Director
Air University Library
Attn: 3T-AUL-59-30
Maxwell Air Force Base
Alabama

Commanding General
White Sands Missile Range
Attn: ORDBS-OM-Tech Library RR-312
New Mexico

Commanding Officer
Diamond Ordnance Fuse Laboratories
Attn: 240
Washington 25, D. C.

Director
U. S. Navy Electronics Laboratory
Attn: Library
San Diego 52, California

Adams-Russell Company
280 Bear Hill Road
Attn: Library (Antenna Section)
Waltham 54, Massachusetts

Aero Geo Astro
Attn: Security Officer
1200 Duke Street
Alexandria, Virginia

NASA Goddard Space Flight Center
Attn: Antenna Section, Code 523
Greenbelt, Maryland

Airborne Instruments Labs., Inc.
Attn: Librarian (Antenna Section)
Walt Whitman Road
Melville, L.I., New York

American Electronic Labs
Box 552 (Antenna Section)
Lansdale, Pennsylvania

Andrew Alfred Consulting Engineers
Attn: Librarian (Antenna Section)
299 Atlantic Avenue
Boston 10, Massachusetts

Amphenol-Borg Electronic Corporation
Attn: Librarian (Antenna Section)
2801 S. 25th Avenue
Broadview, Illinois

Bell Aircraft Corporation
Attn: Technical Library
(Antenna Section)
Buffalo 5, New York

Bendix Radio Division of
Bendix Aviation Corporation
Attn: Technical Library
(For Dept. 462-4)
Baltimore 4, Maryland

Antenna Systems, Inc.
Manager Documentation
Grenier Field
Manchester, New Hampshire

Boeing Airplane Company
Aero Space Division
Attn: Technical Library
M/F Antenna & Radomes Unit
Seattle, Washington

Boeing Airplane Company
Attn: Technical Library
M/F Antenna Systems Staff Unit
Wichita, Kansas

Chance Vought Aircraft, Inc.
THRU: Bu AER Representative
Attn. Technical Library
M/F Antenna Section
P. O. Box 5907
Dallas 22, Texas

Collins Radio Company
Research Division
Attn: Technical Library
Cedar Rapids, Iowa

Convair
Ft. Worth Division
Attn: Technical Library (Antenna
Section)
Grants Lane
Fort Worth, Texas

Convair
Attn: Technical Library
(Antenna Section)
P. O. Box 1050
San Diego 12, California

Dalmo Victor Company
Attn: Technical Library
(Antenna Section)
1515 Industrial Way
Belmont, California

Dorne & Margolin, Inc.
Attn: Technical Library
(Antenna Section)
30 Sylvester Street
Westbury, L. I., New York

Dynatronics, Inc.
Attn: Technical Library
(Antenna Section)
Orlando, Florida

Electronic Communications, Inc.
Research Division
Attn: Technical Library
1830 York Road
Timonium, Maryland

Fairchild Engine & Airplane Corporation
Fairchild Aircraft & Missiles Division
Attn: Technical Library
(Antenna Section)
Hagerstown 10, Maryland

Georgia Institute of Technology
Engineering Experiment Station
Attn: Technical Library
M/F Electronics Division
Atlanta 13, Georgia

General Electric Company
Electronics Laboratory
Attn: Technical Library
Electronics Park
Syracuse, New York

General Electronic Labs., Inc.
Attn: Technical Library
(Antenna Section)
18 Ames Street
Cambridge 42, Massachusetts

General Precision Lab , Division of
General Precision, Inc.
Attn: Technical Library
(Antenna Section)
63 Bedford Road
Pleasantville, New York

Goodyear Aircraft Corporation
Attn: Technical Library
M/F Dept. 474
1210 Massilon Road
Akron 15, Ohio

Granger Associates
Attn Technical Library
(Antenna Section)
974 Commercial Street
Palo Alto, California

I-T-E Circuit Breaker Company
Special Products Division
Attn: Research Library
601 E . .e Avenue
Philadelphia 34, Pennsylvania

General Mills Electronics Division
Attn: Dr. H. P Raabe
2003 East Hennepin Avenue
Minneapolis 13, Minnesota

Grumman Aircraft Engineering Corporation
Attn: Technical Library
M/F Avionics Engineering
Bethpage, New York

The Hallicrafters Company
Attn: Technical Library
(Antenna Section)
4401 W. Fifth Avenue
Chicago 24 Illinois

Hoffman Laboratories, Inc.
Attn: Technical Library
(Antenna Section)
Los Angeles 7, California

John Hopkins University
Applied Physics Laboratory
8621 Georgia Avenue
Silver Springs, Maryland

Hughes Aircraft Corporation
Attn: Technical Library
(Antenna Section)
Florence & Teal Street
Culver City, California

ITT Laboratories
Attn: Technical Library
(Antenna Section)
500 Washington Avenue
Nutley 10, New Jersey

U. S. Naval Ordnance Laboratory
Attn: Technical Library
Corona, California

Lincoln Laboratories
Massachusetts Institute of Technology
Attn: Document Room
P. O. Box 73
Lexington 73, Massachusetts

Litton Industries
Attn: Technical Library
(Antenna Section)
4900 Calvert Road
College Park, Maryland

John Hopkins University
Radiation Laboratory
Attn: Library
1315 St. Paul Street
Baltimore 2, Maryland

Lockheed Missile & Space Division
Attn: Technical Library (M/F Dept-
58-40, Plant 1, Bldg. 130)
Sunnyvale, California

The Martin Company
Attn: Technical Library
(Antenna Section) Mail No. T-38
P. O. Box 179
Denver 1, Colorado

The Martin Company
Attn: Technical Library (Antenna
Section)
Baltimore 3, Maryland

The Martin Company
Attn: Technical Library (M/F Microwave Laboratory)
Box 5837
Orlando, Florida

W. L. Maxson Corporation
Attn: Technical Library (Antenna Section)
460 West 34th Street
New York 1, New York

McDonnell Aircraft Corporation
Attn: Technical Library (Antenna Section)
Box 516
St. Louis 66, Missouri

Melpar, Inc.
Attn: Technical Library (Antenna Section)
3000 Arlington Blvd.
Falls Church, Virginia

University of Michigan
Radiation Laboratory
Willow Run
201 Catherine Street
Ann Arbor, Michigan

Mitre Corporation
Attn: Technical Library (M/F Electronic Warefare Dept. D-21)
Middlesex Turnpike
Bedford, Massachusetts

Northeastern University
Attn: Dodge Library
Boston 15, Massachusetts

North American Aviation, Inc.
Attn: Technical Library (M/F Engineering Dept.)
4300 E. Fifth Avenue
Columbus 16, Ohio

North American Aviation, Inc.
Attn: Technical Library (M/F Dept. 56)
International Airport
Los Angeles, California

Northrop Corporation
NORAIR Division
1001 East Broadway
Attn: Technical Information (3924-3)
Hawthorne, California

Ohio State University Research Foundation
Attn: Technical Library (M/F Antenna Laboratory)
1314 Kinnear Road
Columbus 12, Ohio

Ohio State University Research Foundation
Attn: Dr. C. H. Walter
1314 Kinnear Road
Columbus 12, Ohio

Philco Corporation
Government & Industrial Division
Attn: Technical Library (M/F Antenna Section)
4700 Wissachickon Avenue
Philadelphia 44, Pennsylvania

Westinghouse Electric Corporation
Air Arms Division
Attn: Librarian (Antenna Lab)
P. O. Box 746
Baltimore 3, Maryland

Wheeler Laboratories
Attn: Librarian (Antenna Lab)
Box 561
Smithtown, New York

Electrical Engineering Research Laboratory
University of Texas
Box 8026, University Station
Austin, Texas

University of Michigan Research Institute
Electronic Defense Group
Attn: Dr. J. A. M. Lyons
Ann Arbor, Michigan

Radio Corporation of America
RCA Laboratories Division
Attn: Technical Library (M/F Antenna Section)
Princeton, New Jersey

Radiation, Inc.
Attn: Technical Library (M/F)
Antenna Section
Drawer 37
Melbourne, Florida

Ramo-Wooldridge Corporation
Attn: Librarian (Antenna Lab)
Canoga Park, California

Rand Corporation
Attn: Librarian (Antenna Lab)
1700 Main Street
Santa Monica, California

Rantec Corporation
Attn: Librarian (Antenna Lab)
23999 Ventura Blvd.
Calabasas, California

Raytheon Corporation
Equipment Division
Library - J. Portsch
P. O. Box 520
Waltham 54, Massachusetts

Republic Aviation Corporation
Applied Research & Development
Division
Attn: Librarian (Antenna Lab)
Farmingdale, New York

Sanders Associates
Attn: Librarian (Antenna Lab)
95 Canal Street
Nashua, New Hampshire

Southwest Research Institute
Attn: Librarian (Antenna Lab)
8500 Culebra Road
San Antonio, Texas

H R B Singer Corporation
Attn: Librarian (Antenna Lab)
State College, Pennsylvania

Sperry Microwave Electronics Company
Attn: Librarian (Antenna Lab)
P O Box 1828
Clearwater, Florida

Sperry Gyroscope Company
Attn. Librarian (Antenna Lab)
Great Neck, L. I., New York

Stanford Electronic Laboratory
Attn: Librarian (Antenna Lab)
Stanford, California

Stanford Research Institute
Attn: Librarian (Antenna Lab)
Menlo Park, California

Sylvania Electronic System
Attn: Librarian (M/F Antenna &
Microwave Lab)
100 First Street
Waltham 54, Massachusetts

Sylvania Electronic System
Attn: Librarian (Antenna Lab)
P. O. Box 188
Mountain View, California

Technical Research Group
Attn: Librarian (Antenna Section)
2 Aerial Way
Syosset, New York

Ling Temco Aircraft Corporation
Temco Aircraft Division
Attn: Librarian (Antenna Lab)
Garland, Texas

Texas Instruments, Inc.
Attn: Librarian (Antenna Lab)
6000 Lemmon Avenue
Dallas 9, Texas

A. S. Thomas, Inc.
Attn: Librarian (Antenna Lab)
355 Providence Highway
Westwood, Massachusetts

New Mexico State University
Head Antenna Department
Physical Science Laboratory
University Park, New Mexico

Bell Telephone Laboratories, Inc.
Whippany, New Jersey
Attn: Technical Reports Librarian
Room 2A-165

Robert G Hansen
Aerospace Corporation
Box 95085
Los Angeles 45, California

Dr. Richard C. Becker
10829 Berkshire
Westchester, Illinois

Dr. W. M. Hall
Raytheon Company
Surface Radar and Navigation
Operations
Boston Post Road
Wayland, Massachusetts

Dr. Robert L. Carrel
Collins Radio Corporation
Antenna Section
Dallas, Texas

Dr A. K. Chatterjee
Vice Principal and Head of the Department of Research
Birla Institute of Technology
P O Mesra
District-Ranchi (Bihar) India

University of Dayton
Research Institute
Attn: Professor Douglas Hanneman
300 College Park
Dayton, Ohio

Technische Hochschule
Attn H H Meinke
Munich, Germany

NASA Goddard Space Flight Center
Attn: Antenna Branch
Mr Lantz
Greenbelt Maryland

Aeronautic Division
Ford Motor Company
Ford Road - Attn: Mr J M Black
Newport Beach, California

Professor A. A. Oliver
Polytechnic Institute of Brooklyn
Microwave Research Institute
55 Johnson Street
Brooklyn 1, New York

U. S. Naval Ordnance Laboratory
Attn: Technical Library
Corona, California

Avco Corporation
Research and Advanced Development
Division
Attn: Research Library/T.A. Rupprecht
201 Lowell Street
Wilmington, Massachusetts

Raytheon Company
Missile and Space Division
Attn: Research Library
Bedford, Massachusetts

Teledyne Systems, Incorporated
Attn: Technical Library/Antenna Section
1625 E. 126th Street
Hawthorne, California

National Research Council
Attn: Microwave Section
Ottawa 2, Canada

Sichak Associates
Attn: W Sichak
518 Franklin Avenue
Nutley, New Jersey

W. T. Patton
2208 New Albany Road
Cinn Township
Riverton Post Office
New Jersey

Radio Corporation of America
Missile and Service Radar Division
Attn: Manager, Antenna Engineering
Skill Center
Moorestown, New Jersey

Advanced Development Laboratories, Inc.
Haines Street
Nashua New Hampshire

Cornell Aeronautical Lab
Attn Research Library
Buffalo, New York

Fairchild Stratos Corporation
Aircraft-Missiles Division
Attn: Technical Library (Antenna Section)
Hagerstown 10, Maryland

General Electric Company
Light Military Electronics Department
French Road
Utica New York

General Electric Company
General Engineering Laboratory
Bldg 371, Room 478
Schenectady, New York

Goodyear Aircraft Corporation
Antenna Department
Litchfield Park
Phoenix, Arizona

Laboratory for Electronics, Inc.
Antenna Department
1079 Commonwealth Avenue
Boston 15, Massachusetts

Lockheed Aircraft
Electronic and Armaments System Office
Burbank California

Motorola, Inc
Western Military Electronics Division
P O Box 1417
Scottsdale, Arizona

Philco Corporation
Antenna Section
3875 Fabian Way
Palo Alto California

Space Technology Laboratory
Attn Research Library
P O Box 95100
Los Angeles 45, California

Avco Corporation
Electronic and Ordnance Division
Attn: Technical Library
Cincinnati 41, Ohio

Bendix Corporation
Research Labs Division
Attn: G. M. Peace
Southfield (Detroit), Michigan

Douglas Aircraft Co., Inc.
Attn: MSSD Technical Library
(Antenna Section)
3000 Ocean Park Blvd.
Santa Monica, California

Emerson and Cuming, Inc.
Attn: E. J. Luoma
869 Washington Street
Canton, Massachusetts

Radioplane Company
Attn: Librarian (M/F Aerospace Lab)
1515 Rancho Conelo Blvd.
Newbury Park, California

Hughes Aircraft Company
Attn: Antenna Section
Fullerton, California

ANTENNA LABORATORY

TECHNICAL REPORTS AND MEMORANDA ISSUED

Contract AF33(616)-310

"Synthesis of Aperture Antennas," Technical Report No. 1, C. T. A. Johnk, October 1954.* AD-52134

"A Synthesis Method for Broadband Antenna Impedance Matching Networks," Technical Report No. 2, Nicholas Yaru, 1 February 1955. * AD 61049.

"The Assymmetrically Excited Spherical Antenna," Technical Report No. 3, Robert C. Hansen, 30 April 1955. * AD-66220.

"Analysis of an Airborne Homing System," Technical Report No. 4, Paul E. Mayes, 1 June 1955 (CONFIDENTIAL). AD-80147.

"Coupling of Antenna Elements to a Circular Surface Waveguide," Technical Report No. 5, H. E. King and R. H. DuHamel, 30 June 1955. * AD-75733.

"Input Impedance of a Spherical Ferrite Antenna with A Latitudinal Current," Technical Report No. 6, W. L. Weeks, 20 August 1955. AD-75732.

"Axially Excited Surface Wave Antennas," Technical Report No. 7, D. E. Royal, 10 October 1955 * AD-75731.

"Homing Antennas for the F-86F Aircraft (450-2500 mc), Technical Report No. 8, P. E. Mayes, R. F Hyneman, and R. C. Becker, 20 February 1957.

"Ground Screen Pattern Range," Technical Memorandum No. 1, Roger R. Trapp, 10 July 1955. *

Contract AF33(616)-3220

"Effective Permeability of Spheriodal Shells," Technical Report No. 9, E. J. Scott and R. H DuHamel, 16 April 1956. AD-98615.

"An Analytical Study of Spaced Loop ADF Antenna Systems," Technical Report No. 10, D. G. Berry and J. B. Kreer, 10 May 1956.

"A Technique for Controlling the Radiation from Dielectric Rod Waveguides," Technical Report No. 11, J. W. Duncan and R. H. DuHamel, 15 July 1956. * AD-107344

"Direction Characteristics of a U-Shaped Slot Antenna," Technical Report No 12, Richard C. Becker, 30 September 1956. ** AD-116104.

"Impedance of Ferrite Loop Antennas," Technical Report No. 13, V. H. Rumsey and W. L Weeks, 15 October 1956. AD 119780.

Closely Spaced Transverse Slots in Rectangular Waveguide," Technical Report No. 14, Richard F Hyneman, 20 December 1956. AD-127455.

"Distributed Coupling to Surface Wave Antennas," Technical Report No. 15, R. R Hodges, Jr., 5 January 1957. AD-127454.

"The Characteristic Impedance of the Fin Antenna of Infinite Length," Technical Report No 16, Robert L Carrel, 15 January 1957. * AD-127453.

"On the Estimation of Ferrite Loop Antenna Impedance," Technical Report No. 17, Walter L. Weeks 10 April 1957. * AD-143989.

"A Note Concerning a Mechanical Scanning System for a Flush Mounted Line Source Antenna," Technical Report No. 18, Walter L. Weeks, 20 April 1957. AD-143990

"Broadband Logarithmically Periodic Antenna Structures," Technical Report No. 19, R H DuHamel and D. E. Isbell, 1 May 1957. AD-140734.

"Frequency Independent Antennas," Technical Report No. 20, V. H. Rumsey, 25 October 1957. AD-153260.

"The Equiangular Spiral Antenna," Technical Report No. 21. J. D. Dyson, 15 September 1957. AD-145019.

"Experimental Investigation of the Conical Spiral Antenna," Technical Report No 22. R. L Carrel, 25 May 1957. ** AD-144021.

"Coupling between a Parallel Waveguide and a Surface Waveguide," Technical Report No 23. E J Scott, 10 August 1957. AD-144030.

"Launching Efficiency of Wires and Slots for a Dielectric Rod Waveguide," Technical Report No. 24. J. W Duncan and R. H. DuHamel, August 1957. AD-144030.

"The Characteristic Impedance of an Infinite Biconical Antenna of Arbitrary Cross Section," Technical Report No. 25. Robert L. Carrel, August 1957. AD-144121

"Cavity-Backed Slot Antennas," Technical Report No. 26, R. J. Tector, 30 October 1957. AD-149451

"Coupled Waveguide Excitation of Traveling Wave Slot Antennas," Technical Report No 27. W L Weeks, 1 December 1957 AD-155178.

"Phase Velocities in Rectangular Waveguide Partially Filled with Dielectric," Technical Report No. 28. W L Weeks, 20 December 1957 AD-155177.

Measuring the Capacitance per Unit Length of Biconical Structures of Arbitrary Cross Section Technical Report No 29. J D Dyson, 10 January 1958. AD-153561

Non-Planar Logarithmically Periodic Antenna Structure. Technical Report No 30. D E Isbell 20 February 1958 AD-156203

"Electromagnetic Fields in Rectangular Slots," Technical Report No. 31, N. J. Kuhn and P. E. Mast, 10 March 1958. AD-156709.

"The Efficiency of Excitation of a Surface Wave on a Dielectric Cylinder," Technical Report No. 32, J. W. Duncan, 25 May 1958. AD-162052.

"A Unidirectional Equiangular Spiral Antenna," Technical Report No. 33, J. D. Dyson, 10 July 1958. AD-201138.

"Dielectric Coated Spheroidal Radiators," Technical Report No. 34, W. L. Weeks, 12 September 1958. AD-204547.

"A Theoretical Study of the Equiangular Spiral Antenna," Technical Report No. 35, P. E. Mast, 12 September 1958. AD-204548.

Contract AF33(616)-6079

"Use of Coupled Waveguides in a Traveling Wave Scanning Antenna," Technical Report No. 36, R. H. MacPhie, 30 April 1959. AD-215558.

"On the Solution of a Class of Wiener-Hopf Integral Equations in Finite and Infinite Ranges," Technical Report No. 37, R. Mittra, 15 May 1959. AD-220543.

"Prolate Spheriodal Wave Functions for Electromagnetic Theory," Technical Report No. 38, W. L. Weeks, 5 June 1959. AD-226727.

"Log Periodic Dipole Arrays," Technical Report No. 39, D. E. Isbell, 1 June 1959 AD-220651

"A Study of the Coma-Corrected Zoned Mirror by Diffraction Theory," Technical Report No. 40, S. Dasgupta and Y. T. Lo, 17 July 1959. AD-225273.

"The Radiation Pattern of a Dipole on a Finite Dielectric Sheet," Technical Report No. 41, K. G. Balmain, 1 August 1959.

"The Finite Range Wiener-Hopf Integral Equation and a Boundary Value Problem in a Waveguide," Technical Report No. 42, R. Mittra, 1 October 1959. AD-229279.

"Impedance Properties of Complementary Multiterminal Planar Structures," Technical Report No. 43, G. A. Deschamps, 11 November 1959. AD-230625.

"On the Synthesis of Strip Sources," Technical Report No. 44, R. Mittra, 4 December 1959 AD-230624.

"Numerical Analysis of the Eigenvalue Problem of Waves in Cylindrical Waveguides," Technical Report No. 45, C. H. Tang and Y. T. Lo, 11 March 1960. AD-234536.

"New Circularly Polarized Frequency Independent Antennas with Conical Beam or Omnidirectional Patterns," Technical Report No. 46, J. D. Dyson and P. E. Mayes, 20 June 1960. AD-241321.

"Logarithmically Periodic Resonant-V Arrays," Technical Report No. 47, P. E. Mayes and R. L. Carrel, 15 July 1960. AD-246302.

"A Study of Chromatic Aberration of a Coma-Corrected Zoned Mirror," Technical Report No. 48, Y. T. Lo, June 1960. AD-252492.

"Evaluation of Cross-Correlation Methods in the Utilization of Antenna Systems," Technical Report No. 49. R. H. MacPhie, 25 January 1961. AD-252493.

"Synthesis of Antenna Products Patterns Obtained from a Single Array," Technical Report No. 50, R. H. MacPhie, 25 January 1961. AD-252494.

"On the Solution of a Class of Dual Integral Equations," Technical Report No. 51, R. Mittra, 1 October 1961. AD-264557.

"Analysis and Design of the Log-Periodic Dipole Antenna," Technical Report No. 52, Robert L. Carrel, 1 October 1961. AD-264558.

"A Study of the Non-Uniform Convergence of the Inverse of a Doubly-Infinite Matrix Associated with a Boundary Value Problem in a Waveguide," Technical Report No. 53, R. Mittra, 1 October 1961. AD-264556.

Contract AF33(616)-8460

"The Coupling and Mutual Impedance Between Balanced Wire-Arm Conical Log-Spiral Antennas," Technical Report No. 54, J. D. Dyson, June 1962. AD-285678.

"An Investigation of the Near Fields on the Conical Equiangular Spiral Antenna," Technical Report No. 55, O. L. McClelland, May 1962. AD-276463.

"Input Impedance of Some Curved Wire Antennas," Technical Report No. 56, C. H. Tang, June 1962. AD-276461.

"Polygonal Spiral Antennas," Technical Report No. 57, C. H. Tang, O. L. McClelland, June 1962.

"On Increasing the Effective Aperture of Antennas by Data Processing," Technical Report No. 58, R. H. MacPhie, July 1962.

"Theoretical Study of a Class of Logarithmically Periodic Circuits," Technical Report No. 59. R. Mittra, July 1962. AD-282847.

"Backward Wave Radiation from Periodic Structures and Application to the Design of Frequency-Independent Antennas," Technical Report No. 60, P. E. Mayes, G. A. Deschamps, and W. T. Patton, December 1962. AD-291765.

"The Backfire Bifilar Helical Antenna," Technical Report No. 61, W. T. Patton, September 1962. AD-289084.

"On the Mapping by a Cross-Correlation Antenna System of Partially Coherent Radio Sources," Technical Report No. 62, R. H. MacPhie, October 1962. AD-289085.

"On a Conical Quad-Spiral Array," Technical Report No. 63, J. D. Dyson, September 1962. AD-288252.

"Antenna Impedance Matching by Means of Active Networks," Technical Report No. 64, S. Laxpati, R. Mittra, November 1962. AD-291766.

"On Maximizing the Signal-To-Noise Ratio of a Linear Receiving Antenna Array," Technical Report No. 65, R. H. MacPhie, January 1963.

"Application of Cross-Correlation Techniques to Linear Antenna Arrays", Technical Report No. 67, R. H. MacPhie, March 1963.

"A Study of Wave Propagation of Helices", Technical Report No. 68, Paul W. Klock, March 1963.

"Relative Convergence of the Solution of a Doubly Infinite Set of Equations," Technical Report No. 69, R. Mittra, April 1963.

"Theoretical Brillouin (k-β) Diagram for Monopole and Dipole Arrays and Their Application to Log-Periodic Antennas," Technical Report No. 70, R. Mittra and K. E. Jones, April 1963.

---

* Copies available for a three-week loan period.

** Copies no longer available